QUANTIFYING URBAN FORM VIA SPATIAL METRICS AND ITS CLIMATIC IMPLICATIONS

by

NEIL ANDREW DEBBAGE

(Under the Direction of J. Marshall Shepherd)

ABSTRACT

The spatial arrangement of cities can affect how urban environments alter regional moisture and energy balances, but the precise nature of these relationships is still not fully understood. The existing literature suggests that both sprawling and dense urban development can amplify urban heat and dry island intensities. Based on an analysis of PRISM climate data and spatial metrics calculated for the fifty largest metropolitan areas in the United States, it will be argued that a major factor in determining the magnitude of the urban heat and dry island effects is the spatial contiguity of urban development, regardless of its intensity level. At a time when over half the world's population already suffers from the detrimental consequences of the urban heat and dry island effects, unraveling how urban morphology influences these phenomena, and ultimately the overall quality of life in large cities, will only become more important as urban expansion continues.

INDEX WORDS: Urban heat island, Urban dry island, Urban moisture excess, Spatial metrics, Spatial contiguity, Urban climatology

QUANTIFYING URBAN FORM VIA SPATIAL METRICS AND ITS CLIMATIC IMPLICATIONS

by

NEIL ANDREW DEBBAGE

A.B., The University of Georgia, 2012

A Thesis Submitted to the Graduate Faculty of The University of Georgia in Partial Fulfillment of the Requirements for the Degree

MASTER OF SCIENCE

ATHENS, GEORGIA

2014

QUANTIFYING URBAN FORM VIA SPATIAL METRICS AND ITS CLIMATIC IMPLICATIONS

by

NEIL ANDREW DEBBAGE

Major Professor: J. Marshall Shepherd

Committee: John A. Knox
Marguerite Madden

Electronic Version Approved:

Maureen Grasso
Dean of the Graduate School
The University of Georgia
May 2014

ACKNOWLEDGMENTS

Firstly, I would like to thank my advisor, J. Marshall Shepherd, and committee members, John A. Knox and Marguerite Madden, for their invaluable guidance, insight and support. I am deeply indebted to all three individuals as they were instrumental in shaping and improving this work via their constructive criticisms. I would also like to thank my fellow graduate students as well as the faculty of the Department of Geography for providing a stimulating intellectual environment, which has been so influential in my academic development. Finally, I am thankful for my family and friends who provided support when it was most needed.

TABLE OF CONTENTS

LIST OF FIGURES

LIST OF TABLES

Page

CHAPTER 1

INTRODUCTION

The modern expansion of urban environments has not only altered the conceptual frameworks through which urban landscapes are analyzed (Gottmann 1961, Lewis 1983, Lang and Knox 2009), but it has also led to changes in the physical metabolisms of cities that threaten their own sustainability (Kennedy et al. 2007). By altering the fundamental characteristics of the surface, urban development has created imbalances in regional energy and moisture budgets and modified a plethora of other climatic variables. The enhanced anthropogenic energy consumption, lowered surface albedos, reduced evaporative cooling and narrow canyon geometry characteristic of cities often results in the formation of urban heat islands (UHI), as urban temperatures are elevated relative to the surrounding environment (Environmental Protection Agency [EPA] 2008).

While the UHI effect remains the most commonly studied component of urban climatology (Souch and Grimmond 2006), the introduction of impervious surfaces, largely in place of natural vegetation, can alter local water balances (Arnold and Gibbons 1996) and influence precipitation regimes (Shepherd, *in press*). By reducing the amount of moisture stored at the surface and limiting the water available for evaporation, impervious building materials can create precipitation deficits within urban areas (Kaufmann et al. 2007). Conversely, the presence of an UHI can destabilize the atmosphere and actually enhance precipitation downwind of large urban centers such as Atlanta, Georgia (Bornstein and Lin 2000; Mote et al. 2007). The interactions between cities and the water cycle are complex and can vary spatially, diurnally as well as seasonally. This complexity is made particularly evident by the emergence of the seemingly contradictory terms Urban Moisture Excess (UME) (Holmer and Eliasson 1999) and Urban Dry Island (UDI) (Xi and Yan 2010).

Although this research focuses on how the spatial arrangement of cities influences the thermal and moisture facets of the urban climate system, studies have linked urbanization to changes in a vast array of other climatic and physical processes. For example, urban development can affect snowmelt patterns (Todhunter et al. 1992; Semádeni-Davies & Bengtsson 1998), net primary productivity (Imhoff et al. 2004), atmospheric carbon dioxide levels (Jacobson 2010) and the nitrogen cycle (Filoso et al. 2006). Of course, many of these modifications can be at least indirectly and in some cases directly attributed to the same physical processes that produce the UHI and UDI/UME effects.

1.1 Motivation

The urban development responsible for modifying regional climate regimes can largely be attributed to favorable socio-economic conditions causing in-migration (Bhatta 2010), which has in turn led to substantial increases in the number of urban residents worldwide. In 2012, 51% of the world population and 75% of individuals in developed countries resided in urban areas (Population Reference Bureau [PRB] 2012). The same year in the United States, 79% of the population was estimated to be urban dwellers (PRB 2012). Urban population growth is projected to continue, mainly due to ongoing urbanization in developing countries, with approximately 67% of the world population living in urban environments by 2050 (Figure 1.1 and Figure 1.2) (United Nations 2012).

In light of these demographic trends, it seems imperative to work towards a better understanding of the complex processes found at the intersection of urbanization, climate and the human dimension. Continuously growing urban populations will only increase the number of individuals who suffer from the detrimental impacts of the UHI and UDI/UME effects. For example, the higher temperatures produced by the UHI effect catalyze the chemical reactions responsible for near surface ozone formation (EPA 2008). The larger quantities of ozone further degrade urban air quality, which is already plagued by the concentrated combustion of fossil fuels. Furthermore, the UHI effect increases energy consumption, due to the heightened demand for air conditioning during the warm season, forming a positive feedback that further intensifies air pollution as emissions from regional power plants increase (Rosenfeld et al. 1998). Perhaps most significant, however, is the ability of the UHI effect to amplify heat waves and subsequently increase heat-related fatalities (Zhou and Shepherd 2010; Stone 2012; Li and Bou-Zeid 2013).

The European heat wave that occurred during the summer of 2003 provides a somber example of how deadly the UHI effect can be when acting synergistically with an extreme heat event. Over a four-month period that summer more than 70,000 individuals perished due to heat-related illness (Robine et al. 2008). The vast majority of these individuals lived in cities (Stone 2012) where the impacts of the heat wave were greatly exacerbated (Matzarakis et al. 2009). Partially due to the UHI effect, extreme heat events on average are responsible for more climate-related fatalities than any other form of severe weather (Stone et al. 2010).

Although over half of the world population resides in urban environments and is faced with the adverse impacts of the UHI and UDI/UME effects, this scale of analysis is often overlooked (Stone 2012). Instead, climate change research has generally adopted the global scale as a scientific standard, which dilutes the significance of urban development since its impacts are most prominent at the regional and local scales (Stone 2012). Many global climate studies and assessments, most notably the Intergovernmental Panel on Climate Change (IPCC), fail to take into account the important influence of land use/land cover (LULC) change on future climate projections (Stone 2012). It is also common practice to statistically remove the warming signature attributed to urban development from meteorological observation networks when researching climate change (Stone 2012). However, since cities are arguably where climate change is most tangible and will have the most immediate impact on a vast majority of the world's citizens, their climatic influence deserves special attention rather than being obfuscated by statistical adjustments and global scale analyses.

Amongst those studies that have focused on the climatic ramifications of urban development, there is a general agreement that cities have fundamentally altered regional moisture and energy balances. However, the precise relationships between the spatial arrangement of cities and the UHI/UDI effects are still not fully understood. The existing literature suggests that both sprawling (Stone and Rodgers 2001) and dense (Coutts et al. 2007; Martilli 2014) patterns of urban development can amplify UHI intensities while there is a significant lack of research focusing on the potential linkages between urban form and the UDI effect. Accurately understanding the interactions between the UHI and UDI effects and how their intensities are governed by the spatial arrangement of cities are imperative first steps towards developing successful mitigation strategies. Additionally, a more detailed examination of how various urban morphologies impact urban heating and the urban moisture balance could potentially resolve the conflicting results of previous studies and ultimately help make cities more sustainable and livable in the future.

The lack of consensus regarding how urban form impacts UHI intensity can partially be attributed to the large variety of techniques used to evaluate the UHI effect. Many of the current methodologies are fairly subjective since they commonly rely on point comparisons of urban and rural air temperature, which may not be representative of the entire urban and rural environments. Through a systematic review and critique of the extant UHI literature, Stewart (2011) found that a majority of UHI studies fail to control for confounding factors, such as elevation and weather, and do not report important details concerning their methodologies.

Cognizant of the methodological shortcomings outlined by Stewart (2011), this study established a systematic alternative that used gridded air temperature and dew point data. The standardized approach allowed for a more accurate comparison of the UHI and UDI intensities of the 50 Metropolitan Statistical Areas (MSAs) that were considered. Additionally, using the same method to calculate the UHI and UDI effects helped clarify the relationships that existed between the two phenomena. Due to this study's unique interdisciplinary approach, which combined aspects of Geographic Information Science (GIS), landscape ecology and climatology, it has the potential to produce innovative results that will inform environmental planning efforts focused on UHI mitigation. Policies that successfully mitigate the UHI effect will help secure more sustainable futures for our foremost economic and population centers by reducing heat-related fatalities, improving urban air quality and reducing energy consumption.

1.2 Research Objectives

This research focused on the following objectives:

1. Establish a systematic grid-based methodology to estimate the canopy level UHI and UDI intensities of the 50 largest MSAs in the United States.
2. Quantify the urban form of the 50 MSAs using spatial metrics.
3. Evaluate the degree of association between the spatial arrangement of cities and their subsequent UHI/UDI intensities.

The first research objective was to develop a systematic grid-based methodology to estimate the canopy level UHI and UDI intensities of the 50 largest MSAs in the United States. Parameter-Elevation Regression on Independent Slopes Model (PRISM) temperature and dew point data, produced by the PRISM Climate Group at Oregon State University, served as the foundation for the UHI and UDI analysis (Daly et al. 2008). The UHI and UDI intensities were calculated by subtracting the average rural temperatures from the average urban temperatures and the average rural dew points from the average urban dew points, respectively. Since the 50 MSAs included in the study were dispersed throughout the contiguous United States, it was anticipated that regional differences in the UHI/UDI intensities would be revealed. In addition to examining their spatial distribution, the intra- and inter-annual variability of the UHI/UDI effects was evaluated by quantifying the monthly UHI/UDI intensities in 2010 and conducting a long-term historical analysis from 1895 to 2012. It was hypothesized that the UHI/UDI effects varied seasonally and have become more intense over time due to continued urban expansion. Finally, the potential linkages between the dry island and heat island effects were examined, with stronger moisture excesses expected to be correlated with stronger heat islands as observed by Kuttler et al. (2007) and Holmer and Eliasson (1999).

The second research objective was to quantify the urban form of the 50 MSAs using spatial metrics. The public domain software FRAGSTATS (McGarigal et al. 2012) and LULC data obtained from the 2006 National Land Cover Database (NLCD) were used to calculate the spatial metrics. Initially, the LULC data were converted into an urban/non-urban binary to simplify the analysis but this obscured the different influences of the various urban classifications (i.e. high, medium and low-intensity). Analyzing each LULC classification individually produced much more informative results. MSAs located within the same region of the United States were anticipated to have similar urban morphologies due to the comparable economic forces, cultural values and topographic barriers governing urban development patterns. It was hypothesized that MSAs with more sprawling characteristics, as measured by the spatial metrics, would be clustered in the Southeastern portion of the country. Additionally, the spatial metrics were compared to the Sprawl Index created by Ewing et al. (2002). It was hypothesized that the majority of the metrics would be fairly analogous to the Sprawl Index while a small portion would measure highly unique aspects of urban morphology.

The third research objective was to evaluate the degree of association between the spatial arrangement of cities and their subsequent UHI/UDI intensities. This objective was designed to elucidate the apparent contradictions in previous works, which have suggested that both sprawling (Stone and Rodgers 2001) and high-density (Coutts et al. 2007; Martilli 2014) patterns of urban development can amplify the UHI effect. Bivariate and multivariate statistical techniques were used to analyze the relationships between urban morphology, as evaluated by the spatial metrics, and the estimated UHI/UDI intensities. It was hypothesized that denser patterns of urban development would be associated with stronger UHI and UDI effects largely due to the urban canyon geometry, reduced quantities of vegetation and elevated levels of anthropogenic energy consumption characteristic of high-intensity urban development.

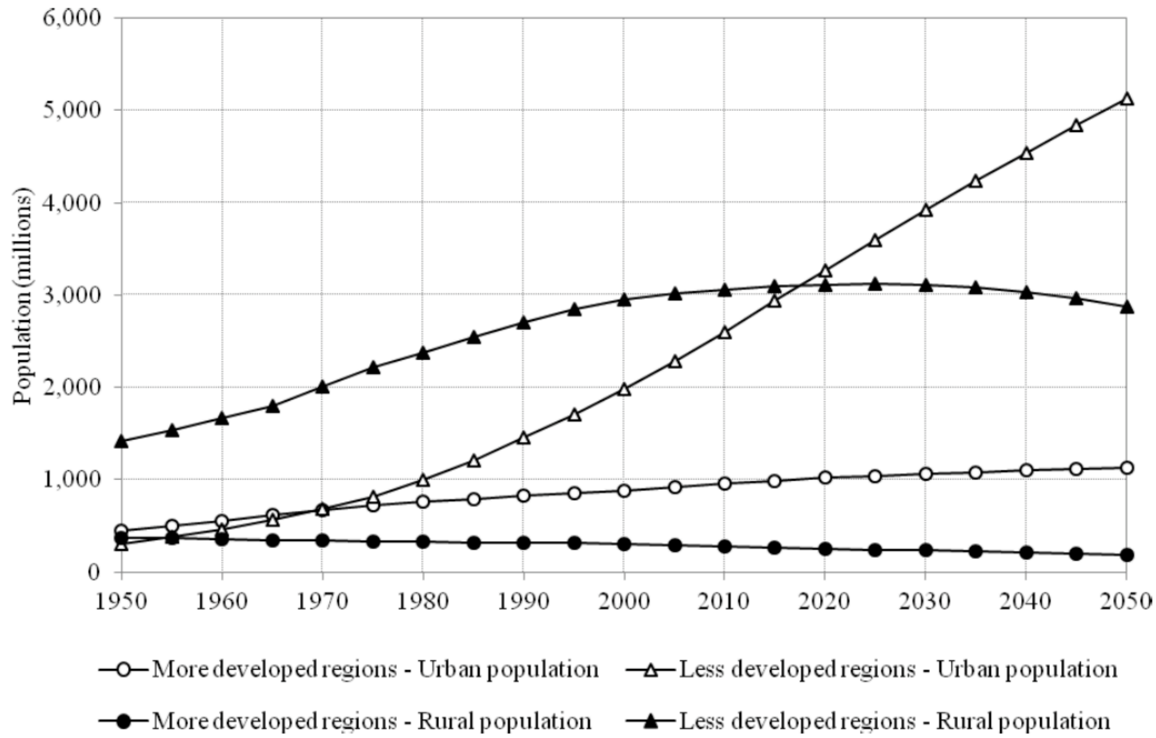

Figure 1.1. Urban and Rural Populations by Development Group, 1950-2050 (United Nations 2012)

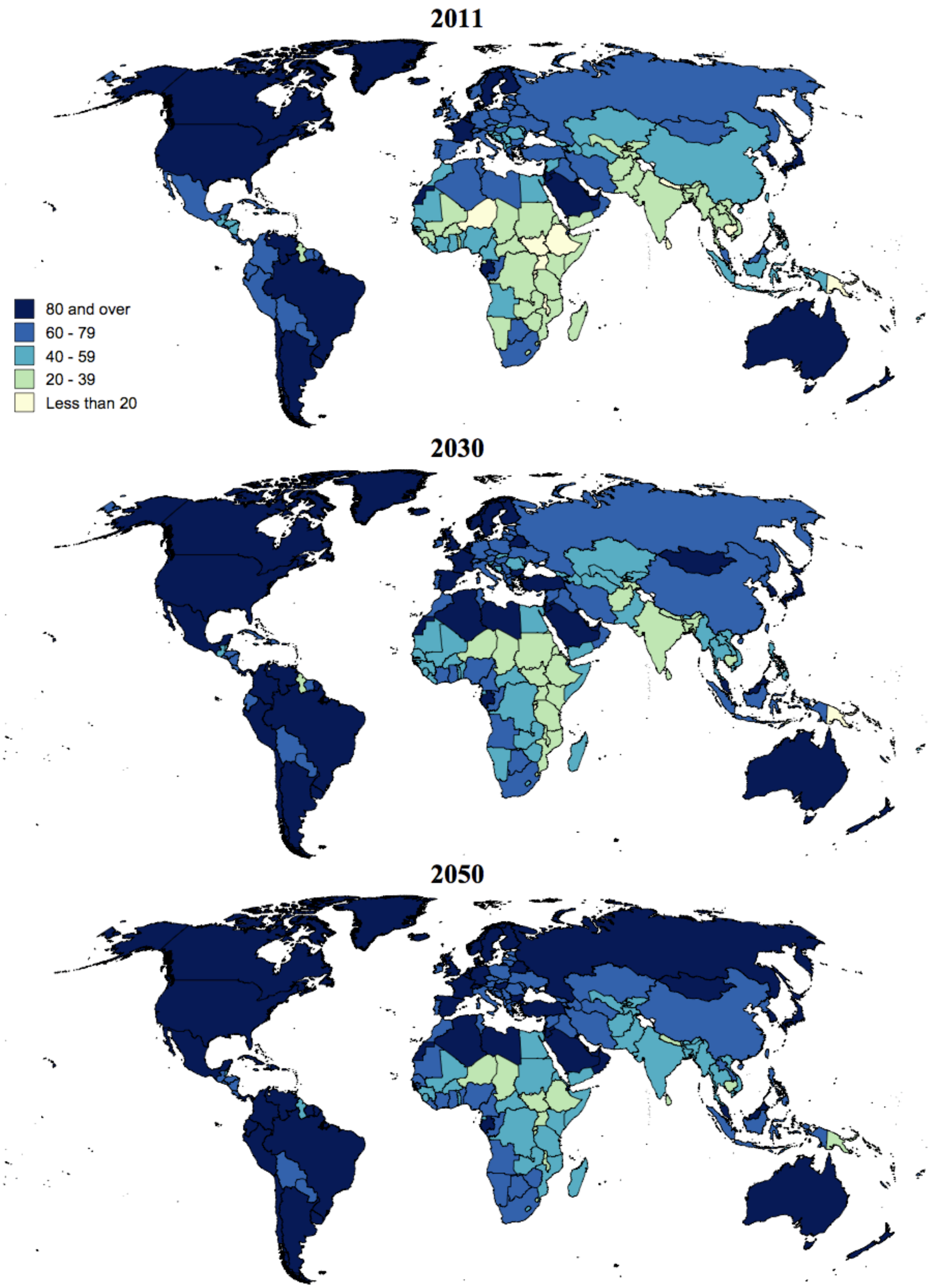

Figure 1.2. Percentage of the Population in Urban Areas: 2011, 2030 and 2050 (United Nations 2012)

CHAPTER 2

LITERATURE REVIEW

2.1 Urban Heat Islands

Luke Howard, who is widely considered a significant pioneer of urban climatology, was the first to identify the influence of urbanization on local climate in his 1833 work, *The Climate of London.* By comparing three temperature records in rural areas outside of London with one urban site, Howard (1833) discovered that the city was on average approximately 2 °F warmer than its surrounding environment (Figure 2.1). This methodology for analyzing the urban effect on temperature, estimating the difference between the urban and rural temperatures (ΔT_{U-R}), has conceptually remained unchanged and is still used in many modern UHI studies (e.g., Stone 2007, Gaffin et al. 2008). Howard (1833) found that London's UHI intensity was greatest during the winter and nighttime, which he presumed to be largely due to anthropogenic heat production. Other causes of the UHI effect identified by Howard (1833) included urban canyon geometry, urban surface roughness and reduced evapotranspiration. Oke (1982) verified the original explanation of the UHI effect provided by Howard (1833) and augmented it slightly by also considering the thermal properties of urban surfaces (Figure 2.2).

Although Howard's (1833) work was pioneering at the time and outlined a majority of the fundamental causes of the UHI effect, it also revealed many complexities that still exist in UHI studies. Firstly, as identified by Oke (1976), there are actually multiple types of UHIs, which are caused by slightly different climatic processes. Oke (1976) distinguished between two atmospheric UHIs: the canopy layer UHI and the boundary layer UHI (Figure 2.3). The canopy layer UHI exists between the surface and the mean roof height. It is strongly influenced by micro-scale variations in local site characteristics such as building geometry and construction materials (Oke 1976). The boundary layer UHI is located above the canopy layer as it begins at the mean roof height and extends upward until the urban environment no longer influences the atmosphere, which is typically no more than two kilometers (Oke 1982). Conditions in the boundary layer are coupled to the urban canopy level but are also governed by more regional or mesoscale climate patterns (Oke 1982).

A third type of UHI, the surface UHI, has emerged more recently partially due to enhanced thermal remote sensing capabilities (Roth et al.1989; Voogt and Oke 1997; Jin 2012). While elevated urban air temperatures characterize the two atmospheric UHIs, the surface UHI refers to the relative warmth of the actual urban surface (Yuan and Bower 2006). The surface UHI is strongest during the day and summer (Roth et al. 1989), whereas the atmospheric UHIs are typically most intense just after sunset and during winter (EPA 2008). Obviously, it is quite important to clarify which UHI is being analyzed and the methodologies used to estimate UHI intensity often vary with each UHI type.

The most traditional approach used to estimate UHI intensity is to compare point measurements of temperature in the urban area with similar measurements in the surrounding natural environment. This is essentially the original methodology developed by Howard (1833). Since the point comparison method usually involves air temperature measurements near the surface, it is most often used to study the canopy level UHI (Yuan and Bower 2006). For the methodology to yield accurate results, the selection of the individual urban and non-urban sites is of the upmost importance (Mills 2008) since they must be representative of their local-scale surroundings (Stewart 2011). The point comparison approach has been used to calculate the UHI intensity for New York City (Gaffin et al. 2008), London (Howard 1833), Atlanta (Bornstein and Lin 2000; Zhou and Shepherd 2010), 50 of the most populous US cities (Stone 2007) and various urban areas in the Netherlands (Wolters and Brandsma 2012).

Unfortunately, since only a few rural and urban points are considered, the heterogeneity of temperature within the urbanized area as well as in the surrounding natural landscape is often overlooked (Jin 2012). By using automobile transects to gather temperature data instead of relying on fixed weather stations, the spatial resolution of the sampling can be improved (Oke and Maxwell 1975) but large portions of the urban environment are still ignored. Using the point comparison methodology to evaluate the canopy level UHI effect produces UHI intensity estimates that fundamentally depend upon the locations of the rural and urban observations or the paths of the automobile transects (Jin 2012). If the locations of the observations or transects are altered, then the UHI intensity will likely change as well. This complicates the interpretation of the results and makes it difficult to compare the UHI intensities of multiple cities (Jin 2012).

In an effort to create a more systematic methodology for estimating UHI intensities, researchers have started to utilize thermal remote sensing. The most commonly used satellite instruments are the Advanced Very High Resolution Radiometer (AVHRR) (Roth et al. 1989), Landsat Thematic Mapper (TM) (Yuan and Bauer 2006), Landsat Enhanced Thematic Mapper Plus (ETM+) (Yuan and Bauer 2006) and NASA's Moderate Resolution Imaging Spectroradiometer (MODIS) (Imhoff et al. 2010; Peng et al. 2011; Jin 2012). Urban surface temperatures can be derived from the AVHRR, Landsat and MODIS because they measure the amount of longwave radiation emitted within a given field of view (Jin 2012). Although the precise accuracy of remotely derived surface temperatures is dependent upon the sensor, the uncertainties are generally less than 2 degrees Kelvin (Yuan and Bauer 2006; Imhoff et al. 2010).

Since satellite instruments are measuring the urban surface or earth skin temperature, remote sensing techniques are most often used to evaluate the surface UHI. Overall, remote sensing platforms improve the spatial resolution and increase the coverage area of temperature data especially when juxtaposed with the traditional point comparison methodology (Jin 2012).

Despite these advantages, UHI intensity estimates based on remotely sensed temperature data appear to suffer from a lack of standardization with regard to how rural is defined. Peng et al. (2011) used a buffer method to establish a surrounding rural area, which was equivalent in size to the area occupied by the city. A different approach was adopted by Jin (2012), who used MODIS land classification data within a 0.6° by 0.6° box surrounding New York and Beijing to delineate rural and urban areas. Alternatively, Imhoff et al. (2010) defined rural areas as the pixels in a 5 km buffer located between 45 and 50 km away from the urban core that had less than 5% impervious surface coverage. Unfortunately, these various definitions of what constitutes “rural” make drawing meaningful comparisons between studies challenging.

One final perspective used to evaluate UHIs relies upon a combination of observational data and computer modeling. Some of the earliest UHI modeling techniques developed by Myrup (1969) were quite simple and only considered surface energy fluxes (sensible, latent and soil) over a city represented in the model as a concrete slab. By including the radiative contributions of the urban canyon, Oke et al. (1991) were able to improve modeling capabilities and more accurately depict the nighttime UHI maximum as indicated by observational data. Although modeling approaches are not based solely on observed data, the simulations allow researchers to examine how UHI intensities vary under different weather conditions (Hafner and Kidder 1999). Additionally, modeling enables the individual factors influencing UHI intensity to be isolated and tested for importance (Atkinson 2003).

2.2 Urban Dry Islands/Urban Moisture Excess

Just as urbanization can alter the thermal properties of local and regional climate systems, it can also dramatically modify moisture levels relative to the surrounding natural environment. Many of the factors responsible for the UHI effect, such as the introduction of impervious surfaces, are also thought to influence urban-rural moisture differences (Ackerman 1987). However, unlike the UHI effect, which is much more dominant than its counterpart the Urban Cool Island (UCI), urban-rural moisture differences are highly variable. A given city can often be drier or moister than the surrounding natural environment depending upon the time of day, season and climatological context. The term Urban Dry Island (UDI) is used to describe a scenario where the city is drier than its surroundings while the opposite state is referred to as an Urban Moisture Excess (UME).

The Urban Dry Island (UDI) effect is most prevalent during the daytime especially throughout the warmer summer months (Hage 1975). A case study of St. Louis (Sisterson and Dirks 1977) revealed that the driest regions within the city correlated well with the most densely populated areas presumably due to the high percentage of impervious surface coverage. Sisterson and Dirks (1977) concluded that the reduced amount of surface moisture found in the urban environment, due to accelerated surface runoff and a lack of vegetation, contributed to the UDI effect. During warm summer afternoons, the UDI effect is also magnified by the high rate of evapotranspiration that occurs in the surrounding natural landscape (Charciarek 2003).

UME is actually most common during nighttime throughout the entire year (Figure 2.4) (Holmer and Eliasson 1999). UMEs occur during the night largely because dewfall is much less prevalent in cities when compared to their natural surroundings (Kuttler et al. 2007). The large quantity of dewfall in rural areas removes moisture from the atmosphere (Holmer and Eliasson

1999), which results in urban areas becoming relatively moister. Additionally, the UME is enhanced by the higher nighttime temperatures within cities that enable evapotranspiration to continue while in rural areas evapotranspiration rates are hindered considerably by rapidly decreasing temperatures after sunset (Charciarek 2003).

UME conditions typically occur during both day and night throughout the colder winter period because large portions of the plant life in the surrounding natural landscape are dormant, which reduces rural atmospheric water vapor (Ackerman 1987). Contrastingly, moisture sources are still prevalent within cities partially due to the combustion of fossil fuels (Ackerman 1987). For cities located in higher latitudes, such as Edmonton, snow and ice often increase the wintertime UME since they melt preferentially in warmer urban areas (Hage 1975). Similar mechanisms can produce UMEs during summertime droughts as urban water vapor sources, such as vehicle exhaust, industrial emissions and irrigation, are still ubiquitous but moisture levels in rural areas are reduced due to the stressed state of the natural vegetation surrounding the city (Holmer and Eliasson 1999).

The techniques for estimating UDI and UME intensities often suffer from shortcomings similar to those encountered in UHI analysis. Firstly, the UDI/UME calculations are almost exclusively based on comparisons of moisture levels at one rural station and one urban station (e.g. Hage 1975; Ackerman 1987; Holmer and Eliasson 1999). Unfortunately, researchers very rarely address how the traditional urban-rural point comparison methodology may not be representative of the entire urban or rural environments especially under varying weather conditions (Hage 1975). An additional complicating factor is selecting a metric to evaluate atmospheric moisture content. Relative humidity (Hage 1975; Ackerman 1987), specific humidity (Sisterson and Dirks 1977), absolute humidity (Hage 1975), dew point (Ackerman

1987) and vapor pressure (Ackerman 1987; Kuttler et al. 2007) have all been used to estimate UDI/UME intensity.

Selecting different metrics to evaluate the UDI/UME effect can profoundly influence the results. When relative humidity is used, the city is typically drier than its natural surroundings during both day and night throughout the majority of the year (Hage 1975). However, the prevalent UDI signature portrayed by relative humidity is largely an artifact of the UHI effect since relative humidity is very sensitive to temperature (Ackerman 1987). In actuality, it is best to utilize variables such as dew point and/or vapor pressure since they are less sensitive to temperature variations (Ackerman 1987). Obviously, the usage of different atmospheric moisture measurements, which are often made at different time intervals, makes it extremely difficult to compare the results of various studies (Kuttler et al. 2007).

2.3 Climatic Variables and Urban Form

Previous efforts have been made to analyze how UHI and, to a lesser extent, UDI/UME intensities vary with different forms of urban development. Early work by Oke (1973) revealed that UHI intensities were approximately proportional to the fourth root of city population. However, using only population size to explain the UHI effect ignores many other intrinsic properties of the city that could influence urban-rural temperature differences. Chandler (1964) opposed the general theory that city size was the most influential factor governing UHI intensity and instead argued that urban fabric and geometry were more important contributors. More recently, Streutker (2003) distinguished between the potential effects of total population and population density on the characteristics of the UHI. Streutker (2003) speculated that total population largely determines the spatial extent of the UHI, while the UHI intensity is likely more heavily influenced by population density. In addition to the effects of city size, as evaluated by both population and area, UHI intensity has been found to depend upon building density and land use distribution (Oke 1982) as well as the quantity of upstream urbanization (Zhang et al. 1999). Presumably, since many of the physical factors that govern UHI intensities also influence the UDI effect (Ackerman 1987), both may be enhanced by similar patterns of urban development.

Although much progress has been made since the formative works of Oke (1973) and Chandler (1964), a general lack of consensus concerning how urban form influences the UHI effect still exists. By analyzing cities in the Northeastern portion of the United States, Imhoff et al. (2010) concluded that UHI intensity increases with city area. Zhou et al. (2013) also found that UHI intensity increased with city area by evaluating the UHIs of all European cities. However, the numerical modeling of the UHI effect conducted by Atkinson (2003) suggests that city size has a minimal influence on UHI intensity. Atkinson (2003) contends that other factors, which are usually strongly correlated with increases in city size, are actually responsible for the ostensible relationship between city size and UHI intensity.

Traditionally, UHIs have been associated with the dense urban development located in city centers largely due to the climatic ramifications of the urban canyon geometry and the lack of vegetation (Oke 1982). However, more recent studies have reached the conflicting conclusions that both more sprawling (Stone and Rodgers 2001; Stone 2012) and denser (Coutts et al. 2007; Martilli 2014) patterns of urban development can produce a stronger UHI. Stone and Rodgers (2001) analyzed the thermal efficiency of single-family residential parcels in suburban Atlanta, Georgia and found that lower density patterns of development contributed more radiant energy to surface heat island formation than urban densification. Based on these findings, Stone (2012) has argued that sprawling urban development increases UHI intensity, especially when evaluated at the MSA scale, since it results in more land clearances, impervious surfaces and excess heat generated per capita when compared to higher density development. Contrastingly, by conducting a series of surface energy balance measurements, Coutts et al. (2007) found greater nocturnal temperatures to be associated with higher densities throughout Melbourne, Australia, which was in part attributed to the urban canyon morphology altering heat storage release. Martilli (2014) also concluded that more compact cities decrease thermal comfort by performing numerous idealized mesoscale simulations.

Potentially most significant are the drastically different planning implications of these disparate studies. Stone (2012) and Emmanuel and Fernando (2007) both advocate high-density urban development as a strategy to mitigate the UHI effect since it increases thermal efficiency and makes strategies such as installing white and green roofs more economically feasible. However, Coutts et al. (2007), whose work was motivated by a long-term strategic urban planning document that aimed to make Melbourne more sustainable, livable and economically prosperous by encouraging high-density compact growth, fear that increasing urban densities will actually make cities less livable due to an intensification of the UHI effect. Although some of the discrepancies outlined above can potentially be attributed to the different cities analyzed in the various case studies (i.e. Atlanta vs. Melbourne), the type of UHI evaluated (i.e. surface vs. canopy) and the diverse methodologies developed to estimate the UHI intensity, the overall lack of understanding regarding the relationships between urban form and the UHI effect, as well as the confusion this has likely engendered amongst urban planners, validates the importance of this study. As noted by Ewing and Rong (2008, pg. 9), “the impact of urban form on the formation of UHIs is ambiguous and calls for empirical analysis.” More recently, Martilli (2014) also called for further observational-based research to evaluate the findings of model-driven studies.

Spatial metrics offer a unique and underutilized perspective to analyze how UHI and UDI/UME intensities may vary with different patterns of urban development. Essentially, spatial metrics are algorithms that quantify categorical map patterns (McGarigal et al. 2012). In landscape ecology, where they are typically referred to as landscape metrics, spatial metrics have been frequently used to quantify the shapes and arrangements of natural environments and to explore the linkages between ecological pattern and ecological function or process (Naveh and Lieberman 1984; Forman and Godran 1986; Gustafson 1998). Herold et al. (2005) suggested that the more general term spatial metrics be used especially when referring to studies that focus on different environments such as urban areas. The application of spatial metrics in urban studies has focused primarily on comparative analysis between cities (Huang et al. 2007; Bereitschaft and Debbage 2013b) as well as the quantification and modeling of urban expansion (Herold et al. 2002; Herold et al. 2005; Ji et al. 2006; Jat et al. 2008). However, a few researchers have adopted a more traditional ecological perspective by investigating the relationships between urban land use patterns and urban processes such as surface temperature (Liu and Weng 2008; Connors et al. 2013) and air quality (Makido et al. 2012; Bereitschaft and Debbage 2013a).

Spatial metric algorithms can be used to quantify specific spatial characteristics at three different levels: patches, classes of patches or the entire landscape mosaic (Forman and Godran 1986; McGarigal et al. 2012). The patch is the most fundamental level and represents a discrete area of homogeneous LULC such as an individual patch of trees. The class level metrics integrate all patches that belong to a common classification. For example, a class level metric for a land cover type forest would evaluate every individual patch of trees. Finally, the landscape level metrics are calculated by considering every patch, regardless of class, within the extent of the study area. Within each of the three levels, spatial metrics can be divided into two general categories based on if they consider spatial information (McGarigal et al. 2012). Composition metrics analyze the variety and abundance of patch types, but do not consider the spatial arrangement of the patches within the landscape. Configuration metrics are more complex because they do include a spatial component by evaluating the shape, arrangement and/or orientation of the LULC patches.

The majority of spatial metrics (Herold et al. 2002; Herold et al. 2005; Ji et al. 2006; Bereitschaft and Debbage 2013a) are calculated using the public domain software FRAGSTATS, created originally in 1995 by McGarigal et al. (2012). However, alternative programs such as APACK (Mladenoff and DeZonia 1997) have also been used (Li et al. 2005). These software packages have made it very simple to calculate an immense number of spatial metrics without the user necessarily understanding their mathematical foundations, which can lead to erroneous interpretations (Li et al. 2005). The most challenging aspects of landscape pattern analysis are selecting the correct spatial metrics to capture the phenomenon being studied and accurately interpreting the results (Li et al. 2005). Since the importance of different spatial metrics varies depending on the overall research objectives, a standard suite of metrics for urban applications has not been identified (Herold et al. 2005). However, if a set of spatial metrics appropriate for analyzing urban climatological phenomena was selected and interpreted correctly, the results would have great potential to elucidate how the spatial configuration of cities influences UHI/UDI intensities.

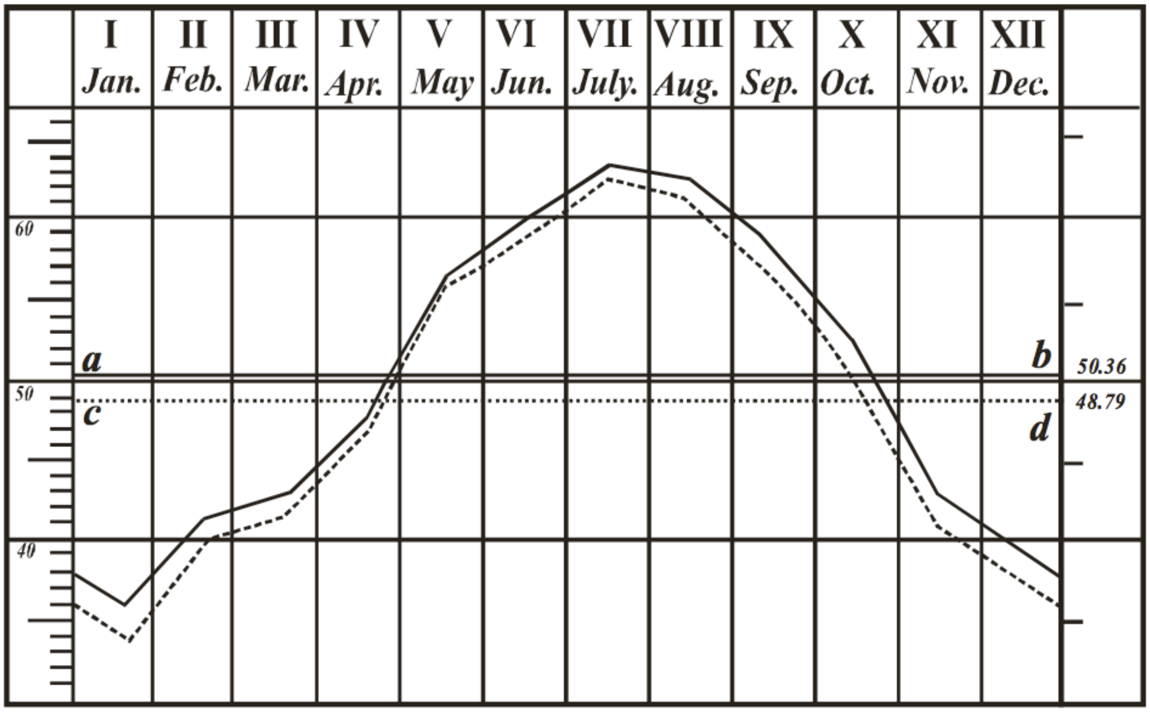

Figure 2.1. London UHI: Solid Line Represents Urban Temperature and Dotted Line Represents Rural Temperature (Howard 1833)

Energy budget term	Urban feature	Meteorological effect
Increased absorption of solar radiation (K^*).	Canyon geometry	Increased surface area and multiple reflection
Increased long-wave radiation received from the sky ($L\downarrow$).	Air pollution	Greater absorption and re-emission
Decreased long-wave radiation loss from surfaces of buildings and streets ($L\uparrow$).	Canyon geometry	Reduced sky view factor
Heat added by human activities (Q_F).	Buildings & traffic	Direct addition of heat
Increased storage of heat in city fabric (ΔQ_S).	Construction materials	Increased thermal admittance
Decreased latent heat exchange (Q_E).	Construction materials	Increased water-proofing
Decreased sensible and latent heat exchange ($Q_H + Q_E$).	Canyon geometry	Reduced wind speed

Figure 2.2. Suggested Causes of Modern Canopy Layer UHI Effect (Oke 1982, Mills 2008)

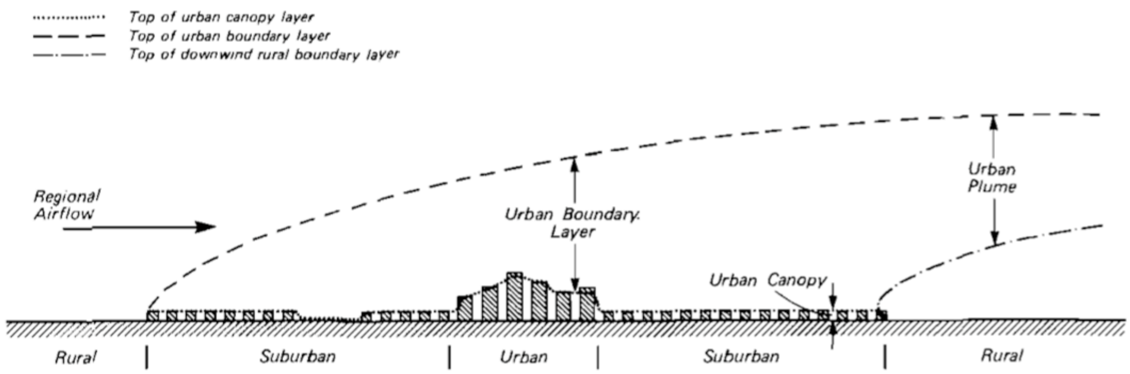

Figure 2.3. Schematic Representation of the Urban Atmosphere Illustrating a Two-Layer Classification of Thermal Modification (Oke 1976)

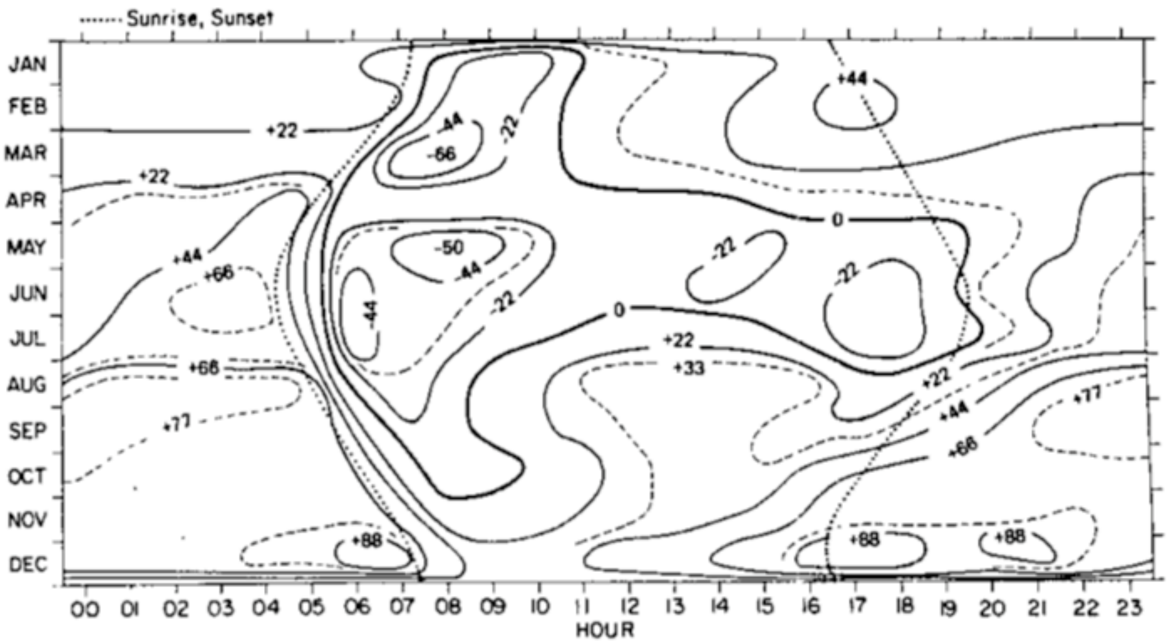

Figure 2.4. Contours of Average ΔDP (Urban – Rural) by Hour for Each Month in Chicago (Ackerman 1987)

CHAPTER 3

RESEARCH DESIGN AND METHODOLOGY

3.1 Study Area

The study area included the 50 largest MSAs in the United States, in terms of population, according to the 2010 US Census (Figure 3.1). A MSA consists of at least one urban core with a population of 50,000 or greater and the adjacent counties that are socio-economically tied to that core, which is determined by commuting data. As of 2010, approximately 54% of the United States population resided within the 50 largest MSAs. Only MSAs located in the contiguous United States were considered so the San Juan, Puerto Rico MSA was not included despite having a population of nearly 2.5 million. By selecting 50 MSAs, a wide variety of city sizes and forms were evaluated. For example, the radically different urban morphologies of Atlanta and Portland were both included in the study. Additionally, the spatial distribution of the MSAs throughout the United States enabled an assessment of how climatological context potentially influenced UHI and UDI/UME intensities.

3.2 Estimating Urban Heat Island/Urban Dry Island Intensities

PRISM (Parameter-Elevation Regression on Independent Slopes Model) climate data (Prism Climate Group) were used to calculate the UHI and UDI/UME intensities for each MSA. PRISM is an analytical model that creates gridded estimates of temperature and dew point by incorporating discrete measurements of climatic variables (temperature, precipitation, etc.), expert knowledge of complex climatic events (rain shadows, temperature inversions and coastal regimes) and a digital elevation model into a knowledge-based system. The gridded data has a resolution of approximately 4 km, which allows numerous grid points to exist within the urban areas of each MSA. Since the vast majority of this research was conducted prior to the PRISM version update that began at the end of 2013 and was still ongoing as of March 2014, the previous version of PRISM was used. Additionally, updated dew point datasets were still not available at the time of writing. Using the previous PRISM version, instead of a combination of the updated for temperature and previous for dew point, ensured that the comparison of the UHI and UDI/UME effects was as accurate as possible. However, to verify that no significant differences existed between the two versions a small portion of the analysis was rerun using an updated PRISM dataset and a two-sample difference test was conducted.

In order to systematically estimate the canopy UHI intensities, the PRISM grids for annual and monthly average minimum temperature were used. Minimum temperatures, rather than maximums or averages, were selected since they most often occur at night when the canopy UHI is strongest. However, to test this assumption a small segment of the analysis was conducted using maximum temperatures as well. The UDI/UME intensities were estimated using the PRISM grids for annual and monthly average dew point temperatures. Dew point is an appropriate variable to assess the moisture content of the atmosphere because it is less sensitive to temperature changes than other measurements, such as relative humidity.

A Python program was created to automate the UHI and UDI/UME intensity calculations. First, the temperatures/dew points of the PRISM grid cells within the Census Urbanized Areas (UA) and Urban Clusters (UC) included in each MSA were averaged to provide an urban temperature/dew point. UA, as defined by the US Census, contain at least 50,000 people and include one central urban core and the adjacent densely settled territory. UC are very similar to UA except they must contain only 2,500 individuals. Since UA/UC are largely based on population density, some researchers (Sutton et al. 2010; Bereitschaft and Debbage 2013a) have used nighttime light intensity as an alternative method to delineate urban areas. However, the added criteria in the 2010 US Census that helped identify non-residential urban land uses characterized by high levels of impervious surfaces makes using UA/UC a viable option. Next, a buffer was created to delineate a rural domain outside the UA/UC. The temperatures/dew points of the PRISM grid cells falling within the defined rural area were averaged to provide a background temperature/dew point. The UHI and UDI/UME intensities were calculated by simply subtracting the average rural temperature/dew point from the average urban temperature/dew point for each MSA (Equation 1 and Equation 2). All temperatures are reported in degrees Celsius.

$$UHI = T_{URBAN\ AVG} - T_{RURAL\ AVG} \tag{1}$$

$$UDI = DP_{URBAN\ AVG} - DP_{RURAL\ AVG} \tag{2}$$

Although using a fundamentally areal-based method to estimate the canopy UHI and UDI/UME intensities improves upon the traditional point comparison approach since it is more representative of entire cities and their surroundings, some challenges still exist. Most notable are the difficulties of accurately defining the extent of the "rural" area and controlling for potential confounding factors (Stewart 2011). For example, elevation changes and neighboring urban areas could distort the UHI and UDI/UME estimates if the buffer used to define the rural domain included mountainous terrain or overlapped neighboring MSAs. In order to combat these potential biases, a systematic rule-based system was developed. To begin, a 50 km buffer around the UA/UC was created to define a preliminary rural area. A digital elevation model was then incorporated to limit the defined rural domain to only those regions within +/- 50 meters (Imhoff et al. 2010) of the average elevation of the UA/UC. Finally, any neighboring urban areas included in the buffer were systematically excluded (Figure 3.2). A sensitivity analysis was conducted to explore the differences in the UHI and UDI/UME intensities estimated by the three iterations of the rural domain (i.e. preliminary 50 km buffer, elevation control, elevation and urban control). The finalized buffer, which controlled for elevation and neighboring urbanized areas, was used in all the subsequent UHI and UDI/UME calculations outside of the initial sensitivity analysis.

Using the methodology described above, the UHI and UDI/UME intensities were calculated for each month in 2010 as well as the annual average. Analysis of Variance (ANOVA) tests were used to explore the influence of seasonality and geography on the UHI and UDI/UME effects. In order to conduct such analysis, the UHI and UDI/UME intensities were grouped by season and the MSAs were assigned to the appropriate Census region (South, West, Midwest and Northeast). In those cases where ANOVA revealed statistically significant differences between seasons or regions, Tukey's Honestly Significant Difference (HSD) test was used to identify the seasons/regions that were different from one another in a post-hoc fashion. Finally, the relationship between the UHI and UDI/UME intensities was analyzed using correlation analysis and scatter plots.

In addition to analyzing the UHI and UDI/UME intensities in 2010, a historical analysis was conducted by calculating the annual average UHI and UDI/UME intensities for each MSA from 1895 to 2012. From the historical database, the rate of change of the UHI and UDI/UME effects was determined using two methodologies. First, an ordinary least squares (OLS) regression line was used to estimate the slope of the historical trend. The second method, which enabled a more accurate comparison with Stone (2007), was slightly more complex and involved computing the mean decadal rate of change (i.e. the annual change in UHI or UDI/UME intensity averaged by decade). To evaluate the influence of geography on the rate of change, the Census regions, ANOVA and Tukey's HSD test were again employed.

3.3 Quantifying Urban Form with Spatial Metrics

LULC data obtained from the US Geological Survey (USGS) Multi-Resolution Land Characteristics Consortium (MRLC) served as the foundation for calculating the spatial metrics. The MRLC maintains the National Land Cover Database (NLCD), which is a series of LULC datasets based primarily on the unsupervised classification of Landsat imagery. The NLCD 2006 has a spatial resolution of 30 meters and an overall accuracy of 78% (Wickham et al. 2013). It includes 20 LULC categories (Figure 3.3), which are based on a classification scheme modified from the Anderson Land Cover Classification System.

Since a large number of MSAs were included in the study, the NLCD 2006 was originally reclassified into an urban/non-urban binary to simplify the calculation and interpretation of the spatial metrics. However, by converting the dataset into a binary the various influences of the four developed land use categories (developed open space, low-intensity development, medium-intensity development and high-intensity development) included in the NLCD were obscured. Therefore, in order to investigate how different degrees of urbanization influence the UHI and UDI/UME effects the spatial metrics were calculated individually for each LULC category.

Developed open space (Class 21) is the least urban of the developed land classes as it includes areas where impervious surfaces account for less than 20% of the total land cover. This class usually consists of single-family homes on large parcels as well as vegetation planted within an urban context for recreation, erosion control and esthetics. Low-intensity development (Class 22) and medium-intensity development (Class 23) include areas with a greater abundance of impervious surfaces, 20 – 49% and 50 – 79% respectively, but both are comprised mainly of single-family housing units on smaller lots. Finally, high-intensity development (Class 24) encompasses those areas where people live or work in large quantities and impervious surfaces account for 80 – 100% of the total land cover (Figure 3.4). In addition to calculating the spatial metrics for the four urban categories (Classes 21 – 24), the remaining 11 LULC classes included in NLCD 2006 were also analyzed. The LULC classes do not sum to 20 because four of the categories only exist in Alaska (e.g. lichens and moss) and one, perennial snow, did not occur within any of the MSAs.

Due to the focus on urban climatic processes, the LULC data were not analyzed for entire MSAs because in some cases the MSA boundary includes large amounts of rural land cover. Overbounding metropolitan counties, those whose administrative boundaries include an urban center but also contain large rural expanses not related to the urban core, are partially responsible for this incongruity between urban land use and MSA demarcation. In order to analyze only urban environments, the LULC data within the UA/UC included in each MSA was extracted (Figure 8). These are the same UA/UC used to obtain the urban temperatures and dew points for the UHI and UDI/UME calculations. Overall, focusing on the LULC data within the UA/UC of each MSA established a much more appropriate landscape extent for examining the relationships between urban morphology and urban climatological phenomena.

The public domain software FRAGSTATS (McGarigal et al. 2012) was used to calculate the individual spatial metrics. Although one specific suite of spatial metrics for analyzing urban environments has not been established, reviewing the relevant literature helped identify some of the most frequently utilized metrics. The more commonly employed spatial metrics that were most relevant from an urban climatology perspective and incorporated into this study included:

area-weighted mean patch fractal dimension (AWMPFD), area-weighted mean shape index (AWMSI), clumpiness index (CLUMPY), contagion index (CONTAG), edge density (ED), largest patch index (LPI), patch density (PD), percentage of like adjacencies (PLADJ) and percentage of landscape (PLAND) (Table 3.1). AWMPFD and AWMSI both provide measures of shape complexity based on modified perimeter-area ratios. AWMPFD values vary from 1 (simple shape) to 2 (complex shape) while AWMSI values increase from 1 as the shape becomes more irregular. ED is another metric commonly used to quantify urban shape complexity, but it is not based on patch perimeter-area ratios. Instead, ED calculates the total length of the urban edge segments, which is then divided by the total landscape area. Within the context of urban landscapes, increasingly irregular and complex shapes generally represent more expansive urban morphologies.

PD and LPI are metrics used to evaluate the fragmentation/aggregation of the urban environment. PD is the number of urban patches divided by the entire landscape area. A larger PD proportion is usually indicative of a more fragmented urban morphology. LPI is of interest when analyzing cities because it quantifies the dominance of the urban core by dividing the area of the largest urban patch, which in most cases would be the Central Business District (CBD) if Class 24 were being analyzed, by the total landscape area. Lower LPI values are typically associated with increased polycentrism and fragmentation of the urban environment.

PLADJ, CLUMPY and CONTAG are also measures of fragmentation/aggregation, but they are fundamentally based on adjacency matrices. PLADJ is calculated by dividing the number of like adjacencies involving urban pixels by the total number of adjacencies involving urban pixels. A higher PLADJ indicates a more contiguous urban landscape. CLUMPY builds on the PLADJ metric by comparing the actual proportion of urban like adjacencies to that expected from a spatially random distribution. The values for CLUMPY vary from -1 (maximally disaggregated) to 1 (maximally aggregated) where 0 represents an essentially random distribution. CONTAG is another aggregation metric but it subsumes both interspersion and dispersion by analyzing the entire landscape, not just the urban pixels. CONTAG values range from 0 to 100 with 100 occurring when the landscape is maximally aggregated.

Although described above via an urban-centric perspective, the same suite of spatial metrics was used to evaluate every LULC category included in each MSA. Since the eight class level metrics were calculated for all 15 LULC classifications, in addition to the one landscape level metric (CONTAG), a total of 121 metrics were derived. If a LULC category was not present within a given MSA, the spatial metrics for that class were assigned a value of zero. Once the spatial metrics were calculated, the potential regional variations in urban morphology were analyzed. The MSAs were assigned to their appropriate Census Region and ANOVA was used to identify if any significant regional differences existed. To better understand how the spatial metrics related to existing measures of urban form, they were compared with the Ewing et al. (2002) Sprawl Index (Ewing et al. 2002). The Sprawl Index was created by aggregating four individual factors that represented density, land use mix, degree of centering and street accessibility (Ewing et al. 2002).

3.4 Evaluating the Relationship between Urban Form and Climatic Variables

Both bivariate and multivariate statistical techniques were used to evaluate the degree to which urban morphology influences UHI and UDI/UME intensities. Pearson's correlation coefficient (r) was calculated to analyze how each of the 121 spatial metrics related to the UHI and UDI/UME effects. These relationships were examined for the annual average UHI and UDI/UME effects in 2010, the monthly UHI and UDI/UME effects in 2010 and a longer-term average of the annual UHI and UDI/UME effects from 2006 to 2010. Comparing the results in 2010 to the longer-term average helped determine if the relationships in 2010 were atypical or fairly consistent with recent history. In addition to analyzing the degree of association between the spatial metrics and the UHI and UDI/UME effects, variables previously hypothesized to influence UHI and UDI/UME intensities, such as city area, population, population density and climatological context, were also evaluated. Finally, bivariate scatter plots were produced for those relationships that were found to be statistically significant ($p < 0.05$) in order to aid the multivariate analysis.

Although the bivariate approach provided useful insights into the relationships between urban morphology and the UHI and UDI/UME effects, multivariate techniques more accurately depict reality by allowing several factors (independent variables) to simultaneously influence a single outcome (dependent variable). Multivariate ordinary least squares (OLS) linear regression was used to untangle how sprawling and dense urban development influence UHI and UDI/UME intensities. In all of the models the UHI and UDI/UME intensities served as the dependent variables. Similar to the bivariate analysis, the models were estimated for the 2010 annual averages, the longer-term annual averages from 2006 to 2010 and the 2010 seasonal averages. The models included various independent variables, which were selected based on a consideration of existing theory, the previous bivariate analysis and the overarching research goals. At least two of the urban spatial metrics (i.e. PLADJ_21, PLADJ_22, PLADJ_23 or PLADJ_24) were included in each model in order to evaluate the different influences of sprawling and dense urban development on the UHI and UDI/UME effects.

The remaining independent variables that were considered for inclusion accounted for potential confounding factors, such as the influence of non-urban land covers, additional components of urban morphology and meteorological conditions, that have previously been theorized to impact UHI and UDI/UME intensities. These variables included city area, population density, aridity and wind speed. City area was calculated by summing the area of the UA/UC included in each MSA. The UHI effect of larger cities, in terms of area, is typically more intense (Imhoff et al. 2010; Zhou et al. 2013) although some research has questioned this relationship (Atkinson 2003). Population density was determined using 2010 US Census data by summing the populations of the UA/UC in a given MSA and dividing that total population by the derived city area variable. Although the direction of the relationship between population density and UHI and UDI/UME intensities is not entirely clear based on previous literature, it is a potential confounding factor that was considered for inclusion in the models.

In terms of meteorological conditions, aridity was included since the climatological context of cities has a major influence in determining their subsequent UHI and UDI/UME intensities (Imhoff et al. 2010). Aridity also served as a geographical proxy since the climatological contexts found across the United States are fairly distinct. Aridity was calculated using the updated PRISM datasets for monthly average precipitation and maximum temperature during 2010, as the older versions were no longer available via the PRISM website. Specifically, the monthly average precipitation and maximum temperatures for each city were derived by averaging the pixel values within the same UA/UC employed during the UHI and UDI/UME estimations. Although fairly simplistic, De Martonne's (1926) aridity index was used (Equation 3).

$$I_{AR} = P/(T+10) \tag{3}$$

In Equation 3, P is precipitation measured in millimeters and T is temperature measured in degrees Celsius. The index approaches zero as the environment becomes more arid. An annual average aridity was also calculated for each city from the individual monthly index values. Finally, the monthly and annual average wind speed (m/s) for each city was calculated using NCEP/NCAR reanalysis data. The reanalysis data was re-sampled to a 0.10 by 0.10 degree grid to ensure that numerous pixels fell within the UA/UC of each MSA, which again served as the averaging domain. Overall, examining the most relevant control variables reduced the likelihood of over-estimating the influence of urban morphology (i.e. the PLADJ_21, PLADJ_22 and PLADJ_24 variables) on the UHI and UDI/UME effects.

Despite the advantages of multivariate techniques, namely the ability to analyze the partial effects of multiple variables while controlling for potential confounding factors, OLS regression models are built on a set of assumptions that must be considered (Hamilton 1992). Although in actual research these assumptions are seldom, if ever, literally met (Hamilton 1992), a series of diagnostics can be used to discern the severity of the violations, help evaluate the overall robustness of the results and determine if any corrective measures should be pursued. Firstly, OLS regression fits the best linear relationship between the dependent and independent variables, which is obviously inappropriate if the functional form is fundamentally non-linear. To determine if the relationships between urban morphology and UHI and UDI/UME intensities were linear, the functional form of the bivariate scatter plots and the added-variable plots created during the regression analysis were examined.

For the estimated parameters to be unbiased all relevant independent variables must be included in the model. Determining if all pertinent variables are included is difficult, due to the infinite number of potential independent variables, and typically relies heavily on theoretical justification. Generally, a certain degree of specification bias is unavoidable in regression analysis since all relevant independent variables cannot be included due to data limitations. To soundly conduct inferential tests on regression model coefficients the error terms must be: homoskedastic (have constant variance across all values of X), uncorrelated with each other (no autocorrelation) and normally distributed. The error terms of all the models were checked for heteroskedasticity (unequal variance across the values of X) using White's Test and normalcy was evaluated using histograms. Finally, regression models are sensitive to influential observations (outliers) and multicollinearity (correlation between the independent variables). Influential observations were tested for using Cook's D and DFBETAS while the presence of multicollinearity was determined by calculating the correlation coefficients of the independent variables as well as their respective variable inflation factors (VIF).

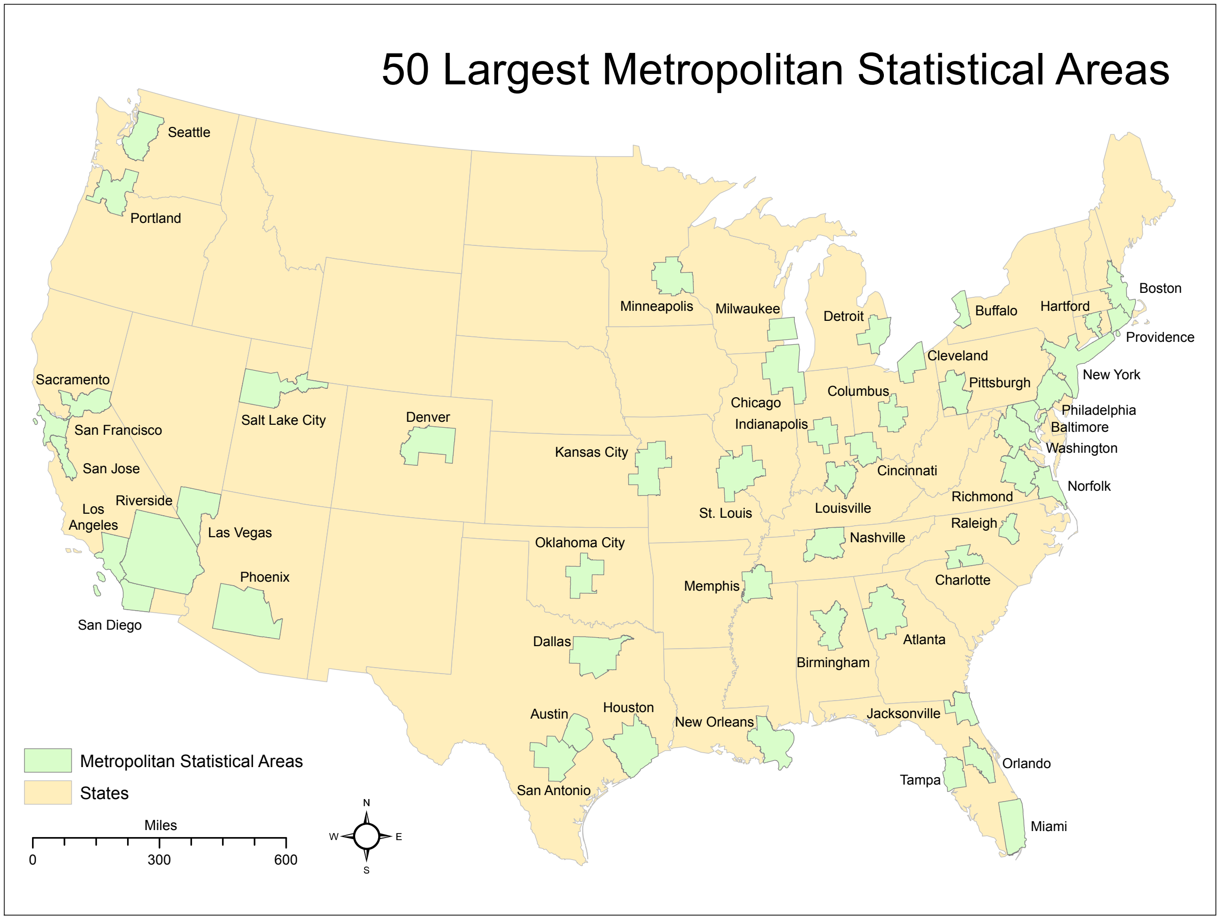

Figure 3.1. Study Area: The Fifty Largest Metropolitan Statistical Areas in Terms of Population

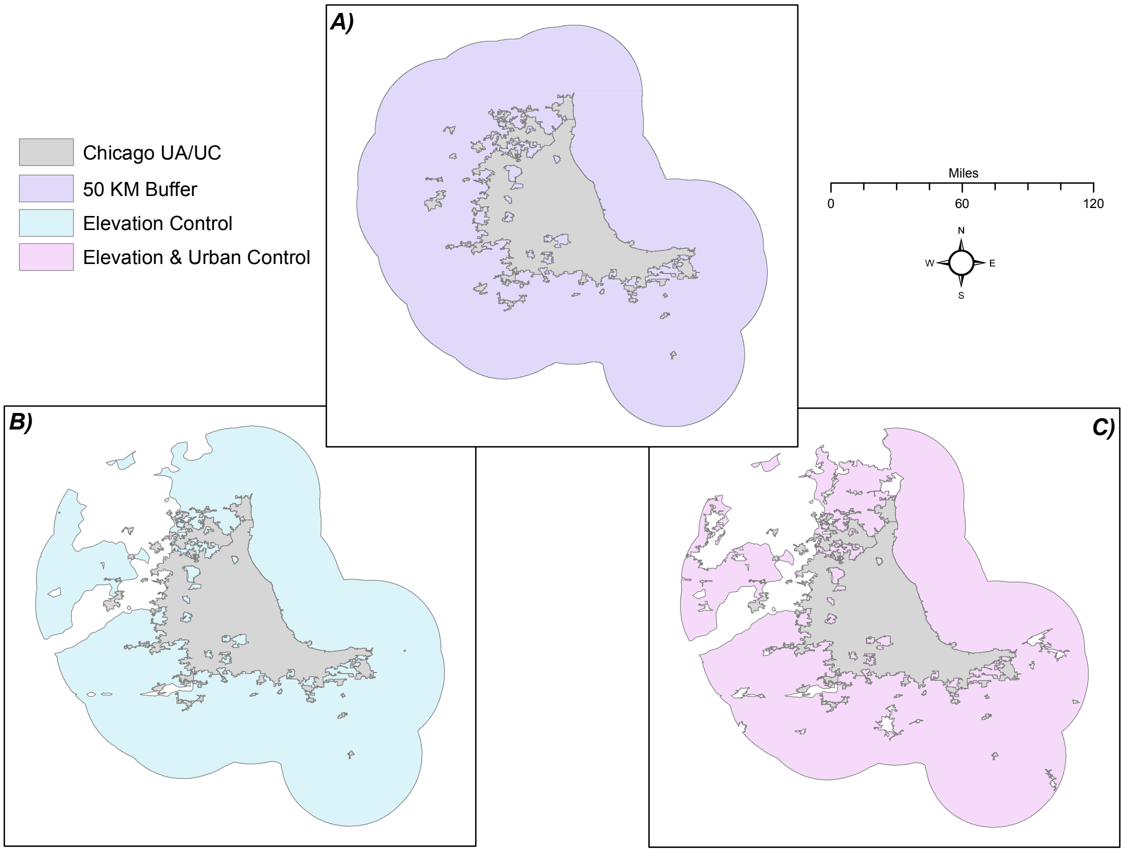

Figure 3.2. Example of the Three Buffer Types for the Chicago MSA: A) 50 km Buffer, B) Elevation Control and C) Elevation and Urban Control

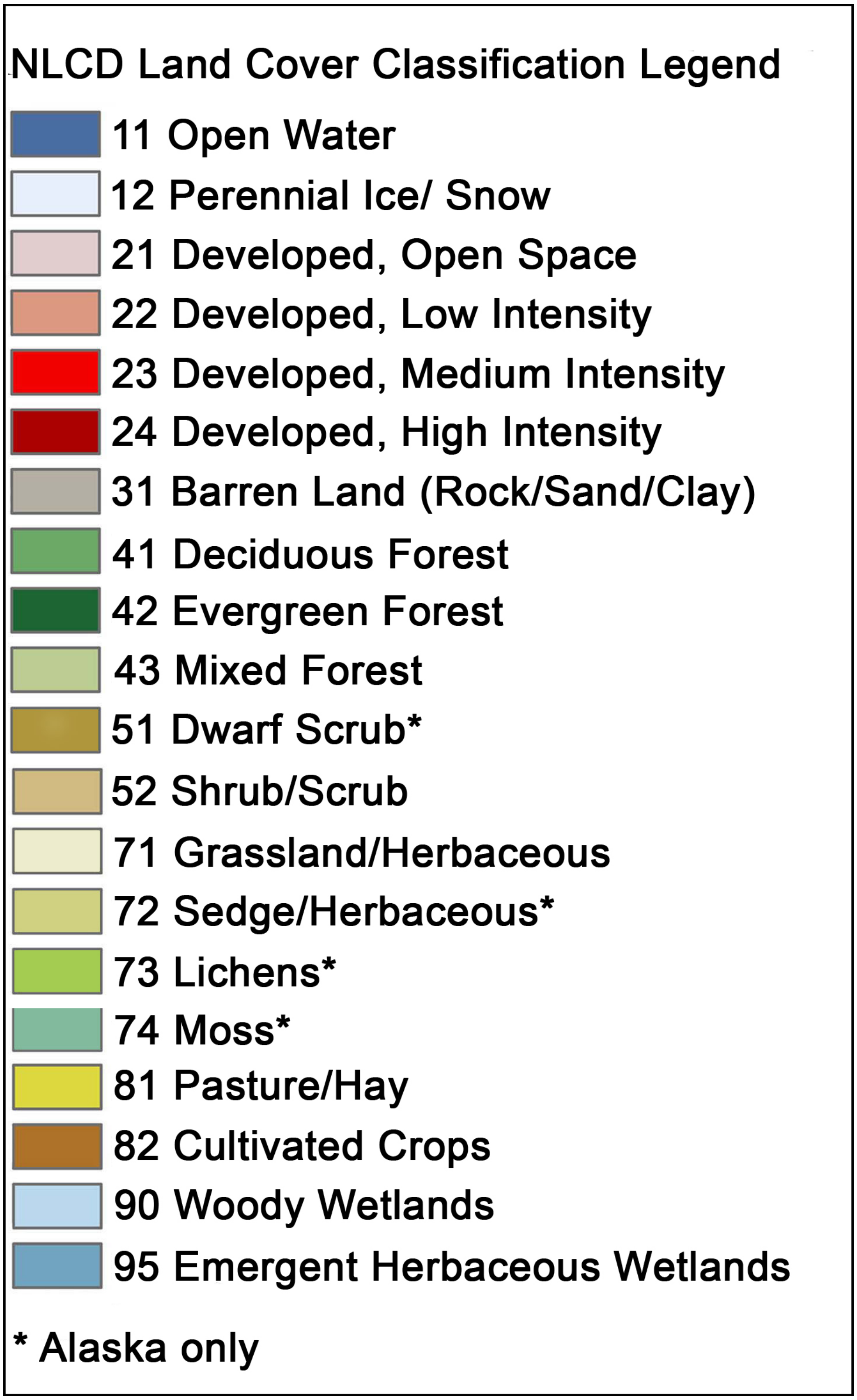

Figure 3.3. Legend for NLCD 2006 Land Cover Classification (MRLC)

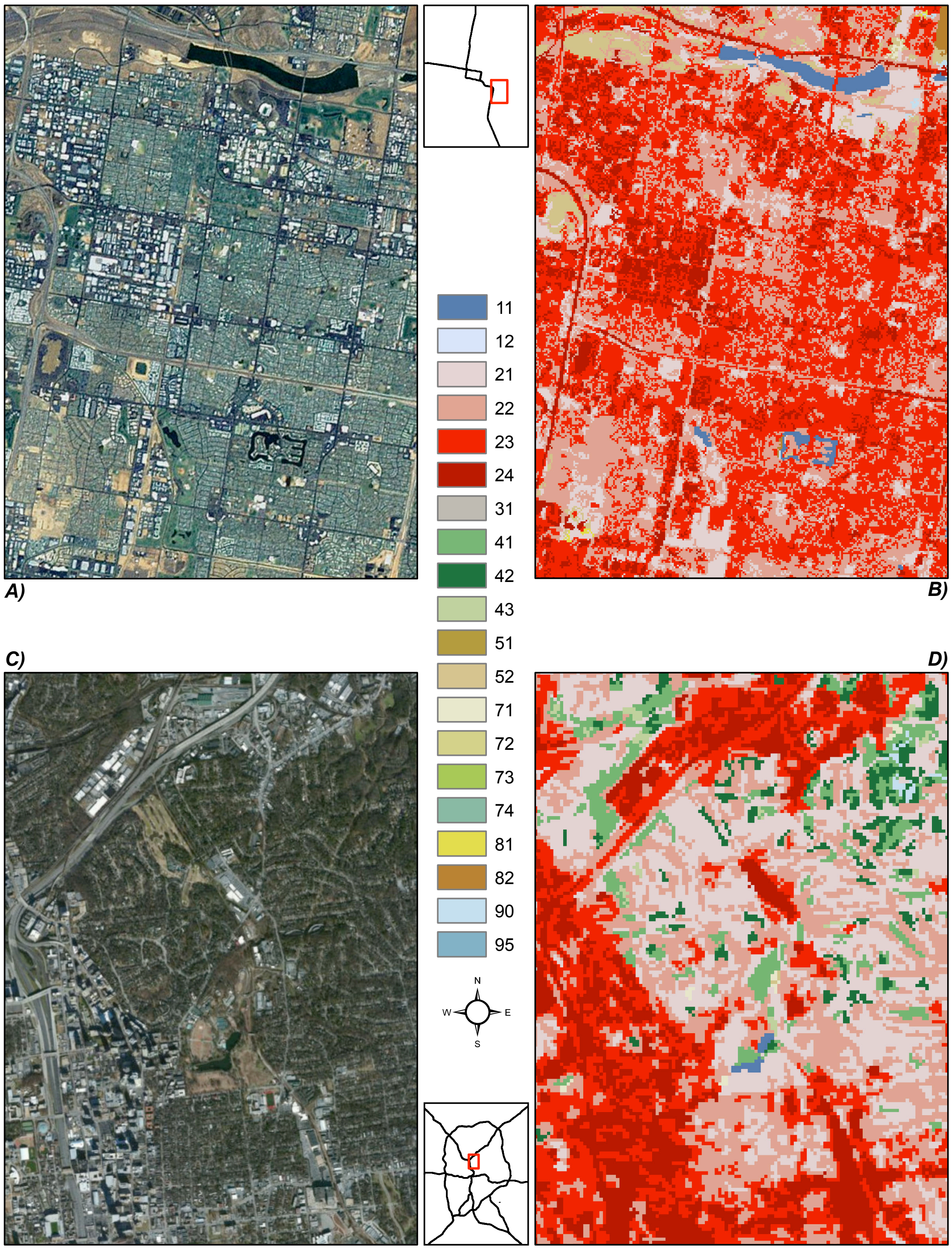

Figure 3.4. Aerial Imagery and Corresponding NLCD 2006 LULC Classifications for Phoenix, Arizona (A & B) and Atlanta, Georgia (C & D)

Table 3.1. Equations and Descriptions of the Spatial Metrics (McGarigal et al. 2012; Makido et al. 2012, Bereitschaft and Debbage 2013a)

Spatial Metric	Equation	Description
Area-Weighted Mean Patch Fractal Dimension (AWMPFD)	$AWMPFD = \sum_{j=1}^{n}\left[\left(\frac{2\ln(0.25p_{ij})}{\ln a_{ij}}\right)\left(\frac{a_{ij}}{\sum_{j=1}^{n} a_{ij}}\right)\right]$	Where p_{ij} is the perimeter of patch ij and a_{ij} is the area of patch ij (i = number of patch types, j = number of patches)
Area-Weighted Mean Shape Index (AWMSI)	$AWMSI = \sum_{j=1}^{n}\left[\left(\frac{0.25p_{ij}}{\sqrt{a_{ij}}}\right)\left(\frac{a_{ij}}{\sum_{j=1}^{n} a_{ij}}\right)\right]$	Where p_{ij} is the perimeter of patch ij and a_{ij} is the area of patch ij (i = number of patch types, j = number of patches)
Clumpiness Index (CLUMPY)	$Given\ G_i = \left(\frac{g_{ii}}{\sum_{k=1}^{m} g_{ik}}\right)$ $CLUMPY = \left[\begin{array}{l} \frac{G_i - P_i}{1 - P_i}\ for\ G_i \geq P_i \\ \frac{G_i - P_i}{1 - P_i}\ for\ G_i < P_i\ \&\ P_i \geq 0.5 \\ \frac{P_i - G_i}{-P_i}\ for\ G_i < P_i\ \&\ P_i < 0.5 \end{array}\right]$	Where g_{ii} is the number of like adjacencies between pixels of patch type i based on the double count method, g_{ik} is the number of adjacencies between pixels of patch types i and k based on the double-count method, and P_i is the proportion of the landscape occupied by patch type i

Contagion Index (CONTAG)	$$CONTAG = \left[1 + \frac{\sum_{i=1}^{m}\sum_{k=1}^{m}\left[(P_i)\left(\frac{g_{ik}}{\sum_{k=1}^{m} g_{ik}} \right) \right] * \left[\ln(P_i)\left(\frac{g_{ik}}{\sum_{k=1}^{m} g_{ik}} \right) \right]}{2\ln(m)} \right] * 100$$	Where P_i is the proportion of the landscape occupied by patch type i, g_{ik} is the number of adjacencies between pixels of patch types i and k based on the double-count method, and m is the number of patch types present in the landscape
Edge Density (ED)	$$ED = \frac{\sum_{k=1}^{m} e_{ik}}{A} * 10{,}000$$	Where e_{ik} is the total edge length (m) of class i in the landscape and A is the total landscape area; the result is multiplied by 10,000 to convert to hectares
Largest Patch Index (LPI)	$$LPI = \frac{\max_{j=1}^{n}(a_{ij})}{A} * 100$$	Where $\max(a_{ij})$ is the area (m^2) of the largest patch of the corresponding class and A is the total landscape area (m^2); the result is multiplied by 100 to convert to a percentage

Patch Density (PD)	$$PD = \frac{n_i}{A} * 10{,}000 * 100$$	Where n_i is the number of patches in the landscape of patch type i and A is the total landscape area (m^2)
Percentage of Like Adjacencies (PLADJ)	$$PLADJ = \left(\frac{g_{ii}}{\sum_{k=1}^{m} g_{ik}} \right) * 100$$	Where g_{ii} is the number of like adjacencies between pixels of patch type i and g_{ik} is the number of adjacencies between pixels of patch types i and k
Percentage of Landscape (PLAND)	$$PLAND = \frac{\sum_{j=1}^{n} a_{ij}}{A} * 100$$	Where a_{ij} is the area (m^2) of patch ij and A is the total landscape area (m^2); the result is multiplied by 100 to convert to a percentage

CHAPTER 4

RESULTS

4.1 Urban Heat Island and Urban Dry Island Intensities

4.1.1 Sensitivity Analysis

By comparing the UHI and UDI/UME intensities estimated by the three different rural delineations (Figure 3.2), a simplistic sensitivity analysis was conducted. Table 4.1 shows the variability of the ten most intense UHIs depending upon which rural domain was utilized. When the initial 50 km buffer was used, Denver, Sacramento, San Diego, Portland and Seattle were all included amongst the most intense UHIs. This is likely due to the mountainous terrain located outside these cities, which would dramatically decrease the average rural temperatures and subsequently inflate the UHI estimates.

When the rural domain was constricted to include only those areas within +/- 50 meters of the average urban elevation, all five of these cities were no longer in the top ten. Overall, the UHI intensities declined for 35 of the 50 MSAs when controlling for elevation, as areas of higher altitude and colder air were generally excluded from the rural temperature averages. The differences between accounting for elevation and controlling both elevation as well as neighboring urban areas were less substantial since 16 of the 50 MSAs had no change in their UHI intensities. This was largely because the elevation threshold already eliminated a sizeable portion of the proximate urban areas. However, 20 MSAs, including half of the top ten (Table 4.1), had slight increases in their UHI intensities as any remaining warmer urban areas were eliminated from the rural temperature averages.

While the analysis above revealed the direction of the UHI intensity changes depending upon the various rural delineations, the standard deviation of the three UHI intensities was calculated for each MSA to capture the overall variability. Not surprisingly, Sacramento, San Diego and Denver had the largest standard deviations, indicating that their UHI intensities varied the most between the three different rural domains (Table 4.2). The extreme topographic relief surrounding these cities likely contributed to the high variability of their UHI intensities. At the bottom of Table 4.2 are those cities with smaller standard deviations, which suggests that their UHI intensities were very similar regardless of if elevation and neighboring urban areas were controlled. The majority of the cities with little UHI variability were located on the coast (i.e. Virginia Beach), in Florida (i.e. Jacksonville, Miami, Orlando and Tampa) or on the Great Plains (i.e. Oklahoma City and Kansas City). In all three of these settings topographic relief and the presence of neighboring urban areas are minimal, which would reduce any differences between the three rural domains. Overall, smaller standard deviations are indicative of higher levels of confidence since the UHI intensities are less sensitive to the precise nature of how "rural" is defined.

Table 4.3 highlights the variability of the ten most intense UDIs depending upon which rural domain was used (Figure 3.2). When the 50 km buffer was restricted by the elevation threshold, the UDI intensities within the top ten increased dramatically. Overall, the UDI intensities increased for 33 of the 50 MSAs when controlling for elevation. This occurred because areas of higher elevation typically have lower dew points, which when omitted would increase the rural average and ultimately increase UDI intensities. Similar to the UHI sensitivity analysis, the differences between accounting for elevation and controlling both elevation as well as neighboring urban areas were less pronounced, as 19 MSAs recorded no change in their UDI intensities. Again, this is likely because the elevation threshold already eliminated a large portion of the proximate urban areas. The standard deviations of the UDI estimates produced by the three rural criteria revealed a comparable pattern to the UHI sensitivity analysis as well (Table 4.4). Substantial topographic relief surrounded those cities whose UDI intensities varied most dramatically while cities located in areas of mild relief displayed less variability.

In order to test the assumption that minimum temperatures, rather than maximum temperatures, should be utilized when analyzing the canopy UHI effect, the 2010 annual average UHI intensities were calculated using both. As expected, the UHI effect estimated with maximum temperatures was less intense (Figure 4.1). When maximums were used almost half of the MSAs were characterized by UCIs (i.e. intensities less than zero) while only 6 UCIs existed when using minimum temperatures. A two-sample t-test indicated that the differences between the UHI intensities estimated using maximum and minimum temperatures were statistically significantly ($p < 0.01$). Since these results support the theory that the canopy UHI is most intense after sunset (EPA 2008), minimum temperatures were used for all subsequent UHI calculations.

The annual average UHI intensities were also estimated using both the updated and previous version of PRISM to verify that no major differences existed (Figure 4.2). The UHI effect was slightly more intense when the update PRISM data were used. However, a two-sample t-test indicated that the differences in UHI intensity were not statistically significant ($p = 0.12$). Since no meaningful differences were discovered, the previous version of PRISM was used to ensure compatibility with the dew point temperature datasets.

4.1.2 Annual UHI and UDI Rankings in 2010

Table 4.5 displays the rankings of the UHI intensities for all 50 MSAs. The UHI intensities were calculated using annual average minimum temperatures in 2010 and the rural criteria that controlled for elevation as well as neighboring urban areas. Initially, the UHI intensities appear fairly unimpressive, as the urban areas were on average only 0.37 degrees Celsius warmer than their surrounding environments. However, since these are annual average UHI intensities, which incorporate both those nights that are optimally and poorly suited for UHI formation, the magnitudes were never expected to approach the maximum thermal modification documented under ideal conditions of approximately 12 degrees Celsius (Oke 1987). The UHI intensities were comparable to Oke (1997), who found that the annual mean temperatures of large cities were typically between 1 and 3 degrees Celsius warmer than their surroundings.

Salt Lake City had the most intense UHI effect (1.49 ºC), which is likely related to the high prevalence of temperature inversions in that region (Pope et. al 2006). Temperature inversions are associated with more intense UHIs since they typically produce calm, clear and stable conditions that are ideal for UHI formation (Hu et al. 2013). In an analysis of 37 American cities, Gallo et al. (1993) also found that Salt Lake City had the most intense UHI, however, their estimated UHI effect was larger since it was based on a weekly average minimum temperature rather than an annual average and contained less stringent controls for elevation biases. The second most intense UHI occurred in Miami (1.34 ºC). The exceptional Miami UHI effect is potentially attributable to the tall skyscrapers along the coastline creating a wall effect (Wong et al. 2010), which prevents the ocean's cooling influence from penetrating the city. Louisville's significant UHI effect (1.12 ºC) was expected, as its UHI intensity has been the fastest growing in America from 1961 to 2010 according to an updated dataset originally created by Stone

(2007). A lack of tree canopy coverage has been hypothesized as a major cause of the intense UHI in Louisville since it is one of very few American cities with no comprehensive tree ordinance. The negative values at the bottom of Table 4.5 indicate that a city was actually cooler than its surroundings. Riverside and Las Vegas had the strongest UCIs (-1.37 and -0.76 ºC, respectively) likely because they are both surrounded by warm desert landscapes.

The rankings for the 2010 annual average UDI intensities are presented in Table 4.6. They were created using the annual average dew point temperature and the rural criteria that controlled for elevation as well as neighboring urban areas. Dew point temperatures were on average 0.08 degrees Celsius higher within the cities relative to their surrounding natural environments. The average effect was essentially nil because the MSAs were almost evenly split between UDI and UME conditions. Surprisingly, Las Vegas ranked as the most intense UDI. When examined in more detail, the rural area defined for Las Vegas appeared to follow the valley created by the Las Vegas Bay and Colorado River, which may have inflated the rural dew point temperatures. Additionally, barren arid regions were included within the Census UA/UC, due to leapfrog development, which may have decreased the urban dew points. Collectively, these two factors could potentially result in a strong UDI effect.

Those cities at the bottom of Table 4.6, with positive values, are actually characterized by UME conditions. Phoenix, Riverside and Salt Lake City had the most intense UMEs due to the increased amount of moisture found within the cities especially relative to their surrounding arid environments. In particular, the UMEs can largely be attributed to the anthropogenic water vapor sources prevalent in urban environments such as the irrigation of lawns and parks. Although the UHI and UDI rankings presented in Table 4.5 and Table 4.6 are informative, it is important to bear in mind that they simply provide snapshots of two continuously changing phenomena. UHI and UDI intensities vary from year to year as the mesoscale and synoptic climate conditions differ and over longer time scales as urban morphologies transform.

4.1.3 Spatial Analysis of UHI and UDI Intensities in 2010

The intensities of the 2010 annual average UHI effects were mapped to examine their spatial variability. Hotspot analysis, using the Getis-Ord Gi* statistic, was performed to highlight clusters of low and high values. The Getis-Ord Gi* statistic produced higher z-scores for more significant clusters of intense UHIs and lower z-scores for more significant clusters of intense UCIs. The UCIs in Boston, Providence, Las Vegas and Riverside clearly stood out in Figure 4.3. Additionally, the hotspot analysis deemed the Northeast and Southwest UCI clusters significant, as their z-scores were less than -1.96 (Figure 4.3). Since the MSAs with stronger UHI effects were dispersed throughout the country, the clustering was not as significant although a concentration of intense UHIs, anchored by Miami, was identified in Florida.

ANOVA was used to test for UHI intensity differences between the various Census Regions of the United States. The annual average UHI intensities showed no significant ($p = 0.13$) differences between regions, but this was partially due to the relatively small sample size ($N = 50$) (Figure 4.4 A). Significant ($p < 0.01$) differences were discovered when the UHI intensities for every month of the year were analyzed (Figure 4.4 B). In this case, Tukey's HSD test revealed that all the regions were distinguishable from one another at the 95% confidence level except for the South and Midwest. Specifically, cities in the Northeastern region exhibited substantially less intense UHI effects.

The monthly UHI intensities were partitioned by season to analyze how the regional differences varied throughout the year. ANOVA identified significant ($p < 0.05$) differences during each season but the specific regions that were distinguishable from one another varied according to Tukey's HSD test (Figure 4.4 C – F). The regional variability of the UHI effect was most pronounced during the winter, as cities in the Northeast exhibited significantly ($p < 0.05$) weaker UHI intensities than cities in every other region. During the spring, the variation between regions was less noticeable. Northeastern cities were significantly ($p < 0.05$) cooler than cities located in the South but no other differences were statistically discernible. Although the ANOVA analysis revealed significant ($p < 0.05$) variation during the summer, Tukey's HSD test did not identify any differences between the individual regions. It appears that the UHI intensities likely differed during the summer but Tukey's HSD test could not determine with sufficient confidence the particular regions that were distinct from one another. The pattern of regional variability in the fall was very similar to that in the winter, as cities in the Northeast had significantly ($p < 0.05$) weaker UHI intensities than cities in every other region. Overall, it appears that the UHI effect tends to be less intense for Northeastern cities with these regional differences being most pronounced during the fall and winter months.

Figure 4.5 maps the spatial distribution of the annual average UDI intensities. The Northeastern Megalopolis region was generally characterized by an UDI effect while cities in the arid Southwestern portion of the United States, with the exception of Las Vegas, were moister than their surrounding environments. When analyzing the UDI/UME effect, the Getis-Ord Gi* statistic used for the hotspot analysis produced higher z-scores for more significant clusters of intense UMEs and lower z-scores for more significant clusters of intense UDIs. The cluster of UMEs in the Southwest was only marginally significant, as the z-scores were generally not greater than 1.96 (Figure 4.5). In contrast, the hotspot analysis deemed the Northeastern UDI cluster significant, as the z-scores were less than -1.96.

To examine the differences in UDI intensity between Census Regions, ANOVA was performed. The annual average UDI intensities showed no significant ($p = 0.18$) regional variation (Figure 4.6 A), but this was partially due to the small sample size. Significant ($p < 0.05$) differences were discovered when the UDI intensities for every month of the year were analyzed (Figure 4.6 B). In this case, Tukey's HSD test revealed that the UDI intensities of all the regions were distinguishable from one another at the 95% confidence level except for the South and Midwest. In particular, Northeastern cities exhibited more intense UDIs.

The monthly UDI intensities were partitioned by season to analyze how the regional differences varied throughout the year (Figure 4.6 C – F). ANOVA identified significant ($p < 0.05$) differences during each season but the specific regions that were distinguishable from one another varied according to Tukey's HSD test. The regional variations in the UDI effect were most pronounced during the fall, as Northeastern cities had significantly ($p < 0.05$) more intense UDIs than cities in every other region. During the spring and summer, regional variability was less noticeable. For both seasons, Northeastern cities had significantly ($p < 0.05$) more intense UDIs than Western cities but no other differences were statistically discernible. Finally, during the winter, Northeastern cities had significantly ($p < 0.05$) more intense UDIs than Western and Midwestern cities but could not be distinguished from cities in the South. Overall, it appears that the UDI effect tends to be more intense for cities in the Northeast with these regional differences being most pronounced during the fall and winter.

4.1.4 Seasonal Analysis of UHI and UDI Intensities in 2010

A monthly ensemble was created to highlight the seasonality of the UHI effect during 2010 (Figure 4.7). Similar to weather model ensembles, Figure 4.7 helped identify both a general consensus as well as those cases that deviated from the broader trends. Lines located above zero indicate that an UHI existed for a given month while those below zero signify that the city was cooler than its natural surroundings. Throughout 2010, the vast majority of MSAs had UHI intensities between 0 – 1 ºC. Riverside and Las Vegas clearly diverged from the general trend and were extreme cases of UCIs. The Riverside UCI peaked in the summer while the Las Vegas UCI reached its maximum later in October. Salt Lake City stood out as the most intense UHI with peaks in September and January. The January UHI maximum provides support for the theory that the city's UHI intensity is influenced by temperature inversions since they most commonly occur during the winter months (Pope et al. 2006). The Miami UHI effect appeared bi-modal with maximums occurring during the transitional seasons of spring and fall. Conversely, the UHI in Los Angeles was well defined by a summer maximum. Of the strongest UHIs, Louisville had the smallest seasonal variation, as its UHI intensity remained fairly close to 1 ºC throughout the entire year. This absence of seasonality supports the hypothesis that a lack of vegetation is largely responsible for Louisville's intense UHI effect.

ANOVA was used to examine the seasonality of the UHI effect in more detail. When all the MSAs were tested together, no significant seasonal pattern in the UHI intensities was discovered (Figure 4.8 A). It was suspected that the geographic scale of the analysis masked the seasonality of the UHI effect since cities in different climatological contexts may have different seasonal trends. Therefore, the MSAs were partitioned by Census Regions to analyze if the UHI effect displayed any seasonality within the more localized geographies. Although slight differences were discovered, none were statistically significant (Figure 4.8 B – E). The lack of any substantial seasonality, even when analyzing only cities within more homogeneous climate regimes, might be due to the small number of MSAs in each region, especially in Northeast where there were only seven. Nevertheless, it appears that the seasonality of the UHI effect is highly localized to each individual city.

The monthly ensemble for the UDI effect is presented in Figure 4.9. Lines below zero indicate that an UDI existed for a given month while those above zero signify UME conditions. The general consensus was centered on zero since the MSAs were almost evenly split between UMEs and UDIs. Of note was Las Vegas' strong UDI, which reached a maximum in the late summer. Boston and Chicago also had relatively strong UDIs, which peaked in the fall and early summer, respectively. In terms of the UME effect, Riverside and Salt Lake City were obviously quite extreme cases. The seasonal variation of the UME effect in these two cities appeared very similar since both had peaks in the early fall and early summer. An intense UME also occurred in Phoenix but it displayed tremendous seasonality, as it reached a maximum during the winter but transitioned to an UDI in June.

ANOVA was used to examine the seasonality of the UDI effect in more detail. No significant seasonal trend in UDI intensity was discovered when all the regions were tested together (Figure 4.10 A). Again, to ensure that the national scale analysis was not masking any regional seasonality, each Census Region was examined individually. However, no significant seasonal patterns existed even within the more localized geographies (Figure 4.10 B – E). On aggregate the UDI effect actually exhibited even less seasonality than the UHI effect. Overall, it appears that the seasonality of the UDI and UHI effects is very localized and dependent upon the specific conditions within each individual city.

4.1.5 Relationship between the UHI and UDI Effects

Scatter plots and Pearson's correlation coefficient were used to explore the relationships between the UHI effect and UDI/UME effect. The relationships were analyzed for the 2010 annual averages and also for the months of each individual season (Figure 4.11). The annual average effects exhibited a significant ($p < 0.05$) positive correlation ($r = 0.32$), meaning more intense UHIs were associated with stronger UMEs. Significant positive relationships also existed during each season expect for the summer, which had a Pearson's correlation coefficient equal to -0.03 (Figure 4.11 D). However, the UHI and UME relationship during the summer was highly influenced by the extreme Riverside UCI. When Riverside was omitted, a positive relationship ($r = 0.57$) of similar magnitude to the other seasons was observed during the summer as well. Riverside was also excluded from the remaining seasons and the annual average to ensure that it was not excessively biasing those relationships. In each case, the omission of Riverside enhanced the strength of the relationship between the UHI and UME effect but the improvement was marginal for the winter months since Riverside was not an extreme observation during that season.

A positive relationship between the UHI and UME effects was expected since more intense UHIs allow evapotranspiration to continue longer within cities after sunset relative to the surrounding natural environment (Charciarek 2003). Additionally, UMEs can amplify the UHI effect as they enhance downward longwave radiation, although urban-rural differences in latent heat flux moderate this magnification (Holmer and Eliasson 1999). The results, particularly when the influential Riverside case was excluded, demonstrated comparable correlation coefficients to Holmer and Eliasson (1999) ($r = 0.52$). The apparent synergies between UHI and UME intensities pose serious health ramifications, as urban dwellers are exposed to a dangerous combination of higher temperatures and higher atmospheric moisture content that undoubtedly increases heat stress.

4.1.6 Historical Analysis

Since PRISM data is available from 1895 to present, a historical trend analysis of the UHI and UDI effects was conducted using the annual average minimum temperature and annual average dew point temperature datasets from 1895 to 2012. It must be noted that PRISM datasets are not corrected for inhomogeneities over this period, such as station movement and instrumentation change, which can potentially bias the historical record. Despite these possible shortcomings, researchers have conducted decadal climate trend analysis using PRISM but suggest that caution be taken when interpreting the results (Beier et al. 2012). Furthermore, averaging the PRISM grid cell values within the entire urban and non-urban domains should reduce the likelihood of station inhomogeneities significantly altering the historical trends.

From 1895 to 2012, the average UHI intensity of the 50 MSAs has steadily increased at a rate of 0.011 ºC per decade (Figure 4.12). Although the magnitude of this increase may be perceived as slight, it was highly significant ($p \sim 0.00$) and year alone explained over half of the temporal variability in annual average UHI intensity. The year-to-year variation exhibited by the record is potentially due to differing meteorological conditions but the general increasing trend is more likely the product of continued urban expansion. Recently since 2000, the average UHI intensity has increased impressively by roughly 0.2 ºC (Figure 4.12). Although it appears fairly extreme, this rate of change is feasible as Gaffin et al. (2008) documented a maximum UHI intensity inter-annual variability of almost 1 ºC. When only the years 1950 to 2012 were analyzed, the UHI intensity decadal rate of change increased slightly to 0.013 ºC. The magnitude of the decadal change in average UHI intensity was comparable to Hansen et al. (2001) (0.015 ºC) but substantially smaller than that observed by Stone (2007) (0.05 ºC).

Since Stone (2007) used the mean decadal rate of change instead of regression slope coefficients, it was also calculated to ensure that any differences were not due to methodological subtleties. However, the rate of increase estimated using this methodology, 0.015 ºC per decade from 1950 to 2012, was similar to that obtained using regression coefficients. It appears that the differences may be due to Stone's (2007) usage of airport weather stations to represent urban temperatures. Since airports were typically located along the urban fringe at the beginning of the historical period, the UHI intensities would have been fairly minimal but undergone substantial growth as the airports were engulfed by urban sprawl. Finally, some of the differences may simply be due to the slightly different time frames and cities being considered.

The UHI intensity decadal rates of change from 1950 to 2012 for each MSA are reported in Table 4.7. The UHI intensity in Las Vegas displayed the most substantial growth as it increased by 0.35 ºC per decade. However, this enhancement of the UHI effect is more accurately characterized as a diminishing UCI, since Las Vegas was approximately 2 ºC cooler than its surrounding environment during the 1950s and is presently only marginally warmer. There were 19 MSAs that actually displayed a reduction in UHI intensity between 1950 and 2012. The most notable cooling trend occurred in Denver, as its UHI intensity decreased by 0.10 ºC per decade. The majority of this decrease was observed at the end of the 1970s and the beginning of the 1980s.

To determine if any regional patterns existed with regard to UHI intensity changes over time, ANOVA was performed using the Census Regions (Figure 4.13). Both the decadal rates of change from 1895 to 2012 and from 1950 to 2012 were tested. The decadal rates of change from 1950 to 2012 suggested that the UHI intensities for Northeastern cities have actually been decreasing (Figure 4.13 A). A similar cluster of diminishing UHIs in the Northeast was also observed by Stone (2007). However, the ANOVA revealed that the UHI intensity decadal rates of change for each region were not statistically discernible from one another. When the longer-term trends from 1895 to 2012 were analyzed, all the regions displayed increases in UHI intensity but there were still no substantial regional differences (Figure 4.13 B). Overall, since any warming due to greenhouse gas emissions is accounted for by the rural baseline temperature used to estimate the UHI effects, the increases in UHI intensity exhibited by most MSAs suggest that cities are warming at a faster rate than the planet as a whole. The aggregate effect of increasing UHI intensities and broader scale climate change is likely to produce exceedingly warm urban environments in the future.

A historical analysis was also conducted for the UDI effect over the same time periods. There was no clear trend from 1895 to 2012, as the average UDI intensity decadal rate of change essentially equaled zero (Figure 4.14). When the analysis was limited to include only those years since 1950, the decadal rate of change was -0.01 ºC. This indicates that on average the MSAs were becoming slightly drier. However, the trend towards increasingly dry cities was largely due to the dramatic amplification of the UDI effect observed since the late 1990s. This recent volatility in the historical record is likely attributable to a complex combination of changing meteorological conditions, alterations in urban morphology and perhaps station inhomogeneities.

The UDI intensity decadal rates of change from 1950 to 2012 for each MSA are reported in Table 4.8. San Jose displayed a substantial increase in UDI intensity, but similar to the average trend this occurred primarily since the 1990s. In 1999 dew point temperatures were still 1 ºC higher in San Jose relative to its surrounding environment but by 2011 the city was characterized by an UDI. Although most cities became relatively drier over the historical period, Las Vegas actually exhibited a decrease in UDI intensity. Since 1970, when dew point temperatures were 3 ºC lower in Las Vegas relative to its surroundings, the UDI has gradually diminished with dew point temperatures currently only 0.14 ºC lower within the city.

To analyze if any regional variability in the UDI intensity decadal rates of change existed, ANOVA between the Census Regions was performed (Figure 4.15). The tests were conducted for the decadal rates of change calculated from the entire record and from the more current subset since 1950. From 1950 to 2012 (Figure 4.15 A), the cities in every region exhibited a drying trend although this was less pronounced in the Northeast. Over the longer-term record (Figure 4.15B), Midwestern and Northeastern cities have become moister while UDI intensities have increased for those cities in the South and West. Although these very slight differences between regions were observable from Figure 4.15, none were statistically significant.

4.2 Urban Morphology

4.2.1. Spatial Metric Values

In total, 121 spatial metrics were calculated, but the results reported herein focus largely on those metrics involving high-intensity urban development (Class 24). Figures 4.16 and 4.17 display the NLCD 2006 LULC of the cities with the minimum, median and maximum values for each Class 24 metric. Since there were an even number of observations, the median value was represented by the city ranked 24th for each metric. Percentage of landscape (PLAND_24) is simply the area of high-intensity urban development divided by the total city area. Despite its reputation as a vast sprawling metropolis, Los Angeles had the largest portion of high-intensity urban development with a PLAND_24 value over 11% (Figure 4.16 A). Kansas City represented a more typical urban morphology since it was the median value, as almost 6% of its area was characterized by high-intensity urban development. In Raleigh, the relatively small central business district (CBD) and the general lack of high-intensity urban development resulted in a minimal PLAND_24, which was only slightly greater than 1%.

Patch density (PD_24) is the number of high-intensity urban patches divided by the total city area (Figure 4.16 B). San Jose had the largest patch density proportion, 2.4 patches per 100 hectares, indicating that its high-intensity urban development was fairly fragmented. The gridded network created by the sizable office parks, particularly around North San Jose, was partially responsible for the large number of high-intensity urban patches. The median value, 1.6 patches per 100 hectares, occurred in San Francisco. This PD_24 ratio was likely heavily influenced by the row house development in the Sunset and Richmond Districts on either side of Golden Gate Park. Finally, Riverside had the lowest PD_24 value (0.79), but this was potentially due to the small proportion of high-intensity development within the city (1.5%).

The largest patch index (LPI_24) quantifies the dominance of the urban core by dividing the area of the largest high-intensity urban patch by the total city area (Figure 4.16 C). Las Vegas had the largest LPI_24, as the patch of high-intensity urban development corresponding to Las Vegas Boulevard and McCarran International Airport made up over 4% of the city's total area. Of course, the large LPI_24 was influenced by the relatively small size of Las Vegas. The median value was substantially smaller than the Las Vegas maximum, as the Milwaukee CBD encompassed only 0.6% of the city's total area. Milwaukee's LPI_24 would have likely been larger had the CBD not been partitioned by the Kinnickinnic and Milwaukee Rivers. The smallest LPI_24 occurred in Orlando since its urban core was responsible for only 0.04% of the city's total area. As made evident by Figure 4.16 C, the extremely low LPI_24 is reflective of Orlando's sprawling urban morphology and polycentrism.

The cities with the minimum, median and maximum values for edge density (ED_24) were Raleigh, Buffalo and Las Vegas, respectively. Since the majority of these cities were mapped in Figure 4.16, they were not included again in Figure 4.17. Las Vegas had the largest ED_24, 37 meters of high-intensity urban development edge per hectare, which is likely reflective of the linearity of the strip development along Las Vegas Boulevard as well as the relatively small area of the city. The median value occurred in Buffalo where there was roughly 21 meters of high-intensity urban edge per hectare. Because of the small proportion of highly developed land use in Raleigh, the ED_24 value was minimal with only 6 meters of high-intensity urban edge per hectare.

The shape index (AWMSI_24) and fractal dimension (AWMPFD_24) metrics shared the same cities with regard to their minimum, median and maximum values. This similarity was expected since both metrics quantify shape complexity using modified perimeter-area ratios. Los Angeles had the largest AWMSI_24 value (25) and AWMPFD_24 value (1.30), which suggests that its high-intensity urban development was amongst the most complexly shaped (Figure 4.17 A). St. Louis was the median value for each metric (AWMSI_24 = 5 and AWMPFD_24 = 1.19), meaning its urban morphology was fairly typical in terms of shape complexity. Raleigh exhibited substantially less complexity (AWMSI_24 = 2 and AWMPFD_24 = 1.12), but this was largely due to the lack of high-intensity urban development within the city.

Percentage of like adjacencies (PLADJ_24) evaluates the spatial contiguity of high-intensity urban development (Figure 4.17 B). Seattle had the largest PLADJ_24, with almost 80% of the total adjacencies for high-intensity urban development being like. Seattle's high PLADJ_24 can largely be attributed to the contiguous pocket of intense development that runs from the CBD southward to King County International Airport. San Antonio had a much more typical urban morphology, with approximately three quarters of all high-intensity urban development adjacencies being like. The PLADJ_24 median value seemed to capture a fairly stereotypical urban morphology for an American city, which is characterized by a single CBD and several auxiliary centers of contiguous high-intensity urban development encircling the city along its beltway. Finally, Phoenix had the smallest proportion of like adjacencies for high-intensity urban development with a PLADJ_24 value of 57%. This is indicative of Phoenix's poorly defined urban core and general sprawling morphology. The results for the clumpiness index (CLUMPY_24) were very similar to PLADJ_24 since Seattle was the maximum value (0.78) and Phoenix was the minimum (0.56). The only discrepancy was that San Diego replaced San Antonio as the median (0.72) value. However, there is little substantive difference between the two metrics, as CLUMPY simply compares the observed proportion of like adjacencies to that expected from a spatially random distribution.

Figure 4.17 C is one example of a metric calculated for a different urban intensity level. In this case, the minimum, median and maximum values for the PLADJ of developed open space (Class 21) are presented. Accordingly, the lightest shade of red in Figure 4.17 C is the focal point. PLADJ_21 was highest in Indianapolis where almost three quarters of all adjacencies for developed open space were like. The large lot single family housing Northeast of the city proximate to Sylvan Ridge and Steinmeier Estates was partially responsible for the high contiguity of developed open space. Birmingham represented a more typical city, with 69% of all adjacencies for developed open space being like. The moderate value can be attributed to the occasional pockets of contiguous developed open space, particularly just north of Birmingham-Shuttlesworth International Airport. Finally, in Boston developed open space was fairly discontinuous, as only 60% of all adjacencies were like.

4.2.2. Spatial Analysis of Urban Morphology

To determine if regional differences in urban morphology existed, ANOVA between the Census Regions was performed. The analysis focused largely on high-intensity urban development (Class 24), since it best captures the urban core. Western cities had the largest relative quantity of high-intensity urban development (PLAND_24), as it typically occupied 8% of their total areas. Amongst Western cities, there was considerable variability because of the drastically different urban morphologies included in the Western Census Region (i.e. Seattle vs. Los Angeles). Relative to the West, the proportion of high-intensity urban development in Southern cities was significantly ($p < 0.01$) smaller and equaled approximately 4% (Figure 4.18 A). The lack of intense urban development in Southern cities is indicative of their low-density, sprawling urban morphologies.

Patch Density (PD_24) also exhibited significant ($p < 0.01$) differences between Southern and Western Cities (Figure 4.18 B). In the West, there were almost 2 patches of intense urban development per 100 hectares while this ratio was below 1.5 in the South. Southern cities also had a significantly ($p < 0.05$) smaller patch density than Midwestern cities. Since the PD_24 metric considers only high-intensity urban development, the small values in the South were likely due to the limited amount of intense urban development especially relative to the fairly large city sizes.

The dominance of the largest high-intensity urban patch, as evaluated by the largest patch index (LPI_24), displayed significant geographical variability (Figure 4.18 C). The largest intensely developed urban patch typically comprised over one percent of the total area in Western cities. This proportion decreased significantly ($p < 0.01$) in Southern cities, as it equaled approximately 0.5%. The smaller largest patch index observed in the South was due to the lack of well-defined urban cores and polycentric nature of many southern cities, such as Orlando.

The spatial variability of edge density (ED_24) mirrored the trends observed for the aforementioned metrics. Western cities had over 25 meters of high-intensity urban edge per hectare while Southern cities had approximately 15, which was significantly smaller ($p < 0.05$) (Figure 4.18 D). The lack of substantial quantities of high-intensity urban development in Southern cities, especially relative to their sizes, appears to have influenced the edge density metric in a similar manner to the patch density metric.

The shape index (AWMSI_24) did not exhibit any significant spatial variability. The F-Value was fairly small ($F = 2.5$), which means none of the regions were statistically discernable from one another ($p = 0.07$). Although substantively very similar, fractal dimension (AWMPFD_24) did exhibit significant regional differences partially because its standardization process produces a bounded metric with values between 1 and 2 (Figure 4.18 E). High-intensity urban development was most complexly shaped in Western and Northeastern cities, as both regions had fractal dimensions greater than 1.20. Southern cities were characterized by more simply shaped urban cores and were statistically distinguishable from Western cities ($p < 0.05$) but not Northeastern cities ($p > 0.05$).

The spatial contiguity of high-intensity urban development did not vary by Census Region. This held true regardless of if the clumpiness index (CLUMPY_24) or percentage of like adjacencies (PLADJ_24) was used to operationalize contiguity. However, there was substantial geographical variability in the contiguity of developed open space (PLADJ_21), as it was significantly ($p < 0.05$) more contiguous in Southern cities than Northeastern cities (Figure 4.18 F). Overall, the urban morphologies of Southern and Western cities exhibited the most substantial differences. In the West, urban cores were more well-defined and dominant with higher levels of shape complexity while in the South they were generally more polycentric and simply shaped.

4.2.3 Comparison of Spatial Metrics and Sprawl Index

The spatial metrics were compared with the Sprawl Index created by Ewing et al. (2003) to better understand how they related to existing measures of urban form. Correlations were calculated between each of the high-intensity urban development (Class 24) metrics and the Sprawl Index. Charlotte, Louisville, Nashville and Richmond were omitted from the analysis since the Ewing et al. (2003) Sprawl Index was not calculated for these four cities. It is important to note that smaller Sprawl Index values are actually indicative of more sprawling urban morphologies.

A vast majority of the spatial metrics had significant correlations with the Ewing et al. (2003) Sprawl Index. The relative abundance of high-intensity urban development (PLAND_24) had a moderately strong positive relationship ($r = 0.46$) with the Sprawl Index, which indicates that greater quantities of intense urban land use were typically associated with less sprawl (Figure 4.19 A). A moderately strong positive correlation ($r = 0.42$) was also observed between high-intensity urban development patch density (PD_24) and the Sprawl Index, suggesting that cities with a greater number of high-intensity urban patches relative to their size were generally less expansive (Figure 4.19 B). Similarly, larger quantities of high-intensity urban edge (ED_24) were correlated with less sprawling urban morphologies ($r = 0.48$) (Figure 4.19 D). Although larger patch density and edge density ratios are typically associated with more fragmented and expansive urban landscapes when analyzing all urban LULC classes collectively (Bereitschaft and Debbage 2013b), the opposite is true in this case since the metrics only considered high-intensity urban development (Class 24).

The dominance of the largest high-intensity urban patch within a city (LPI_24) had a significant but slightly weaker relationship (r = 0.36) with the Sprawl Index, as more sprawling cities typically had less dominant urban cores (Figure 4.19 C). In terms of shape complexity, both AWMSI_24 and AWMPFD_24 had strong positive relationships with the Sprawl Index, as their correlation coefficients equaled 0.43 and 0.56, respectively (Figure 4.19 E). This suggests that more complexly shaped high-intensity urban development was indicative of less sprawling morphologies. The positive relationship was potentially observed because dominant urban cores typically undergo growth and expansion, which results in more complex urban shapes.

The spatial contiguity of high-intensity urban development also exhibited a positive relationship with the Sprawl Index. Although CLUMPY_24 was fairly weakly correlated (r = 0.27), PLADJ_24 displayed a significant association with sprawl (r = 0.33). This implies that higher levels of spatial contiguity, with regard to high-intensity urban development, are generally indicative of more compact growth. Contrastingly, there was no significant relationship between the contiguity of developed open space (PLADJ_21) and the Sprawl Index, which indicates that PLADJ_21 evaluated a unique aspect of urban form.

4.3 Urban Form and its Climatic Ramifications

4.3.1 Bivariate Analysis - Control Variables

When analyzing the relationships between UHI/UDI intensities and urban morphology, it is useful to first consider potential confounding factors such as city size, population and the influence of weather. Figure 4.20 displays the relationships between the 2010 annual average UHI intensities and six variables that have been hypothesized to influence the UHI effect. Firstly, there was not a strong correlation between UHI intensity and city area (Figure 4.20 A), although numerous studies have suggested such a relationship exists (Imhoff et al. 2010; Zhou et al. 2013). This result lends support to Ackerman's (2001) hypothesis that city size has a minimal influence on UHI intensity. There was also no significant relationship between the water area within a city and UHI intensity (Figure 4.20 B). The percent of a city's total area that was water, though not pictured in Figure 4.20, also failed to significantly influence the UHI effect.

Although well documented by Oke (1973), there was a very poor correlation between UHI intensity and population size (Figure 4.20 C). Logarithmic transformations of the population variable were performed but they did not substantially improve the correlations. It appears that the relationship between population size and UHI intensity deteriorates when analyzing exclusively very large cities, since this study only considered the fifty largest MSAs in terms of population. Additionally, there was a very weak correlation between UHI intensity and population density (Figure 4.20 D). This casts doubt on the hypothesis posited by Streutker (2003) that population density, rather than total population, is influential in governing the UHI effect.

Even though climatological factors such as wind speed and aridity are known to influence UHI intensities, the relationships were weak when analyzed on an annual time frame (Figure 4.21 E – F). However, when the monthly UHI intensities were compared to the corresponding monthly wind speed and aridity values significant correlations were discovered for certain cities. Figure 4.20 illustrates how the seasonality of the UHI effect appeared to be heavily influenced by wind speed in Boston and Providence and aridity in Riverside. Boston and Providence exhibited wintertime peaks in UCI intensity, which corresponded to the periods of highest wind speed (Figure 4.21 A – D). Contrastingly, the Riverside UHI effect was modulated by aridity, with the summertime UCI peak occurring during a phase of extremely arid conditions (Figure 4.21 E – F).

A similar process was conducted to analyze if any significant relationships existed between UDI/UME intensities and the same set of control variables. Fairly weak negative correlations were observed for both city area ($r = -0.21$) and water area ($r – 0.22$) (Figure 4.21 A – B). Total city population and population density also appeared to have minimal influence on UDI intensities (Figure 4.21 C – D). At least on an annual time frame, wind speed was not significantly associated with the UDI effect either (Figure 4.21 F). Interestingly, there was a marginally significant ($p = 0.06$) relationship between aridity and the UME effect, with UME intensities generally increasing as the environment became more arid (Figure 4.21 E). Overall, it seems that differences in city area, the presence of water, wind speed, population and population density do not explain the variability in the annual average UHI or UDI/UME intensities amongst very large American cities.

Boston, Providence and Riverside were used as examples to analyze the potential relationships between the monthly UDI/UME intensities and the corresponding monthly values for wind speed and aridity. Relative to the influence of wind speed on Boston's UHI effect, the correlation between wind speed and its UDI intensity was substantially weaker and not significant ($p = 0.21$) (Figure 4.23 A – B). In Providence, the relationship between wind speed and UDI intensity ($r = -0.83$) was even more pronounced than that observed for the city's UHI effect, with higher wind speeds generally associated with more intense UDIs (Figure 4.23 C – D). Finally, aridity did not appear to influence the seasonality of the UDI effect in Riverside (Figure 4.23 E – F), but this weak relationship was at least partially due to the simplicity of the

De Martonne Index (1926) since it cannot reveal subtle variations in aridity when no precipitation occurred (Equation 3).

4.3.2 Bivariate Analysis – Urban Spatial Metrics

Of the spatial metrics calculated for the urban classes (21 – 24), the percentage of like adjacencies (PLADJ) had the strongest correlations with UHI and UDI/UME intensities. It is worth noting that the amount of urban land cover, across all four intensity levels, was not as strongly correlated with either UHI or UDI/UME intensities. This suggests that the spatial configuration of urban development, not merely its quantity, is of importance. Figure 4.24 displays the relationships between the PLADJ for the four urban classes and the annual average UHI intensity in 2010. The PLADJ for developed open space (21), low-intensity development (22) and high-intensity development (24) all had significant positive correlations with UHI intensity. This suggests that increasing the spatial contiguity of urban development across a wide spectrum of intensity levels enhances the UHI effect. Finding that more contiguous urban development, regardless of intensity level, magnifies the UHI effect potentially clarifies how studies have suggested that both sprawling (Stone 2012) and high-density (Coutts et al. 2007) urban development can amplify the UHI effect. It appears that the spatial contiguity of urban development, rather than its density or intensity, is a critical factor influencing the UHI effect amongst large US cities. In other words, sprawling and dense urban development patterns both have the propensity to increase UHI intensities if they are highly contiguous.

The correlations between the spatial contiguity of urban development and UHI intensity varied throughout the year due to the seasonality of the UHI effect. In the bottom portion of Figure 4.25, the bar lengths correspond to Pearson's correlation coefficient between the monthly UHI intensities in 2010 and the PLADJ for the four urban classes. Some very clear seasonal trends were apparent, as the PLADJ for high-intensity urban development (24) was most strongly correlated with UHI intensity during the summer months of June, July and August. Contrastingly, the contiguity of developed open space (21) and low-intensity development (22) displayed stronger relationships with UHI intensity during the late fall and winter. The top portion of Figure 4.25 graphs the correlation coefficients between the urban spatial metrics and the annual average UHI intensity in 2010 as well as the longer-term annual average estimated from 2006 to 2010. The differences in Pearson's r between the 2010 annual average and the longer-term average were minimal, suggesting that the relationships between the spatial contiguity of urban development and UHI intensity observed in 2010 were not abnormal and fairly consistent with previous years.

In terms of UDI/UME intensities, PLADJ was still the most influential metric for the urban land use classes. The PLADJ for developed open space (21) had a significant ($p < 0.05$) positive relationship with the UDI effect (Figure 4.26 A), meaning more contiguous developed open space increased UME intensities. This is likely due to the large quantities of vegetation, which serve as potential water vapor sources, included in the developed open space LULC classification. For example, in the Southeast developed open space consists predominately of large-lot single-family housing units while in the Southwest it is comprised mainly of urban parks (Figure 3.4). The spatial contiguity of low-intensity (22) and medium-intensity (23) urban development displayed no significant relationships with UDI intensity (Figure 4.26 B – C). For high-intensity urban development, PLADJ had a negative correlation with the UDI effect. This suggests that more contiguous high-intensity urban development was generally associated with relatively drier urban environments (Figure 4.26 D). Since impervious surfaces make up between

80 and 100 percent of the land cover in highly developed areas, the lack of vegetation and water vapor sources was partially responsible for the observed negative relationship.

The strength of the relationships between the spatial contiguity of urban development and UDI intensity varied throughout the year due to the seasonality of the UDI effect. In the bottom portion of Figure 4.27, the bar lengths depict Pearson's correlation coefficient between the monthly UDI intensities in 2010 and the PLADJ for the four urban classes. Seasonal trends were made apparent, as the PLADJ for high-intensity urban development (24) was most strongly correlated with the UDI effect during the winter months. The relationships between UDI intensity and the spatial contiguity of low-intensity (22) as well as medium-intensity (23) urban development were weak and statistically insignificant for all months. With the exceptions of May and June, the contiguity of developed open space (21) displayed a fairly stable relationship with UDI intensity throughout 2010. The top portion of Figure 4.27 graphs the correlation coefficients between the urban spatial metrics and the annual average UDI intensity in 2010 as well as the longer-term annual average estimated from 2006 to 2010. The differences in Pearson's r between the 2010 annual average and the longer-term average were minor, indicating that the relationships between the spatial contiguity of urban development and UDI intensity observed in 2010 were not abnormal and fairly consistent with recent history.

4.3.3 Multivariate Analysis – UHI

In total, seven multivariate regression models were estimated to explore the relationships between UHI intensity and urban morphology. In each model the dependent variable was either the seasonal, annual or long-term average UHI intensity. The independent variables were held constant across all the models and included: the spatial contiguity of low-intensity urban development (PLADJ_22), the spatial contiguity of high-intensity development (PLADJ_24), the percentage of barren land (PLAND_31), the shape complexity of deciduous forest (AWMPFD_41), the percentage of shrub land (PLAND_52) and the annual average aridity in 2010 (Aridity). In order to better meet the assumptions of multivariate regression modeling, five cities were omitted from the UHI analysis because they were characterized by extreme values that were overly influential. Firstly, Miami and Tampa were omitted because they did not contain any deciduous forest, which meant their respective values for AWMPFD_41 were assigned to zero and therefore fairly extreme. Secondly, Las Vegas, Phoenix and Riverside were omitted because the lack of other arid cities within the sample made them exceedingly influential, particularly during the summer.

However, for the sake of clarity and to provide a point of reference, Model 1 was estimated without omitting any cities and with the annual average UHI intensity in 2010 as the dependent variable. The model performed fairly well, as it explained almost 45% of the variability in UHI intensity (Table 4.9). Relative to the R-Squared value, the adjusted R-Squared did not decrease substantially, which suggests that the model was not overly complex. The partial slope coefficients indicated that the spatial contiguity of high-intensity urban development (PLADJ_24) did have a significant ($p < 0.05$) relationship with UHI intensity while the contiguity of low-intensity development (PLADJ_22) did not. The other variables included in the model accounted for the influence of non-urban land covers and climate type on the annual average UHI intensity. Although many of these relationships were significant, they were heavily influenced by the cities that were omitted from the remaining models. Model 1 also suffered from heteroskedasticity, which can partially be attributed to the difficulty of predicting the extreme values.

The remaining regression models were calculated while excluding the five cities mentioned earlier, which provided much more robust estimates as indicated by the model diagnostics. Highly influential observations were not present, as Cook's Distance values never exceeded 0.32 for Models 2 – 7 (Cook's Distance values greater than 1 are considered to be highly influential). Multicollinearity was also minimal in Models 2 – 7 since the VIFs were less than 1.6 (VIFs greater than 4 are typically indicative of problematic levels of multicollinearity). Finally, heteroskedasticity was negligible as the p-values for White's Test were never below 0.07 (p-values less 0.05 would result in a rejection of the null hypothesis of homoskedasticity).

Model 2 shared the same specification as Model 1 except the influential cities were excluded (Table 4.10). Overall, the model performed well as it explained almost half of the variability in annual average UHI intensities. There was little drop off in the adjusted R-Squared value, which suggests that the model was not overly complex. The partial slope coefficients indicated that the spatial contiguity of high-intensity urban development (PLADJ_24) had a significant ($p < 0.05$) relationship with UHI intensity. Specifically, a ten percentage point increase in the spatial contiguity of high-intensity urban development, the equivalent of shifting from Riverside (PLADJ_24 = 64%) to San Antonio (PLADJ_24 = 74%), was predicted to enhance a city's UHI intensity by 0.4 degrees Celsius. This is quite a substantial amplification, especially when considering that the original magnitudes of the annual average UHI effects were fairly modest. The partial slope coefficient for the spatial contiguity of low-intensity urban development (PLADJ_22) was also significant, as a ten percentage point increase was predicted to enhance a city's UHI intensity by 0.3 degrees Celsius. Therefore, as suggested by the bivariate analysis, both low and high-intensity patterns of urban development can amplify the UHI effect if they are highly contiguous.

The remaining variables included in Model 2 accounted for the influence of non-urban land covers and aridity on the annual average UHI intensity. The partial slope coefficient for the proportion of barren land (PLAND_31) was significant, with increased quantities of barren land predicted to increase the UHI intensity. The direction of this relationship was opposite to that observed in Model 1, because in the original model the relationship was heavily influenced by the arid cities, particularly Las Vegas. It appears that the thermal properties of barren land relative to urban surfaces and their natural surroundings provide a cooling effect for cities in arid environments but a warming effect for cities in non-arid climates. The partial slope coefficient for the shape complexity of deciduous forest (AWMPFD_41) was also significant, with increasingly complex forest shapes predicted to enhance UHI intensities. Again, the direction of this relationship was opposite to that in Model 1, but the positive relationship observed in the original model was largely spurious since it was the product of Miami and Tampa being assigned zeros for AWMPFD_41. Since increased deciduous forest shape complexity is likely due to the fragmentation caused by urban expansion, it is logical that more complexly shaped forests were indicative of more intense UHIs. Unlike barren land and forest shape complexity, the presence of shrub land (PLAND_52) actually had a mitigating effect on UHI intensities, albeit insignificant ($p > 0.10$). Finally with regard to climatological context, those cities located in more arid environments were predicted to have stronger UHIs.

To ensure that the relationships between urban form and UHI intensity were not anomalous to 2010, Model 3 was estimated with the longer-term annual average UHI intensity from 2006 to 2010 as the dependent variable (Table 4.11). The similarities between Model 3 and Model 2 suggest that the relationships were temporally stable. Model 3 explained roughly half of the variability in the longer-term UHI intensities. The partial slope coefficient for the spatial contiguity of high-intensity urban development (PLADJ_24) was still significant and had a slightly larger magnitude than that observed in Model 2 (0.043 versus 0.039). Contrastingly, the partial slope coefficient for the spatial contiguity of low-intensity urban development (PLADJ_21) was only marginally significant ($p = 0.05$) and of slightly reduced magnitude (0.024 versus 0.028). The remaining variables, which were included to evaluate the influence of aridity and non-urban land covers on the UHI effect, all had very similar partial effects to those observed in Model 2.

The final four regression models (Models 4 – 7) were estimated to analyze how the relationships between urban morphology and UHI intensity varied by season. The dependent variable in Model 4 was the winter UHI intensity in 2010, which was the average of the December, January and February UHI effects. The predictive power of Model 4 was comparable to the aforementioned models as its R-Squared value was 0.47 (Table 4.12). The spatial contiguity of high-intensity urban development (PLADJ_24) was slightly less influential in governing UHI intensities during the winter relative to the annual average. However, the partial slope coefficient for the spatial contiguity of low-intensity urban development (PLADJ_22) was highly significant ($p = 0.004$), as a ten percentage point increase was predicted to enhance the winter UHI effect by 0.4 degrees Celsius.

The dependent variable in Model 5 was the spring UHI effect in 2010, obtained by averaging the March, April and May UHI intensities. It was the weakest of all the UHI models since it explained roughly one third of the variability in UHI intensity (Table 4.13). The spatial contiguity of high-intensity urban development (PLADJ_24) had only a marginally significant ($p = 0.09$) partial effect on UHI intensity. However, the magnitude of the partial slope coefficient was still relevant, as a ten percentage point increase was predicted to enhance the UHI effect by

0.3 degrees Celsius. At the opposite end of the urban intensity spectrum, the influence of low-intensity urban development on the spring UHI effect was not significant ($p = 0.39$). The partial effects of aridity and deciduous forest shape complexity were comparable to those observed in the previous models with more arid climate regimes and increasingly complex forest shapes predicted to enhance the UHI effect.

Model 6 evaluated the relationships between urban form and the summer UHI effect, the average of the June, July and August UHI intensities. The model performed fairly well as it explained almost half of the variability in the summer UHI effect (Table 4.14). The partial slope coefficient for the spatial contiguity of high-intensity urban development (PLADJ_24) was significant, as a ten percentage point increase was predicted to enhance the UHI effect by 0.4 degrees Celsius. However, if all the cities were included in the model, a ten percentage point increase would yield a magnification of 0.7 degrees Celsius. The increased magnitude of the relationship when no observations were excluded was largely attributable to the influential arid cities, as Riverside, Las Vegas and Phoenix all had Cook's Distance values greater than one. Therefore, omitting the arid cities not only helped better meet the assumptions of multivariate regression modeling but also provided a more conservative estimate of how urban morphology influences the UHI effect. With regard to the spatial contiguity of low-intensity urban development (PLADJ_22), its partial slope coefficient was only marginally significant ($p = 0.10$) during the summer.

The final UHI regression model (Model 7) analyzed the fall UHI effect, which was the average of the September, October and November UHI intensities. The model performed fairly well, as it explained almost half of the variability in the fall UHI effect (Table 4.15). The partial slope coefficients for the spatial contiguity of low and high-intensity urban development were both significant. A ten percentage point increase in the spatial contiguity of either low or high-intensity urban development was predicted to enhance the UHI effect by roughly 0.4 degrees Celsius. Additionally, the fall UHI intensities were magnified by more arid climate regimes, more complexly shape deciduous forest and the increased presence of barren land.

Although the nature of the data, particularly the commonality of extreme outliers and influential observations, created modeling difficulties and resulted in the omission of five cities from the majority of the analysis, the models collectively provided a fairly compelling diagnosis of the UHI effect. Firstly, the results suggest that more contiguous urban development across a spectrum of intensity levels can amplify the UHI effect (Figure 4.28). This seems to partially reconcile how previous research has suggested that both high-density (Coutts et al. 2007) and sprawling (Stone and Rodgers 2001) urban development can enhance the UHI effect. At least amongst large American cities, the spatial contiguity of urban development, regardless of its density or intensity level, appears to be a main driver of UHI intensities. By increasing the spatial contiguity of low or high-intensity urban development ten percentage points, the UHI effect was predicted to increase by a tenth to almost half a degree Celsius (Figure 4.28). Additionally, during the summer when all the cities were included in the model, the UHI amplification predicted by increasing the contiguity of high-intensity urban development ten percentage points reached almost an entire degree Celsius. Therefore, the results presented in Tables 4.9 – 4.15 are inherently conservative estimates of how urban spatial contiguity can influence UHI intensities.

4.3.4 Multivariate Analysis – UDI/UME

In total, six multivariate regression models (Models 8 – 13) were calculated to analyze the influence of urban morphology on UDI/UME intensities. In each model the dependent variable was either the seasonal, annual or longer-term average UDI/UME intensity. The independent variables were held constant across all the models and included: the percentage of like adjacencies for developed open space (PLADJ_21), the percentage of like adjacencies for high-intensity urban development (PLADJ_24), the Ewing et al. (2002) Sprawl Index, the shape complexity of grasslands (AWMPFD_71), the shape complexity of croplands (AWMSI_82) and city area (Land Area). Unlike the majority of the models estimated for the UHI effect, the UDI/UME models included all the cities. As indicated by the model diagnostics, no cities were overly influential since Cook's Distance values never exceeded 0.73 (Cook's Distance values greater than 1 are considered to be highly influential). Additionally, the presence of multicollinearity was negligible, as the VIFs for Models 8 – 13 were all less than 1.4 (VIFs greater than 4 are typically indicative of problematic levels of multicollinearity). Finally, there were no major issues with heteroskedasticity as the p-value to White's test was never below 0.12 (p-values less 0.05 would result in a rejection of the null hypothesis of homoskedasticity).

In Model 8 the annual average UDI/UME intensity in 2010 served as the dependent variable. Overall, the model performed fairly well, as it explained 40% of the variability in the 2010 annual average UDI/UME intensities (Table 4.16). There was a noticeable reduction in the adjusted R-Squared value but this was largely due to the inclusion of PLADJ_24, which had very little influence on the annual average UDI/UME effect. The partial slope coefficient for the contiguity of developed open space (PLADJ_21), however, was significant. Specifically, a ten percentage point increase in the spatial contiguity of developed open space, roughly the equivalent of shifting from Portland (PLADJ_21 = 65) to Indianapolis (PLADJ_21 = 71), was predicted to enhance the UME effect by 0.4 degrees Celsius. This is likely due to the large quantities of vegetation, which serve as potential water vapor sources, found in the large-lot single-family housing units and urban parks included in the developed open space LULC classification.

The Ewing et al. (2002) Sprawl Index also had a significant partial effect on the annual average UDI/UME intensities. It is important to recall that lower values on the Sprawl Index are actually indicative of more sprawling urban morphologies. Therefore, the negative relationship suggests that more sprawling cities generally had stronger UMEs. A 100 point decrease in the Sprawl Index, roughly the equivalent of shifting from Providence (Sprawl Index = 154) to Atlanta (Sprawl Index = 58), would enhance the UME effect by 0.6 degrees Celsius. This is likely due to the higher prevalence of vegetation and potential water vapor sources associated with sprawling morphologies. Specifically, since expansive urban development increases the number of daily vehicle-miles traveled per capita (Ewing et al. 2002), it enhances anthropogenic water vapor sources associated with car exhaust. Of the remaining variables included in Model 8, which accounted for non-urban LULCs and controlled for city size, no significant relationships were observed.

In order to ensure that the relationships between urban morphology and UDI/UME intensities were not anomalous to 2010, Model 9 was estimated with the longer-term (2006 to 2010) annual average intensity as the dependent variable. The general similarity between Model 9 and Model 8 suggests that the relationships observed in 2010 were not spurious. Overall, Model 9 explained approximately 40 percent of the variability in the longer-term annual average UDI/UME intensities (Table 4.17). The partial slope coefficients for the spatial contiguity of developed open space (PLADJ_21) and the Sprawl Index were both significant. Additionally, they were of similar magnitude and had the same direction as the coefficients estimated in Model 8. Although still not statistically distinguishable from zero, the partial effect of the spatial contiguity of high-intensity urban development (PLADJ_24) changed direction, as it was positive in Model 9. Another notable difference between Model 9 and Model 8 was that the partial slope coefficient for the shape complexity of grasslands (AWMPFD_71) increased in significance when analyzing the longer-term annual average. More complexly shaped grasslands were predicted to enhance the UME effect, a relationship that is likely attributable to the highly complex grasslands that contributed to the Phoenix and Riverside UMEs.

The remaining four models (Models 10 – 13) were estimated to analyze how the relationships between urban morphology and UDI/UME intensities varied seasonally. In Model 10, the winter UDI/UME effect (the average of the December, January and February UDI/UME intensities) served as the dependent variable. Model 10 had the largest R-Squared value of all the UDI/UME models, as it explained almost half of the variability in the winter UDI/UME effect (Table 4.18). The partial slope coefficient for the spatial contiguity of developed open space (PLADJ_21) was significant, with a ten percentage point increase predicted to enhance the UME intensity by 0.4 degrees Celsius. Contrastingly, increasing the spatial contiguity of high-intensity urban development (PLADJ_24) by ten percentage points was predicted to decrease the UME intensity by almost 0.3 degrees Celsius. It should be noted, however, that the influence of PLADJ_24 was only marginally significant ($p = 0.07$). With regard to the Sprawl Index, the winter was the only season when it did not have at least a marginally significant partial effect on UDI/UME intensities. Finally, of the non-urban land covers and control variables, cropland shape complexity (AWMSI_82) had the only significant influence on the winter UDI/UME effect. More complexly shaped croplands were predicted to amplify UME intensities.

The spring UDI/UME effect (the average of the March, April and May UDI/UME intensities) served as the dependent variable in Model 11. The model had the weakest predictive power of all the UDI/UME models, as it explained 35% of the variability in the spring UDI/UME effect (Table 4.19). The partial slope coefficient for the spatial contiguity of developed open space (PLADJ_21) was only marginally significant ($p = 0.10$) and had a reduced magnitude relative to its influence on the annual average in 2010 (0.035 vs. 0.041). The Sprawl Index did exhibit a significant partial effect on the spring UDI/UME intensity. Of all the seasons, the influence of sprawl on the UDI/UME effect was actually greatest during the spring. Specifically, a 100 point decrease in the Sprawl Index (i.e. shifting towards a more sprawling urban morphology) was predicted to increase the UME intensity by almost a full degree Celsius. Overall, the poor predictive power of the spring model can partially be attributed to the insignificant partial slope coefficients for the spatial contiguity of high-intensity urban development (PLADJ_24), the non-urban land covers and the city area control.

Model 12 evaluated the influence of urban morphology on the summer UDI/UME effect (the average of the June, July and August UDI/UME intensities). Overall, the model explained almost 40% of the variability in the summer UDI/UME intensities (Table 4.20). The partial slope coefficient for the spatial contiguity of developed open space (PLADJ_21) was significant and of comparable magnitude to that observed in the annual average models (Models 8 and 9), as a ten percentage point increase was predicted to enhance the UME intensity by 0.45 degrees Celsius. Although only marginally significant ($p = 0.05$), the partial effect of the Sprawl Index was similar to that observed in the spring (Model 11), with a 100 point decrease predicted to amplify the UME intensity by 0.7 degrees Celsius. Finally, the shape complexity of grasslands (AWMPFD_71) was also a significant contributor to the spring UME effect.

The last multivariate regression model (Model 13) tested the influence of urban morphology on the fall UDI/UME effect (the average of the September, October and November

UDI/UME intensities). The R-Squared value of Model 13 was comparable to the aforementioned models since it explained roughly 40% of the variability in the fall UDI/UME intensities (Table 4.21). The partial slope coefficient for the spatial contiguity of developed open space (PLADJ_21) was significant and of identical magnitude to that observed in the summer (Model 12). Additionally, the partial effect of the Sprawl Index on the fall UDI/UME intensities was significant and had the same magnitude as the coefficients estimated in the two annual average models (Model 8 and Model 9). Of the non-urban land covers and city size control, the shape complexity of grasslands (AWMPFD_71) was marginally significant ($p = 0.06$). Again, increasingly complex grasslands were predicted to enhance the UME effect.

Collectively, the models provided an insightful analysis of how the spatial configuration of cities can influence moisture differences between urban environments and their surroundings. Firstly, more contiguous developed open space was found to amplify UME intensities. A ten percentage point increase in the spatial contiguity of developed open space was predicted to magnify the UME effect by 0.35 to 0.45 degrees Celsius. At the opposite end of the urban intensity spectrum, the spatial contiguity of high-intensity urban development only had a marginal influence on the UDI/UME effect during the winter. In the winter more contiguous high-intensity development was predicted to increase UDI intensities, but this relationship was not observed in any other season or with respect to the annual averages. Finally, the Ewing et al. (2002) Sprawl Index indicated that more expansive or sprawling urban morphologies generally amplified the UME effect. Overall, it appears that highly contiguous developed open space as well as more general sprawling urban morphologies achieve a delicate balance between the heat contributed by urban land surfaces to power evapotranspiration and maintaining enough vegetation and water vapor sources to create strong UMEs.

In order to fairly compare the importance of urban spatial contiguity and sprawl with regard to the UDI/UME effect, their standardized regression coefficients were graphed in Figure 4.29. Standardized regression coefficients were used because the Sprawl Index has different units and therefore a different statistical distribution than the two spatial metrics (PLADJ_21 and PLADJ_24). Figure 4.29 illustrates that outside of the winter months the spatial contiguity of high-intensity urban development (PLADJ_24) had a very minimal influence on UDI/UME intensities. Secondly, despite their standardized regression coefficients having opposite signs, both sprawling and highly contiguous developed open space enhanced the UME effect throughout the entire year. In terms of which variable was more influential in governing UME intensities, sprawl and the contiguity of developed open space were generally comparable but displayed slightly different seasonalities.

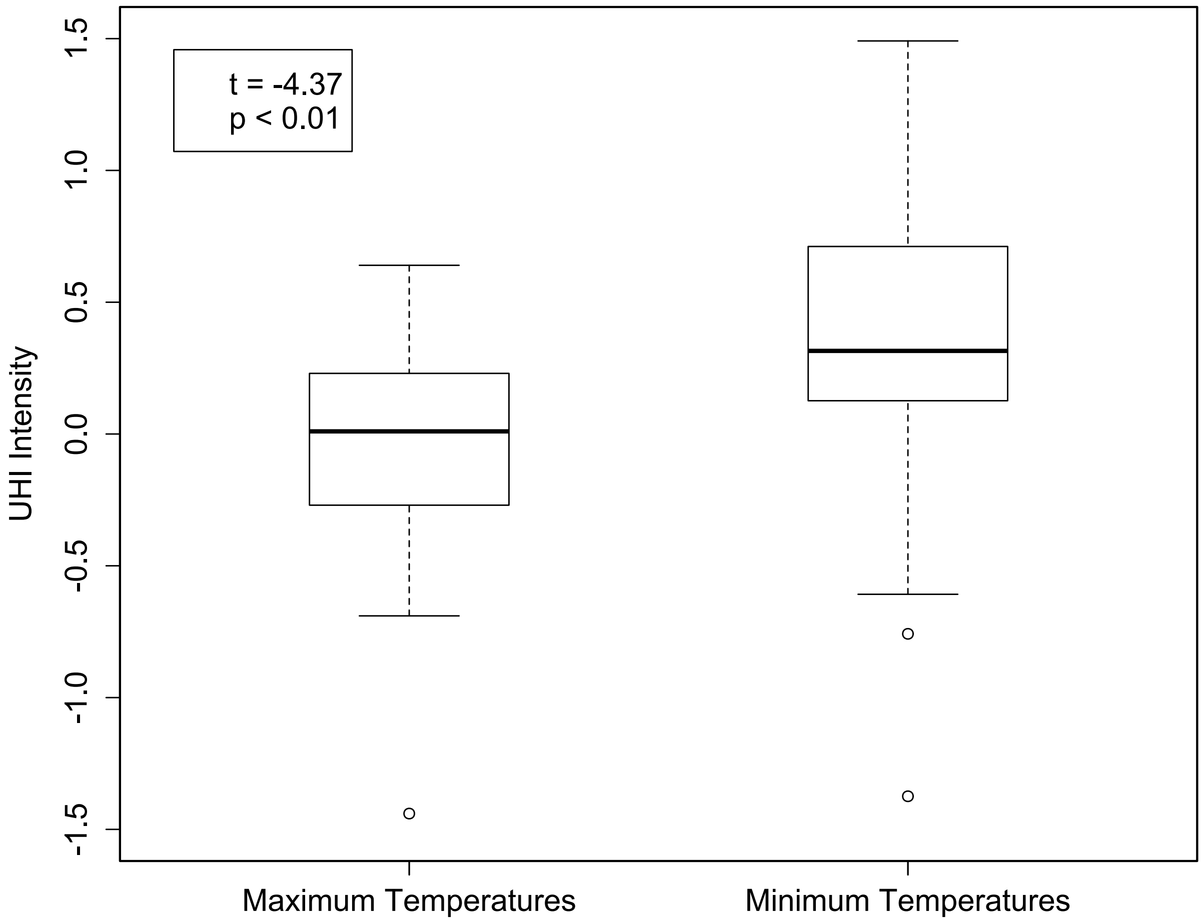

Figure 4.1. Difference in UHI Intensity Between Maximum and Minimum Temperatures

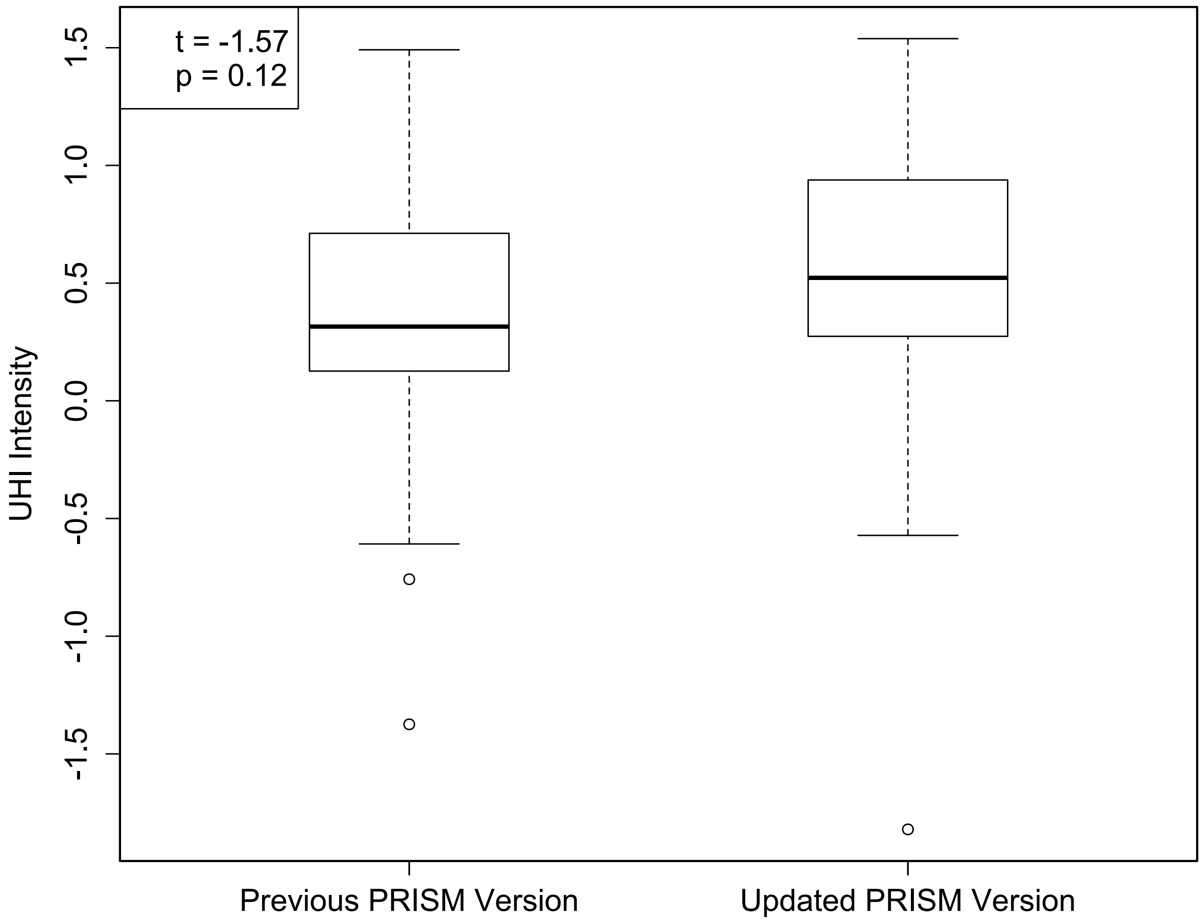

Figure 4.2. Difference in UHI Intensity Between the Previous and Updated PRISM Versions

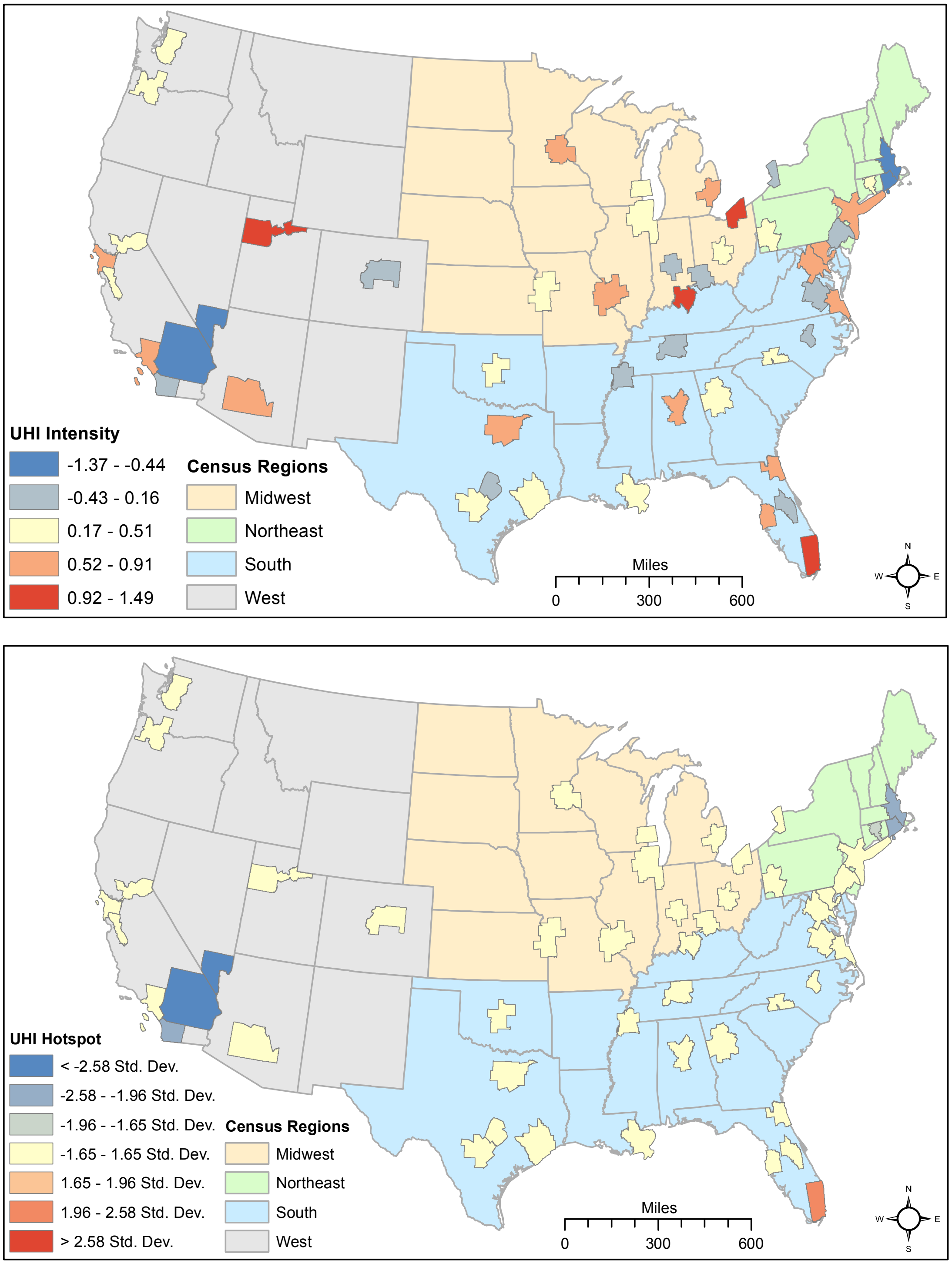

Figure 4.3. Map of 2010 Annual UHI Intensity and Corresponding Hotspot Analysis

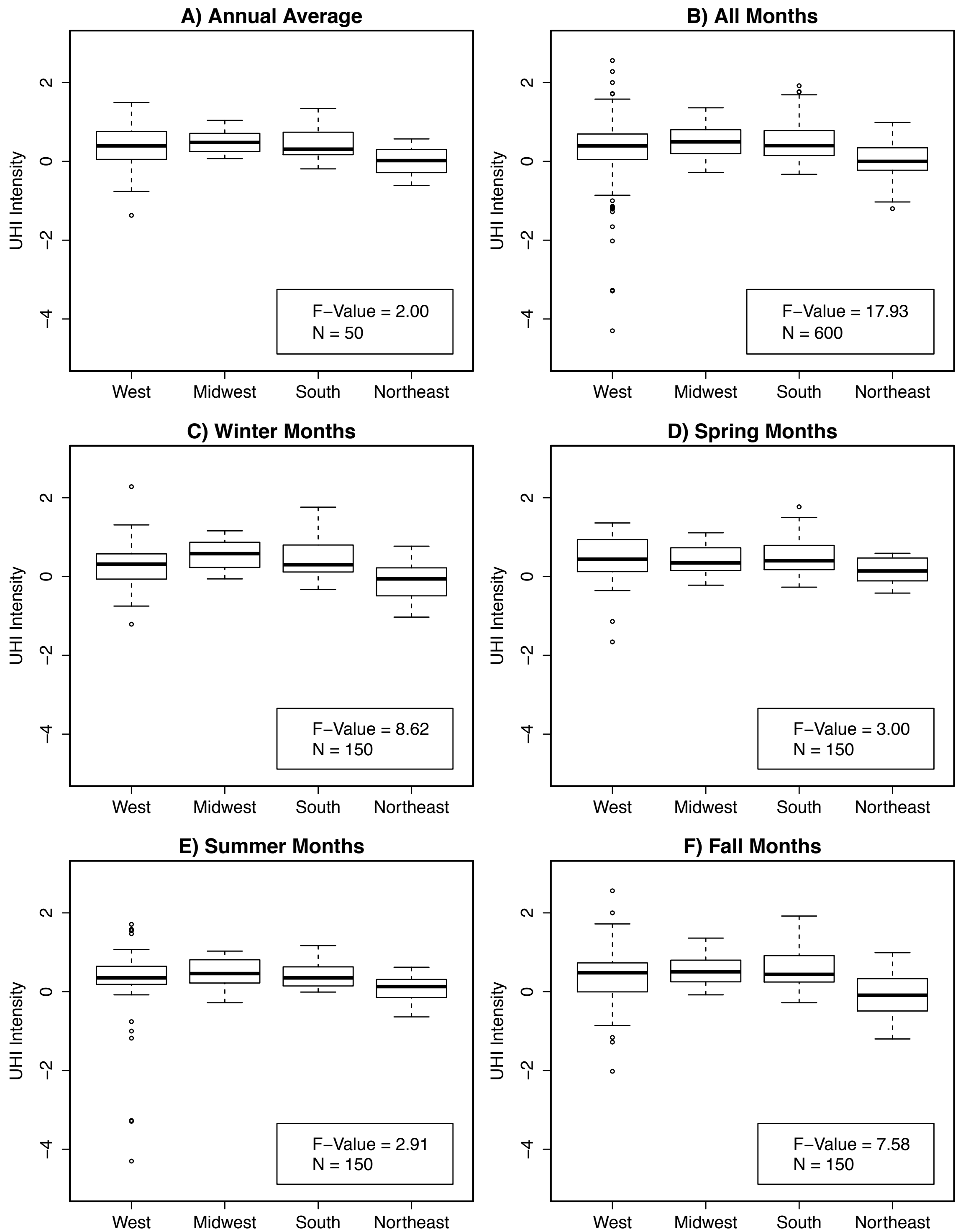

Figure 4.4. Differences in UHI Intensity Between Census Regions for: A) Annual Average B) All Months, C) Winter Months, D) Spring Months, E) Summer Months and F) Fall Months

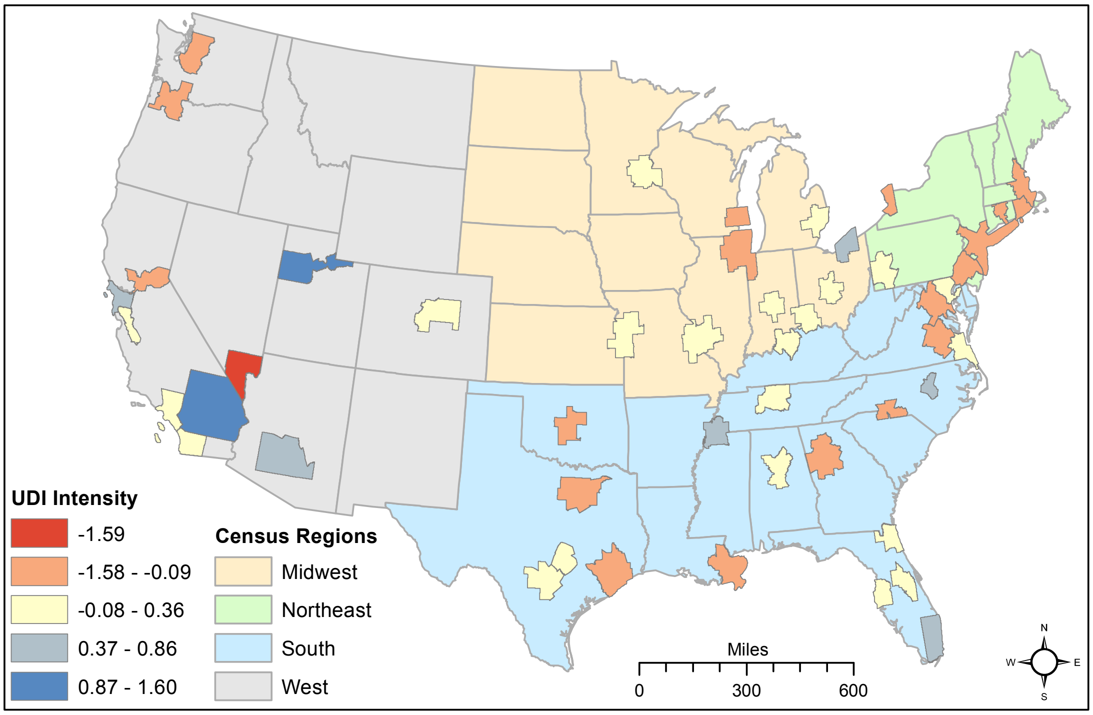

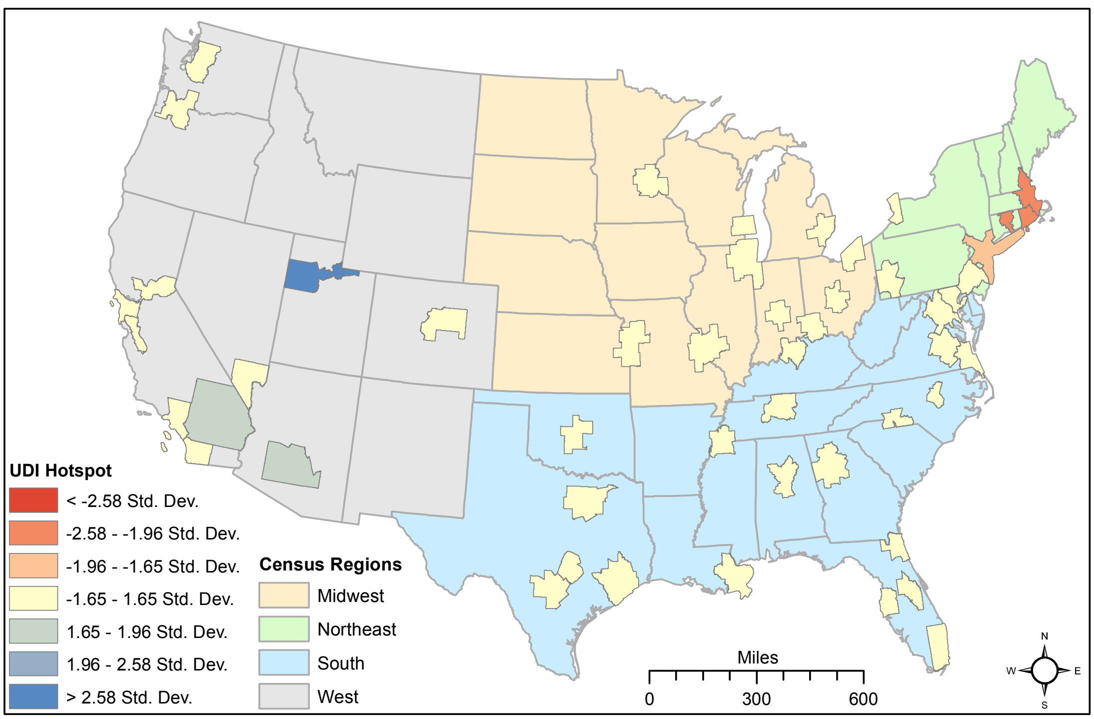

Figure 4.5. Map of 2010 Annual UDI Intensity and Corresponding Hotspot Analysis

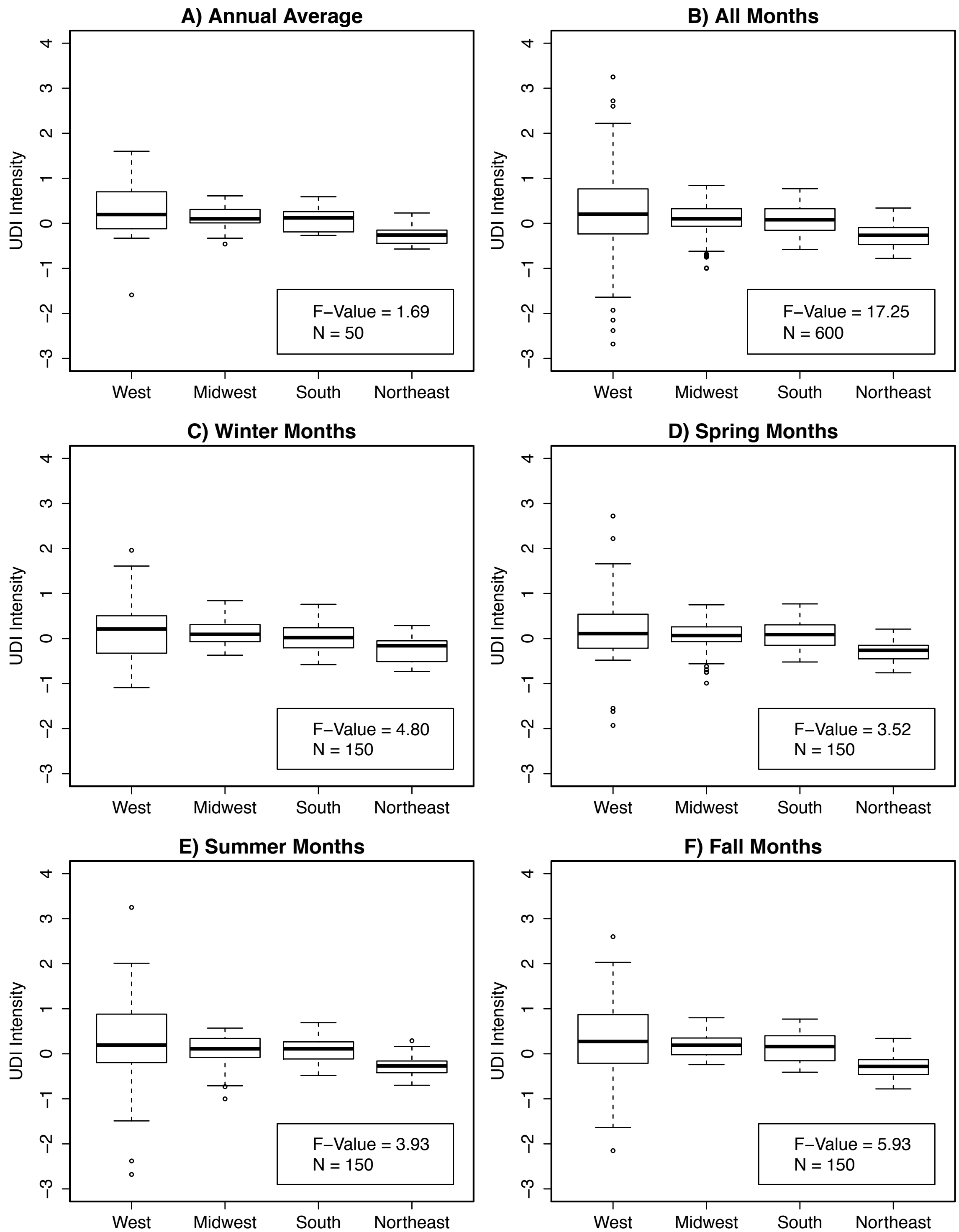

Figure 4.6. Differences in UDI Intensity Between Census Regions for: A) Annual Average B) All Months, C) Winter Months, D) Spring Months, E) Summer Months and F) Fall Months

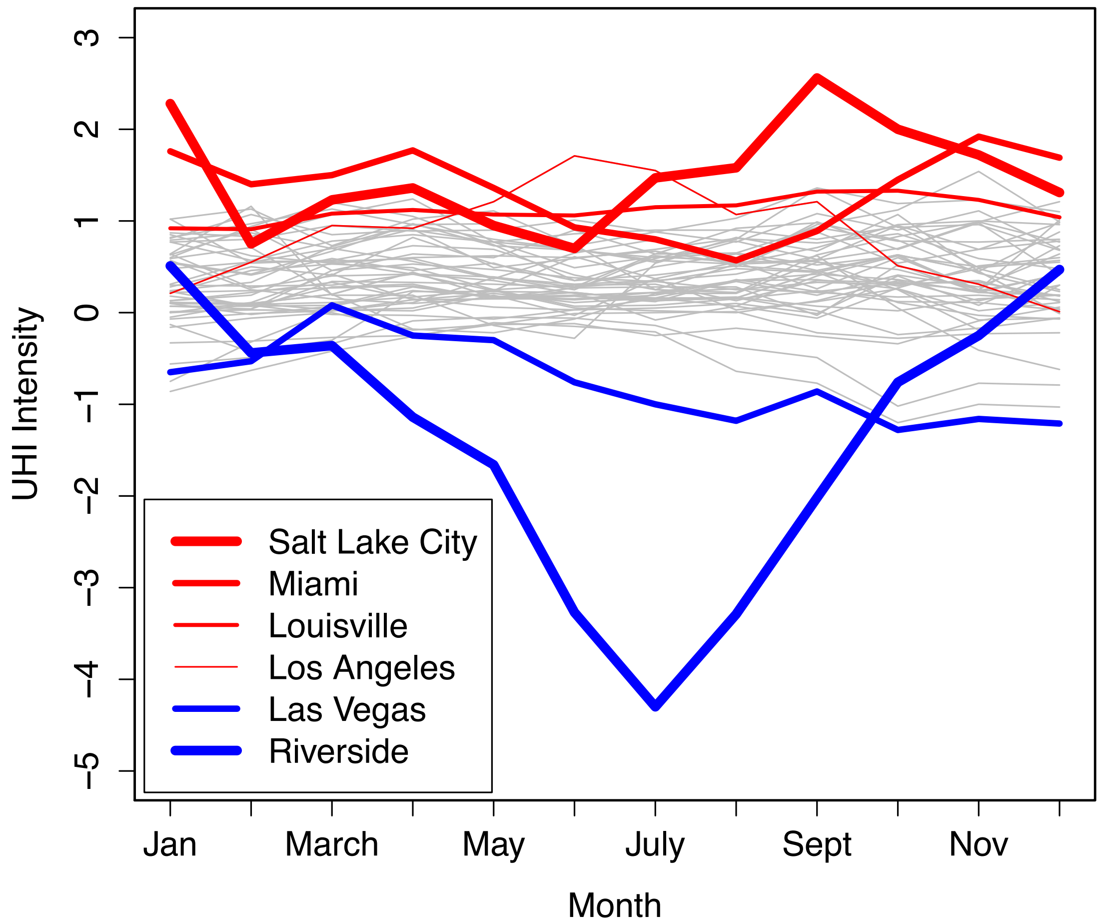

Figure 4.7. UHI Intensity Monthly Ensemble for 2010

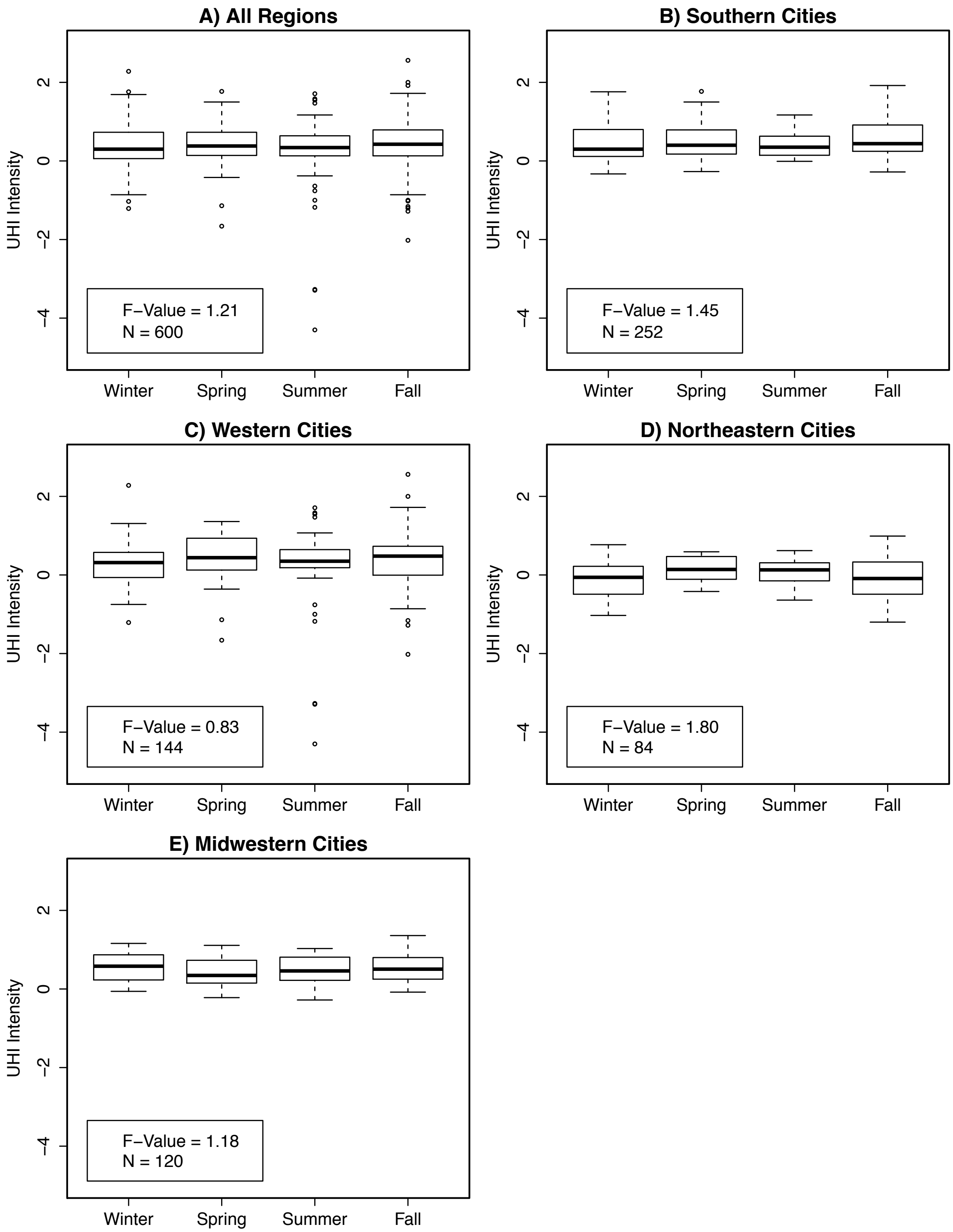

Figure 4.8. Differences in UHI Intensity Between Seasons for: A) All Regions, B) Southern Cities, C) Western Cities, D) Northeastern Cities and E) Midwestern Cities

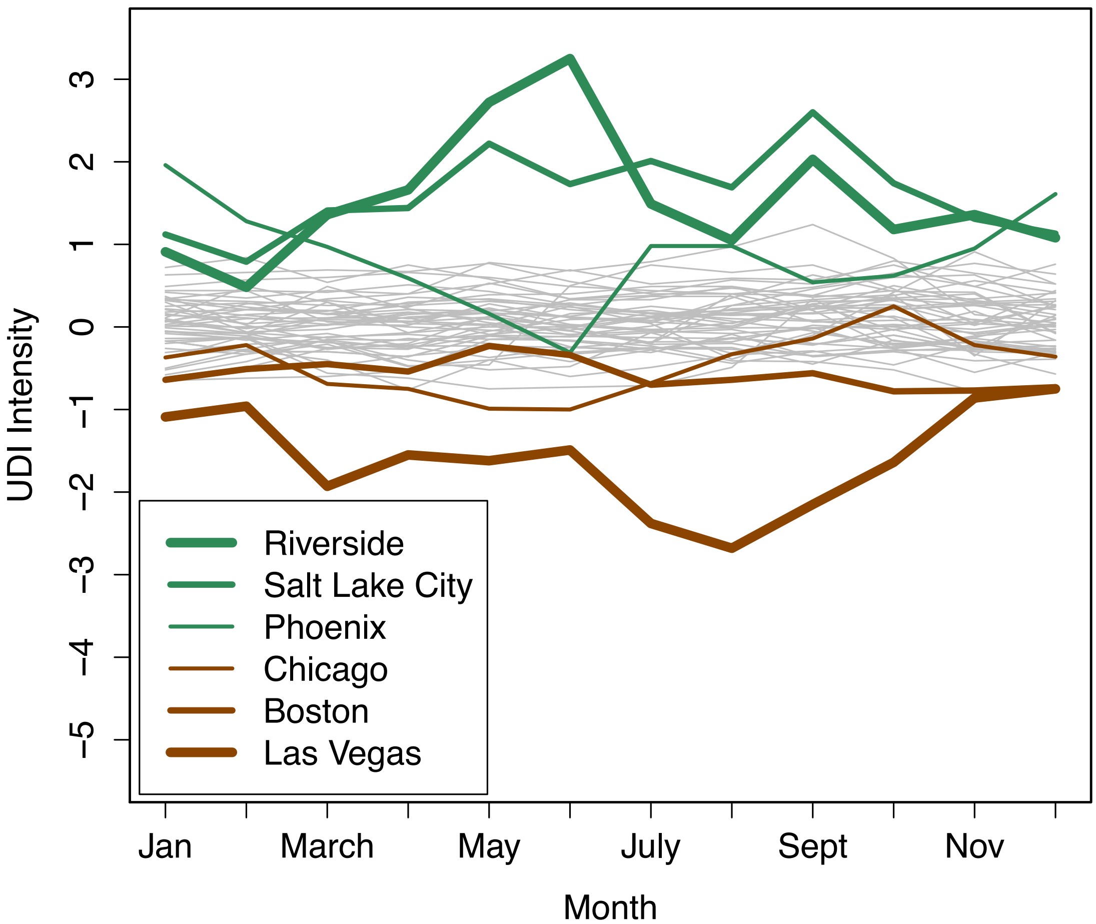

Figure 4.9. UDI Intensity Monthly Ensemble for 2010

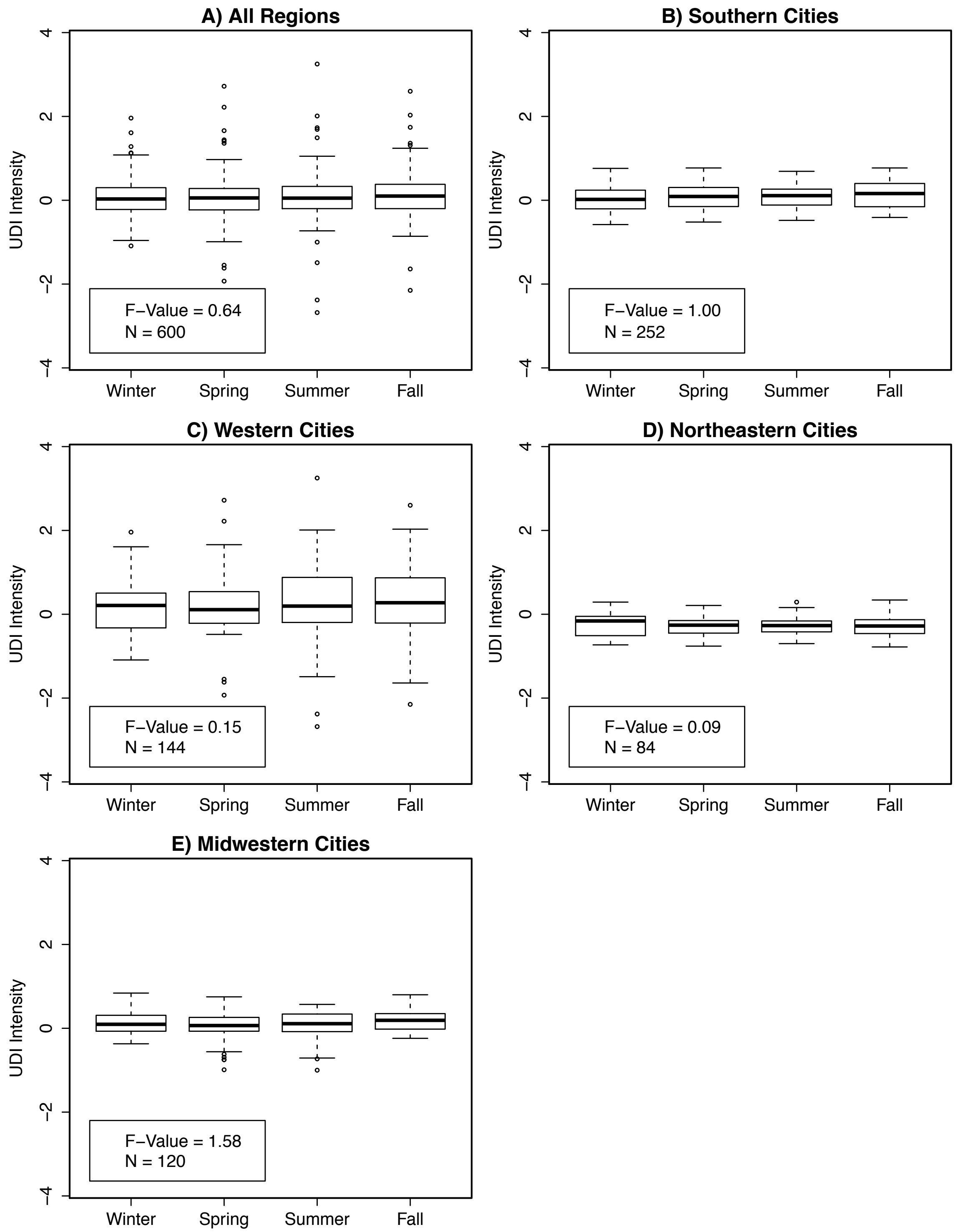

Figure 4.10. Differences in UDI Intensity Between Seasons for: A) All Regions, B) Southern Cities, C) Western Cities, D) Northeastern Cities and E) Midwestern Cities

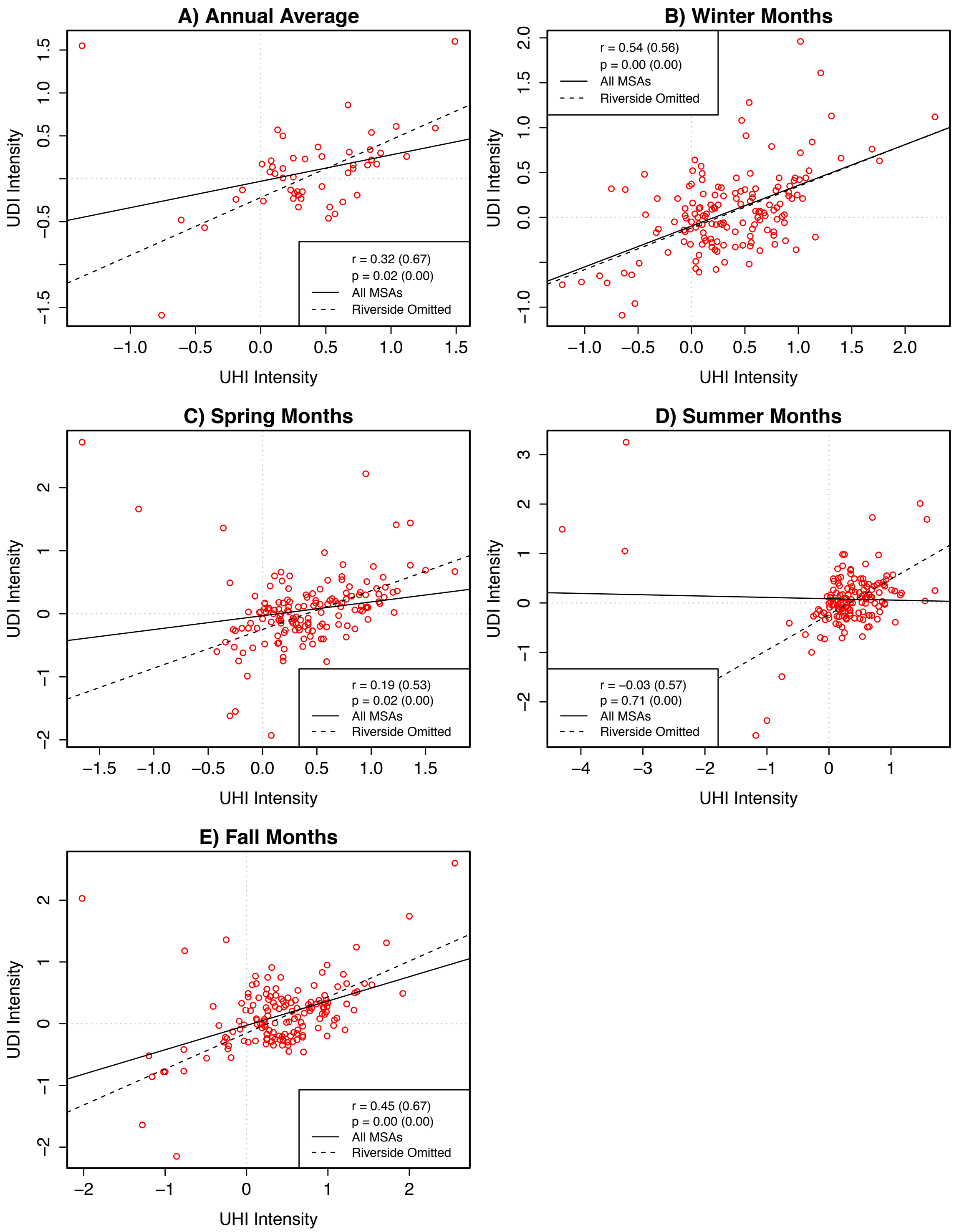

Figure 4.11. Relationships Between UHI Intensity and UDI Intensity for: A) Annual Average, B) Winter Months, C) Spring Months, D) Summer Months and E) Fall Months

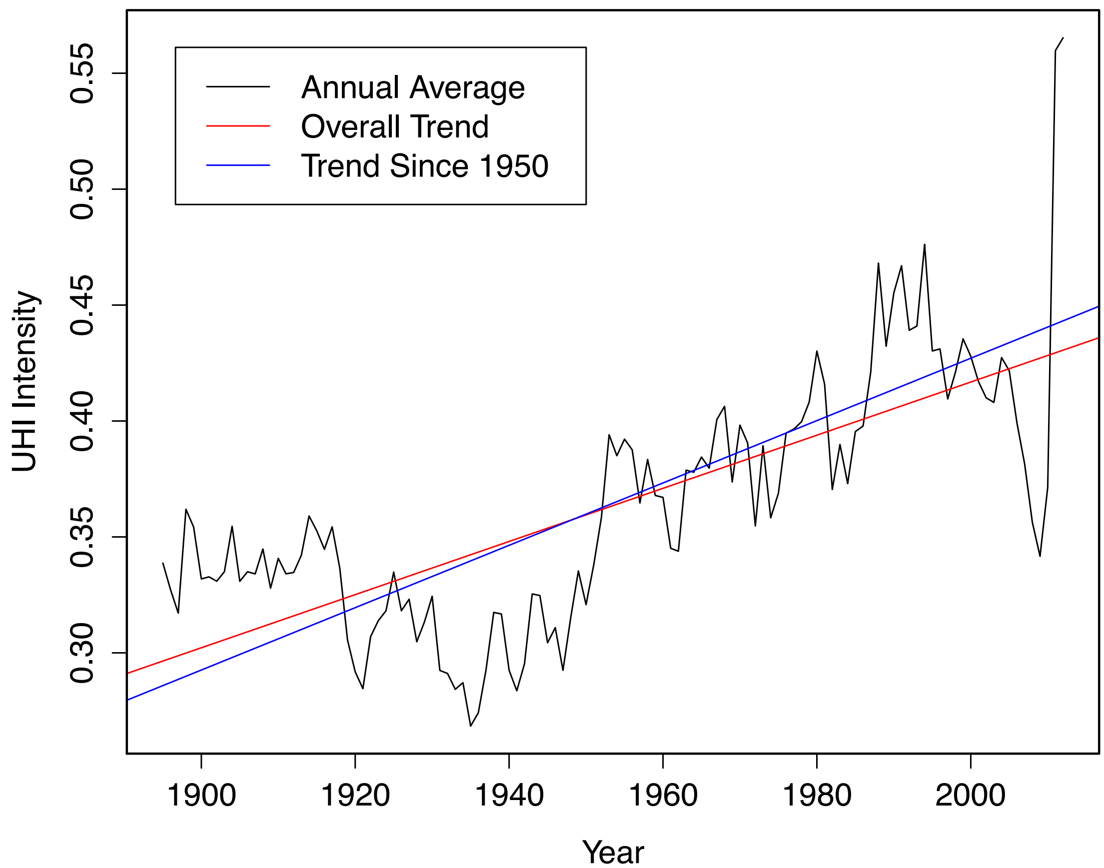

Figure 4.12. Annual Average UHI Intensity of all MSAs from 1895 to 2012

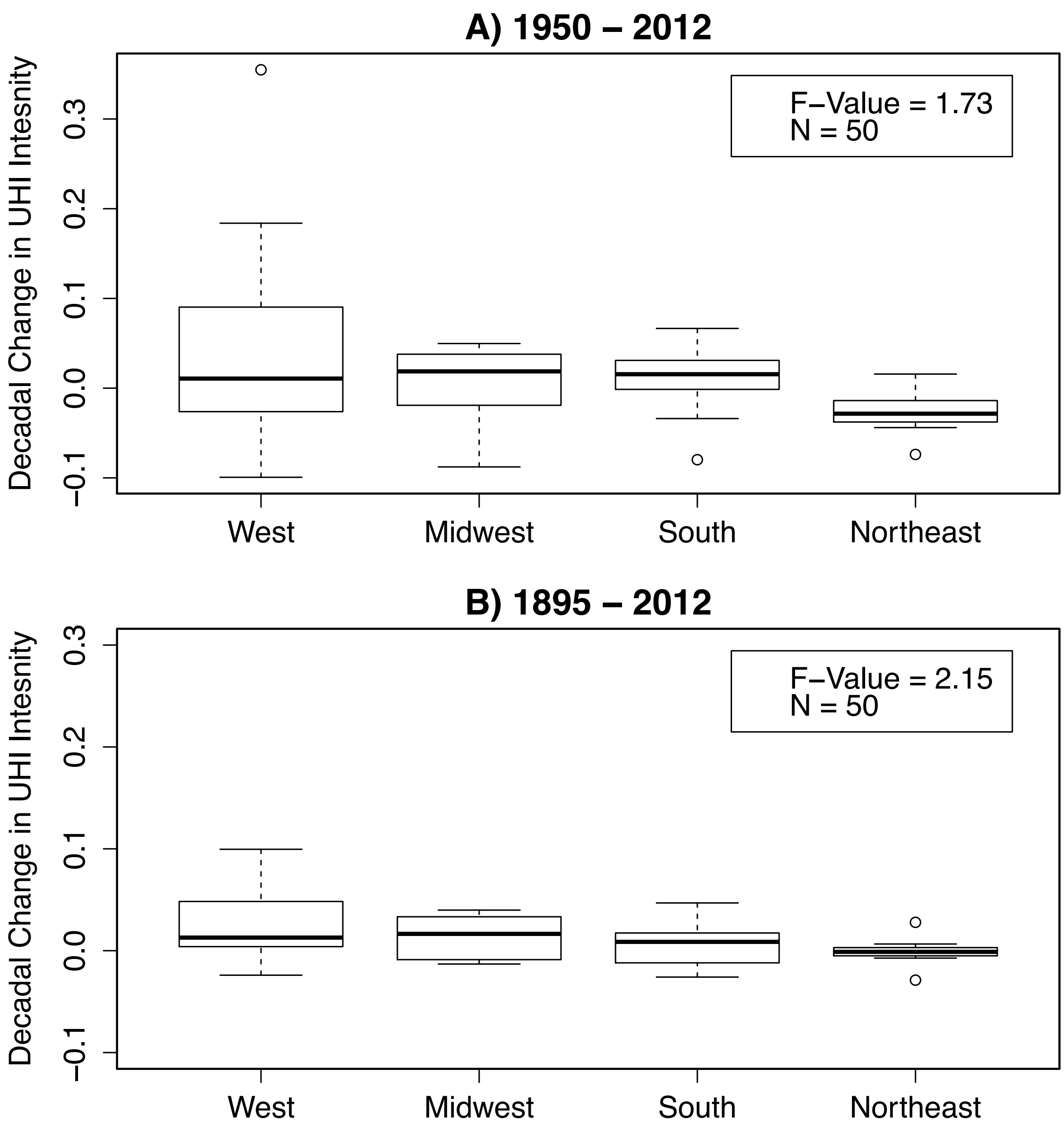

Figure 4.13. Decadal Change in UHI Intensity by Census Region from: A) 1950 to 2012 and B) 1895 to 2012

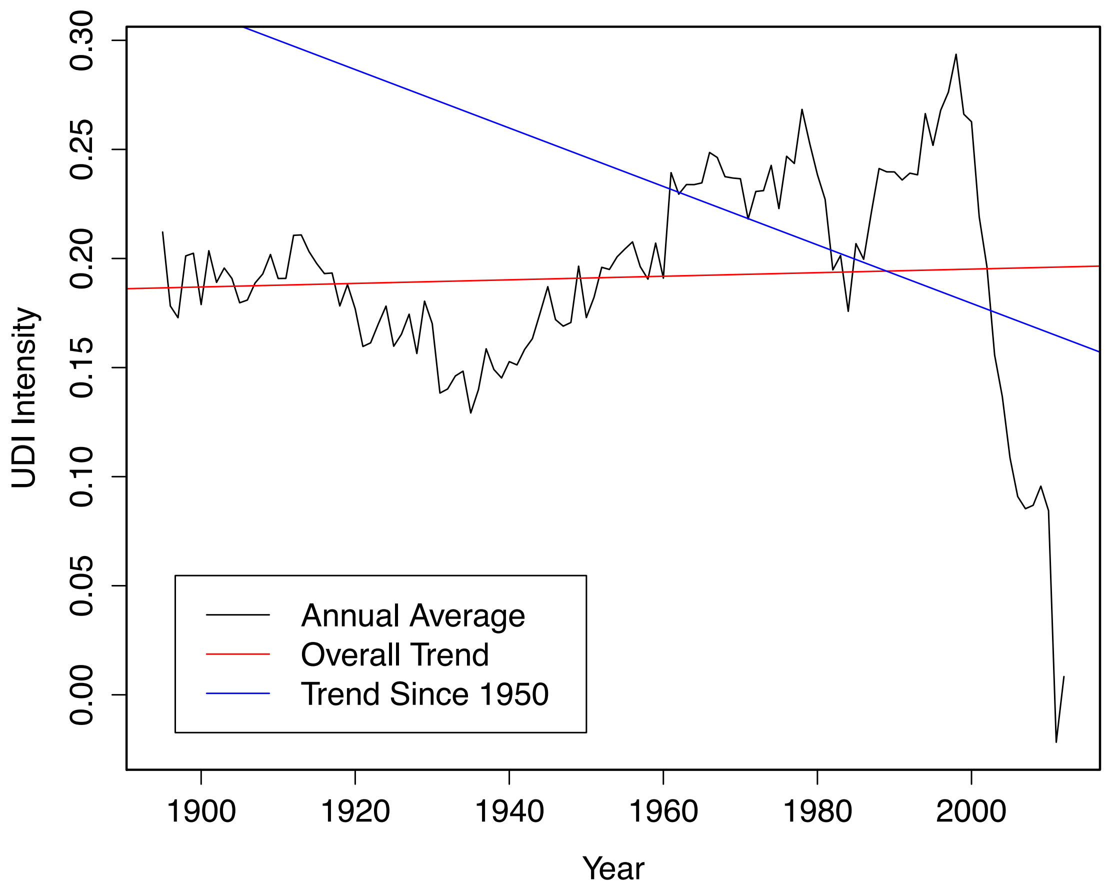

Figure 4.14. Annual Average UDI Intensity of all MSAs from 1895 to 2012

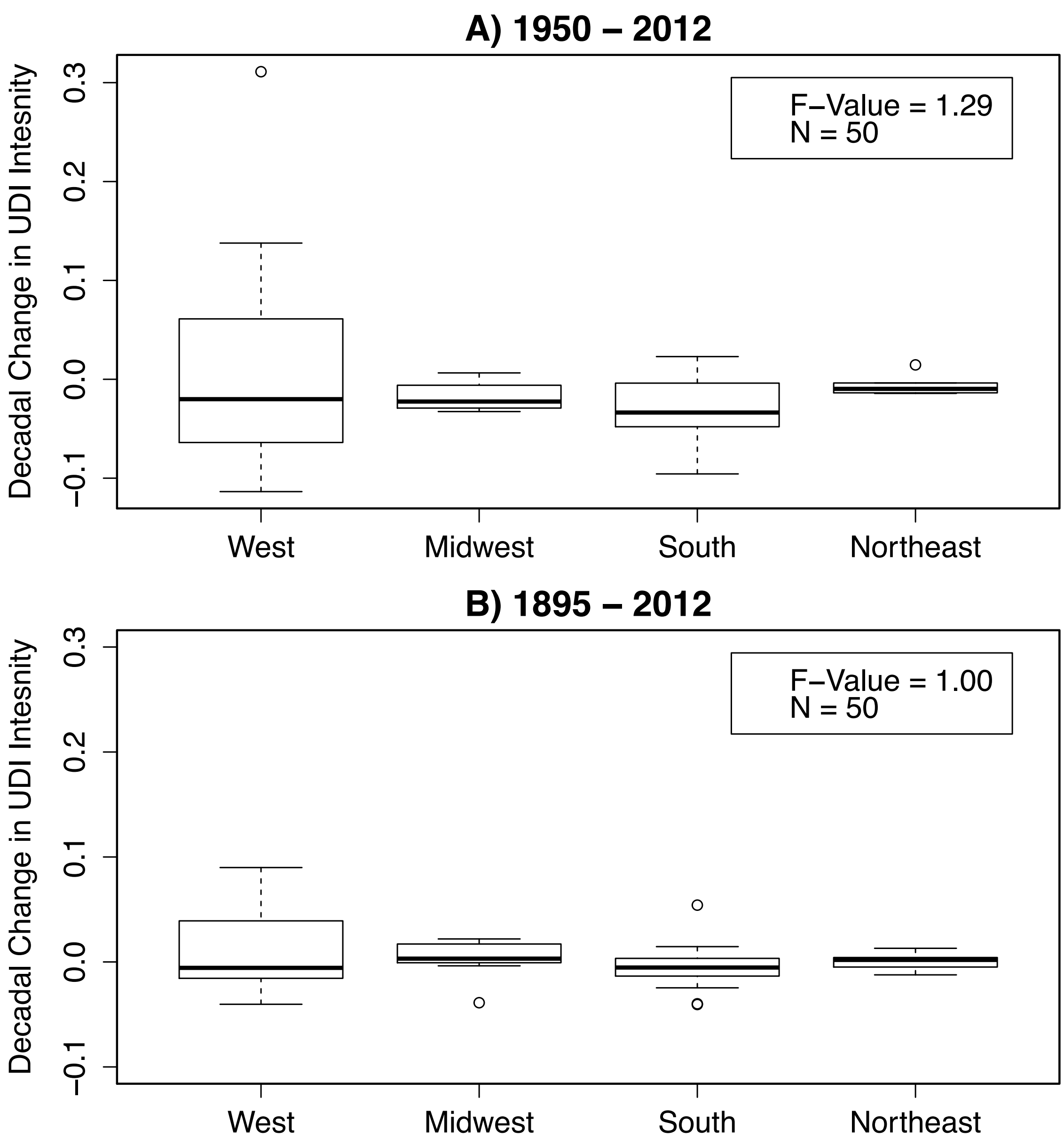

Figure 4.15. Decadal Change in UDI Intensity by Census Region from: A) 1950 to 2012 and B) 1895 to 2012

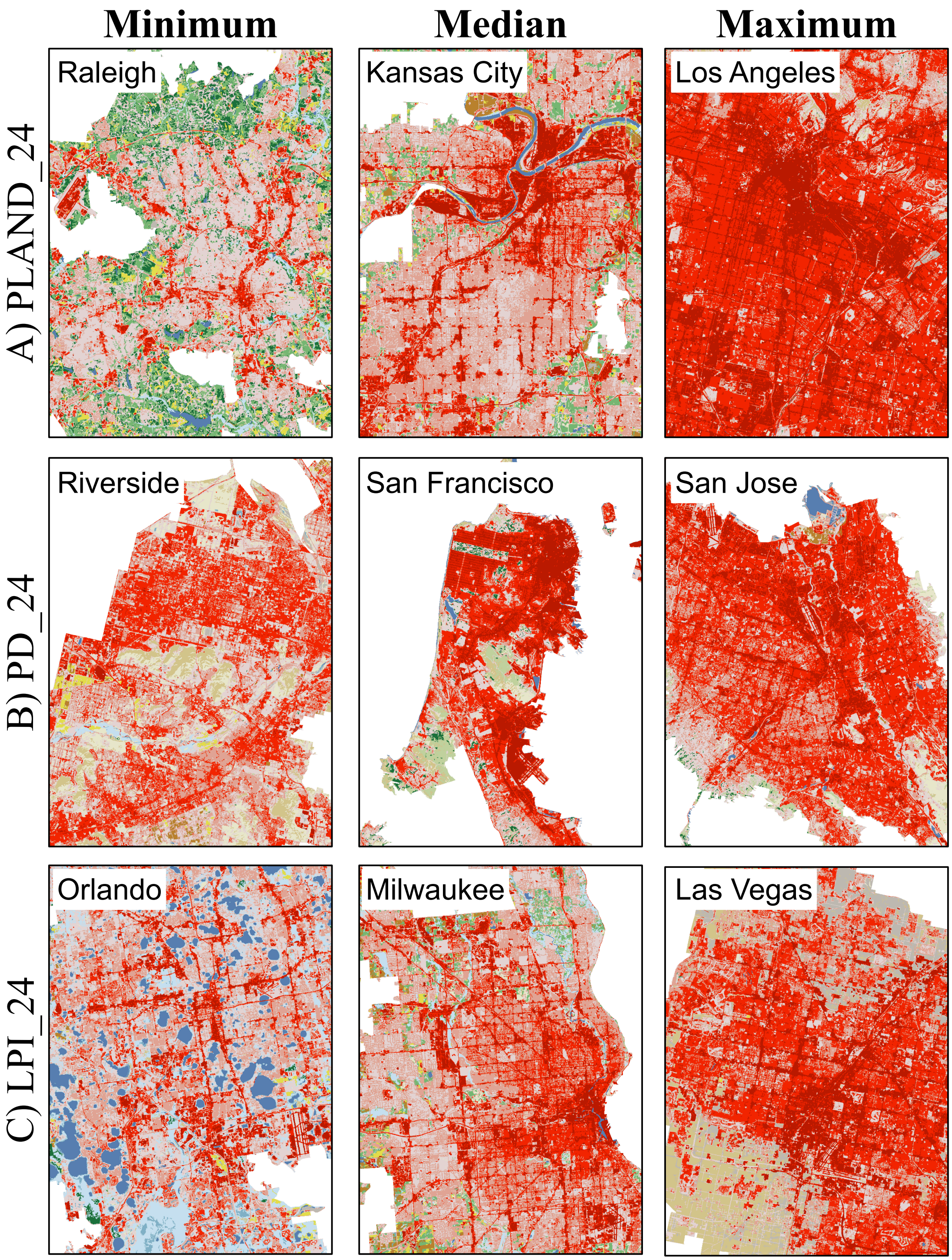

Figure 4.16. Minimum, Median and Maximum Values for A) Percentage of Landscape, B) Patch Density and C) Largest Patch Index Calculated for Class 24 (All Maps at 1:400,000 Scale)

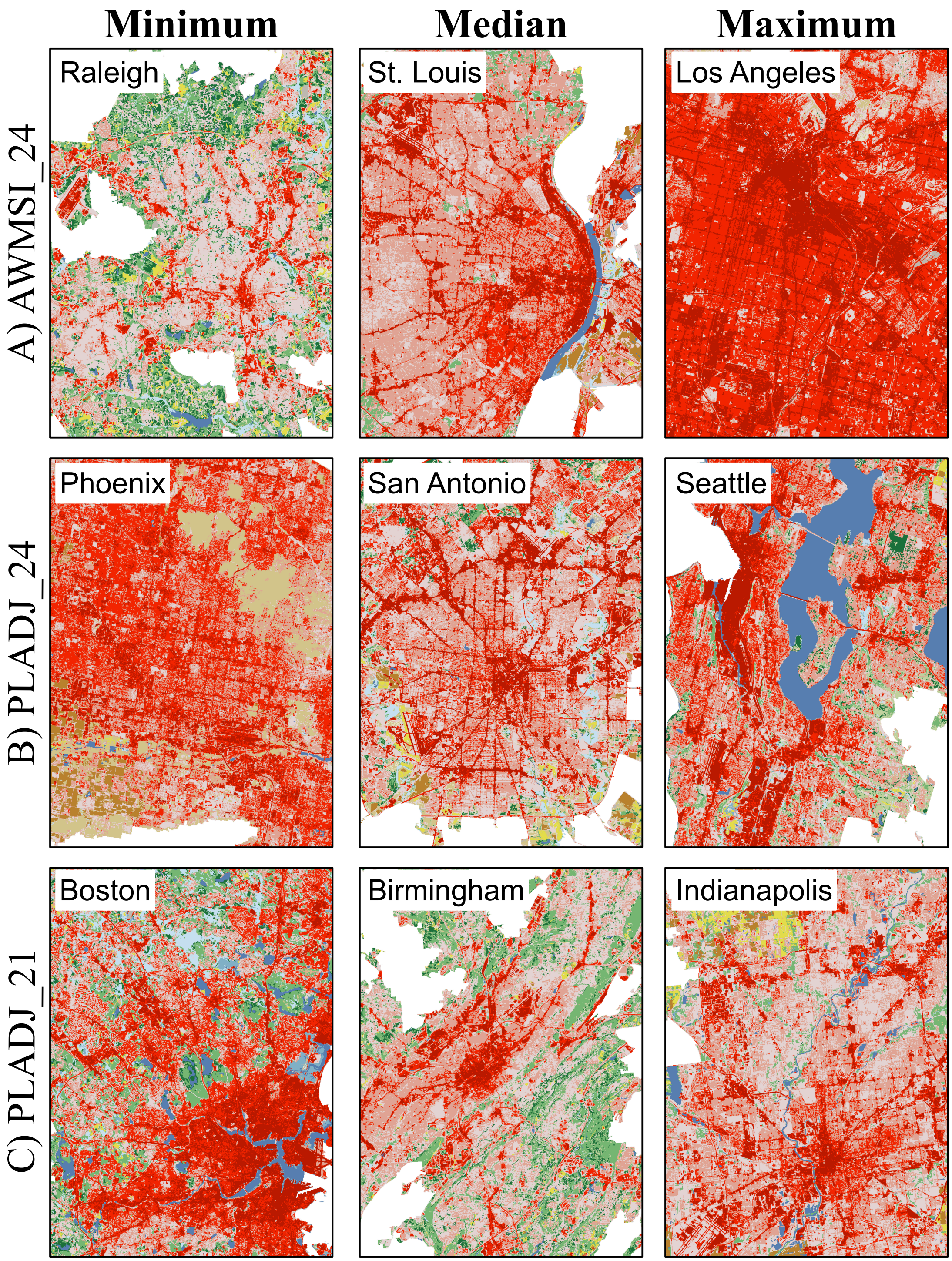

Figure 4.17. Minimum, Median and Maximum Values for A) AWMSI_24, B) PLADJ_24 and C) PLADJ_21 (All Maps at 1:400,000 Scale)

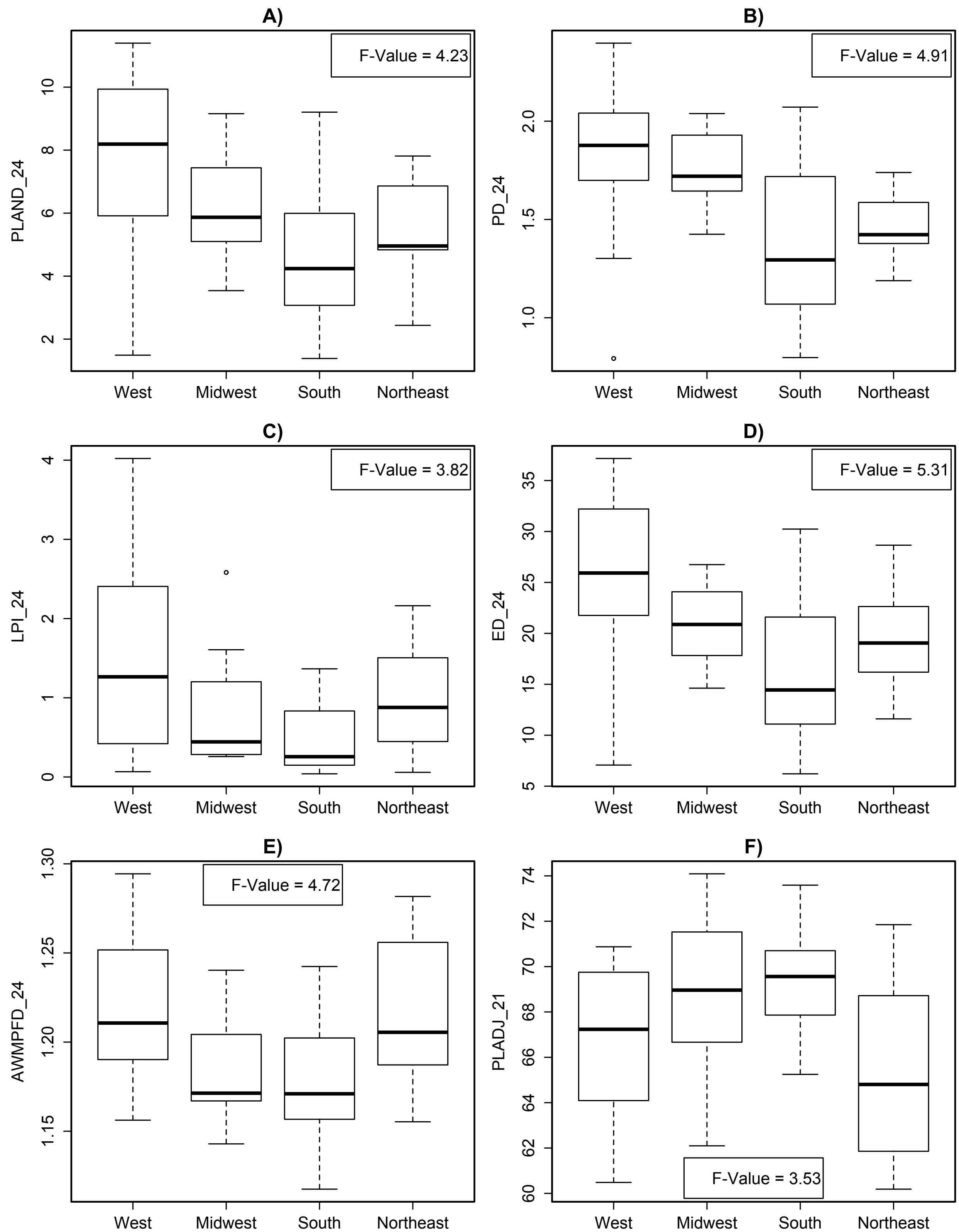

Figure 4.18. Differences in Urban Morphology Between Census Regions

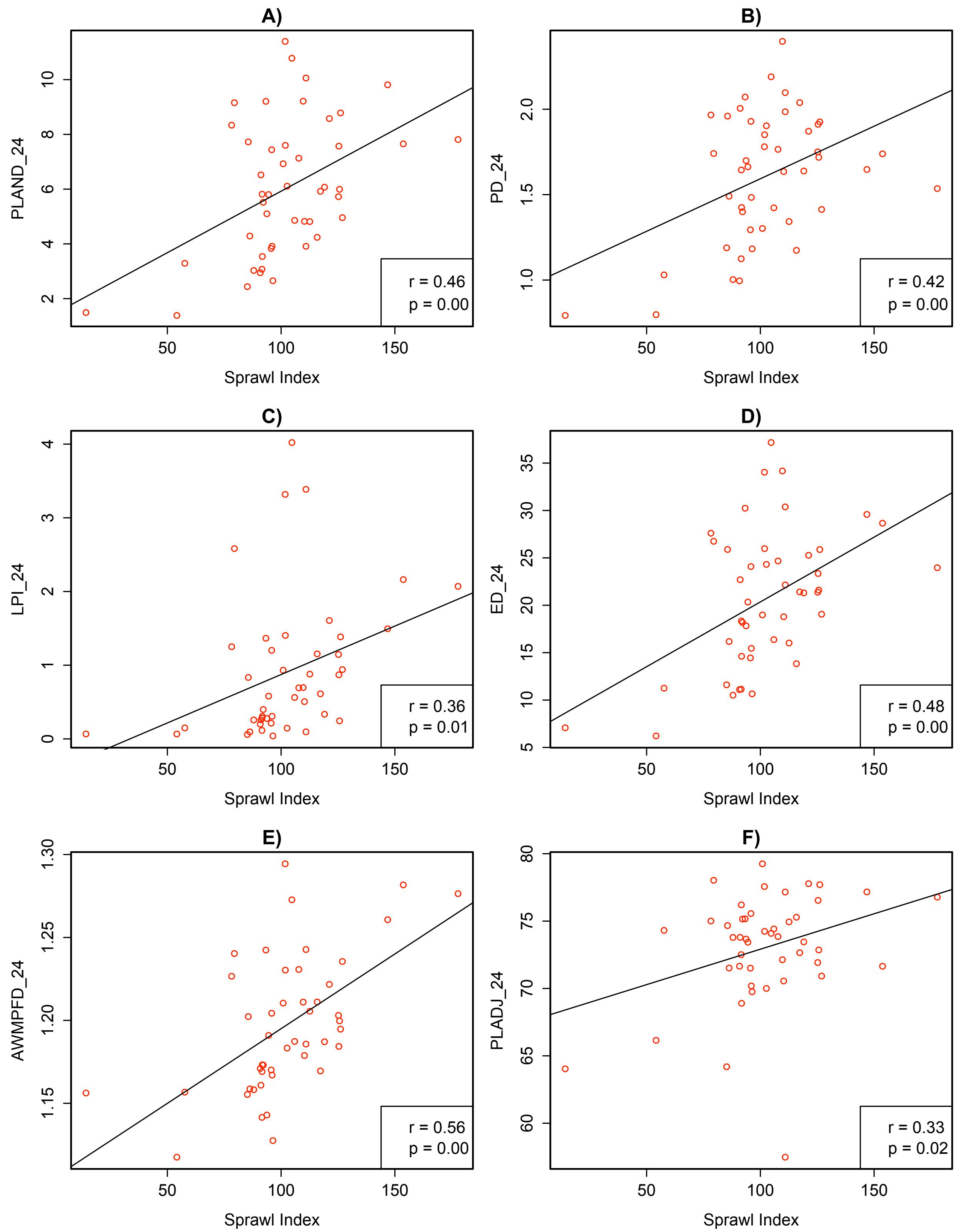

Figure 4.19. Relationships Between Spatial Metrics and Sprawl Index

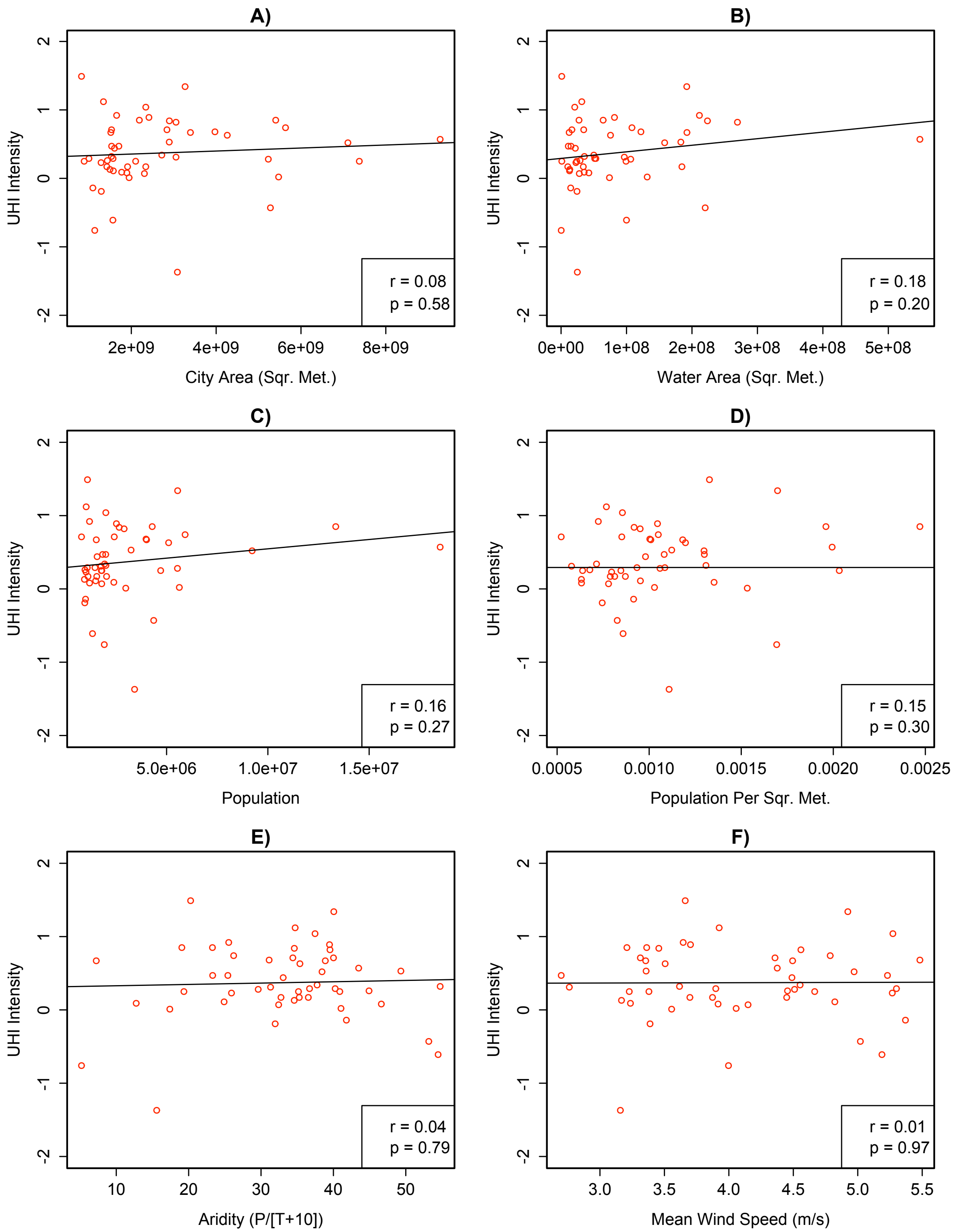

Figure 4.20. Relationships Between 2010 Annual UHI Intensities and Potential Control Variables

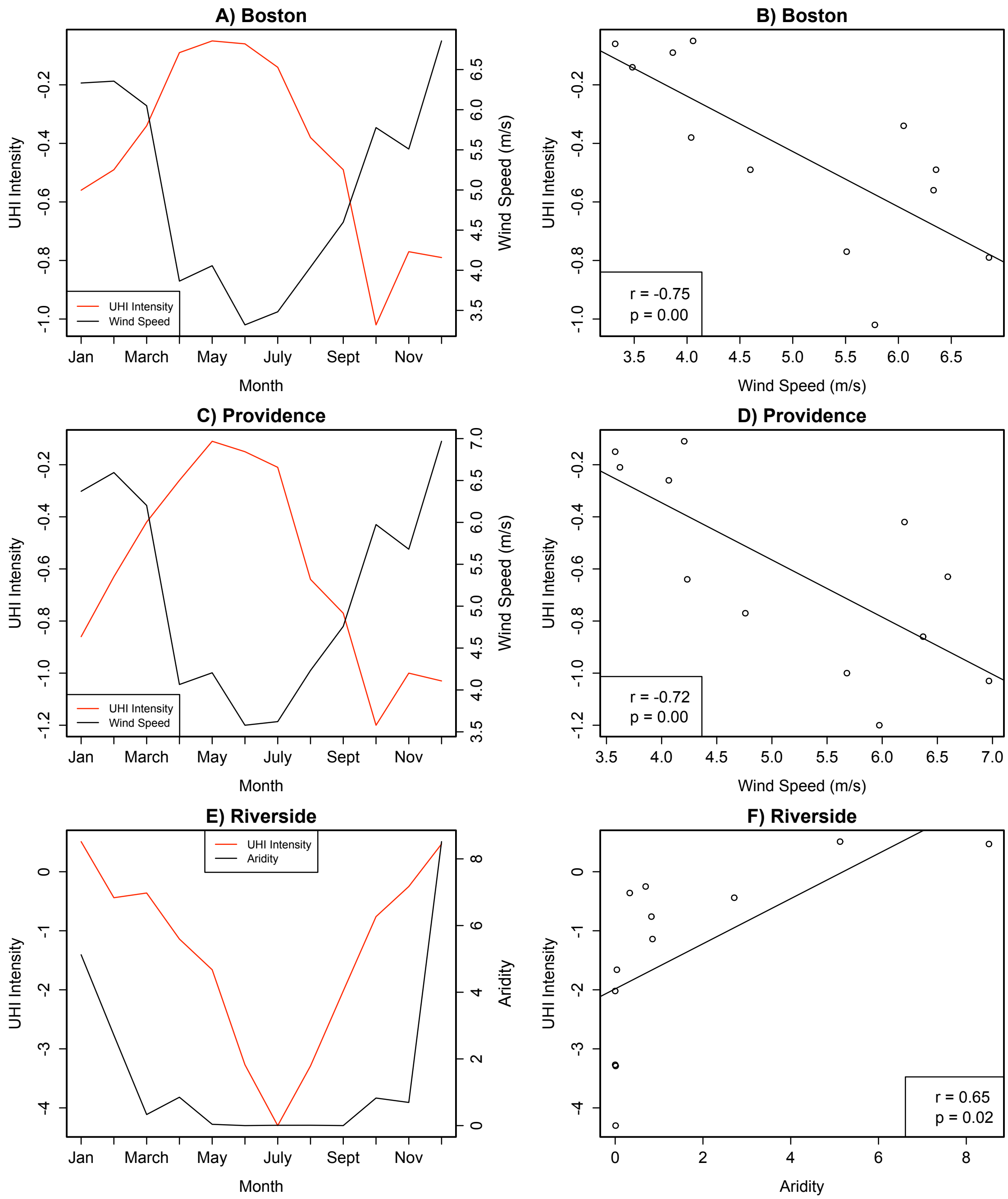

Figure 4.21. Relationships Between Monthly UHI Intensities in 2010 for Boston, Providence and Riverside and Relevant Meteorological Variables

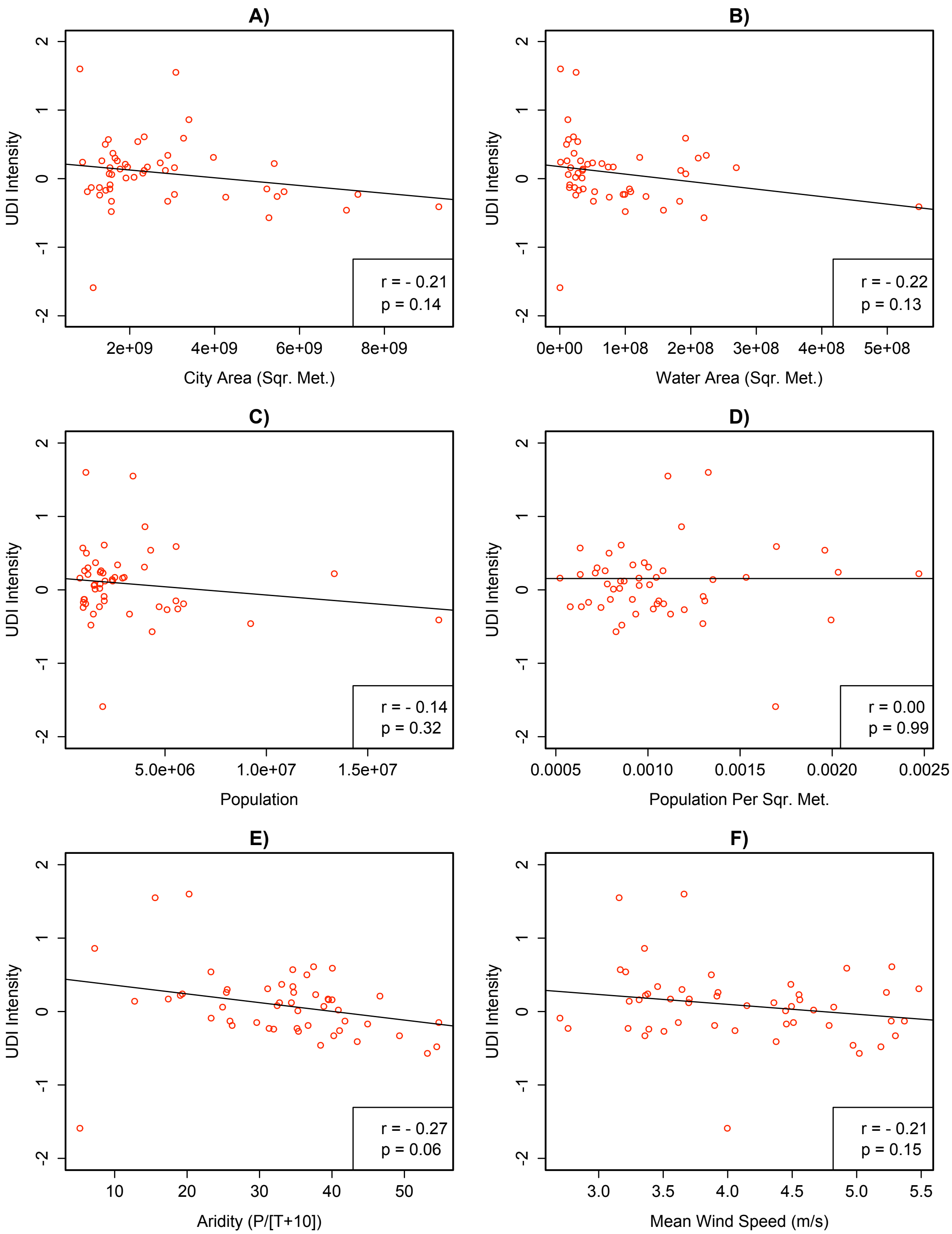

Figure 4.22. Relationships Between 2010 Annual UDI/UME Intensities and Potential Control Variables

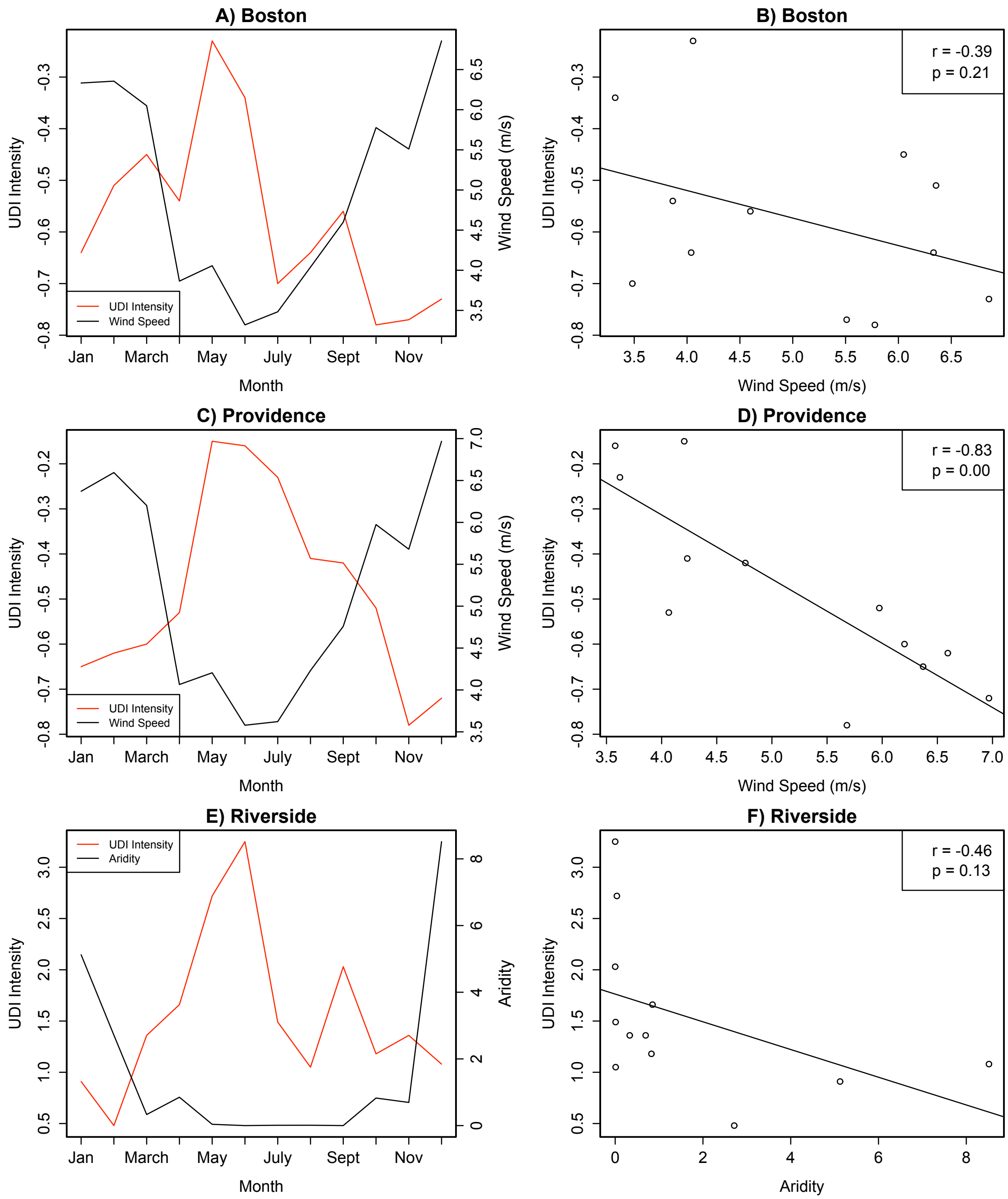

Figure 4.23. Relationships Between Monthly UDI Intensities in 2010 for Boston, Providence and Riverside and Relevant Meteorological Variables

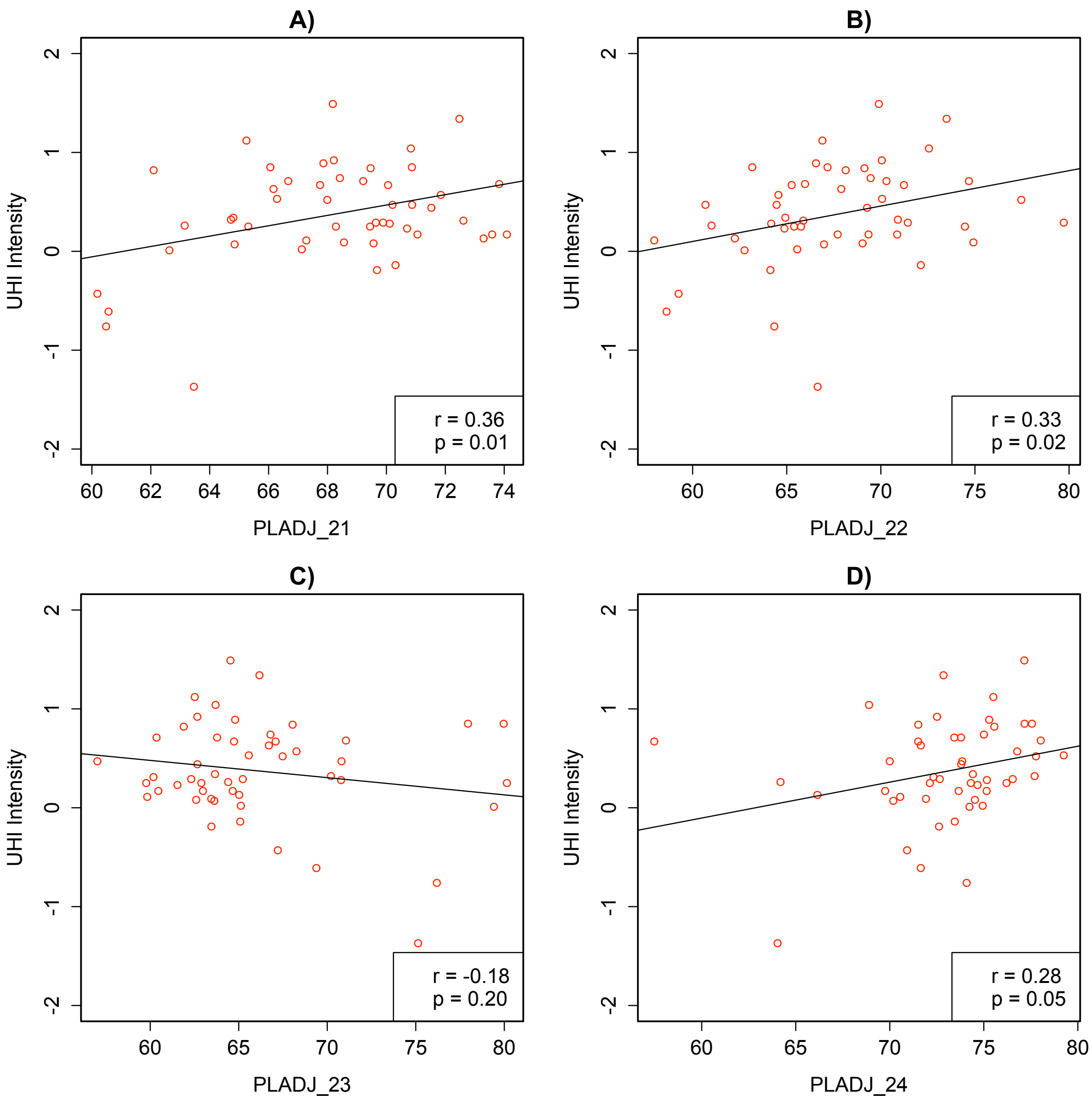

Figure 4.24. Relationships Between Annual Average UHI Intensity in 2010 and Urban Spatial Metrics

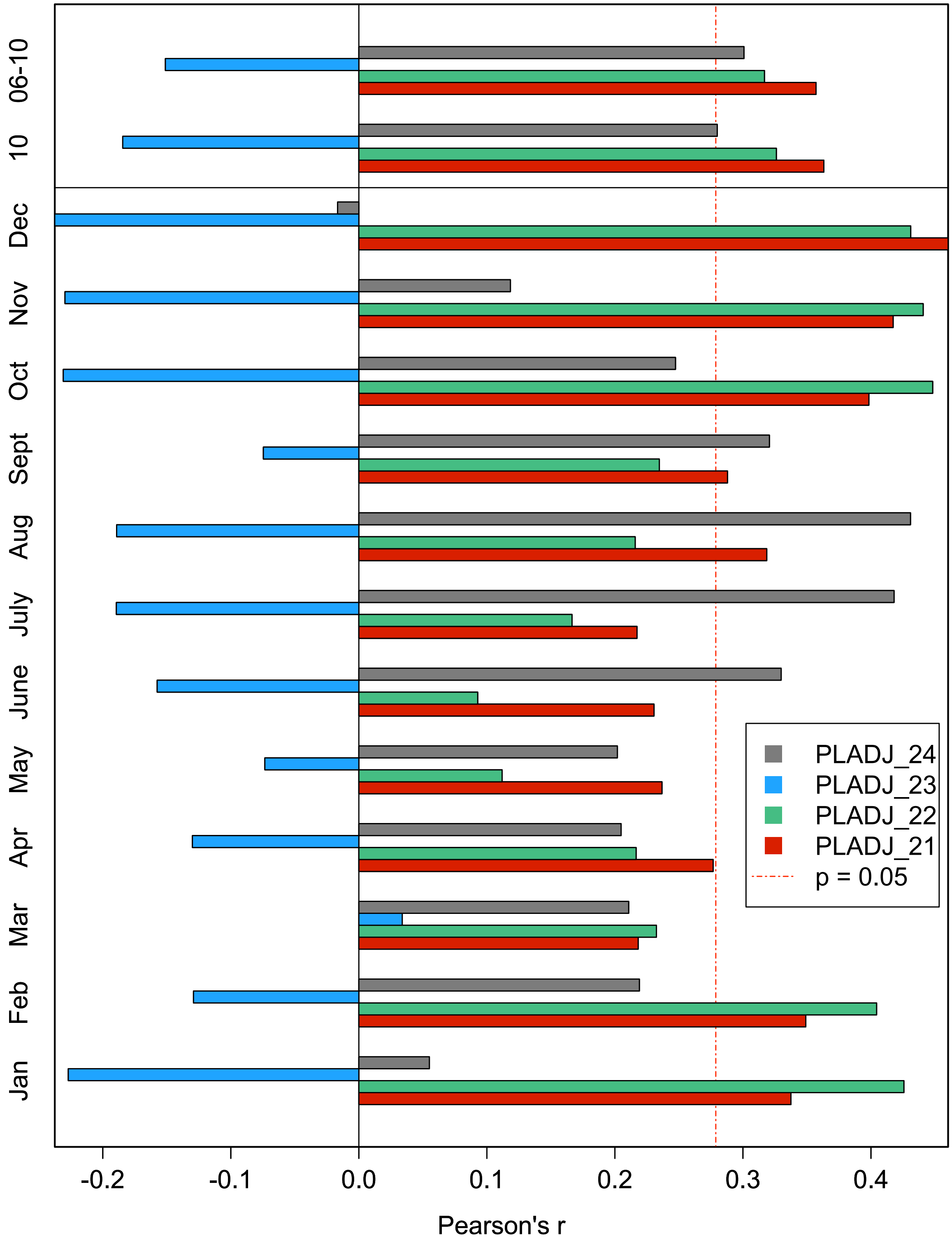

Figure 4.25. Variability in the Relationships Between UHI Intensity and Urban Spatial Metrics by Month in 2010

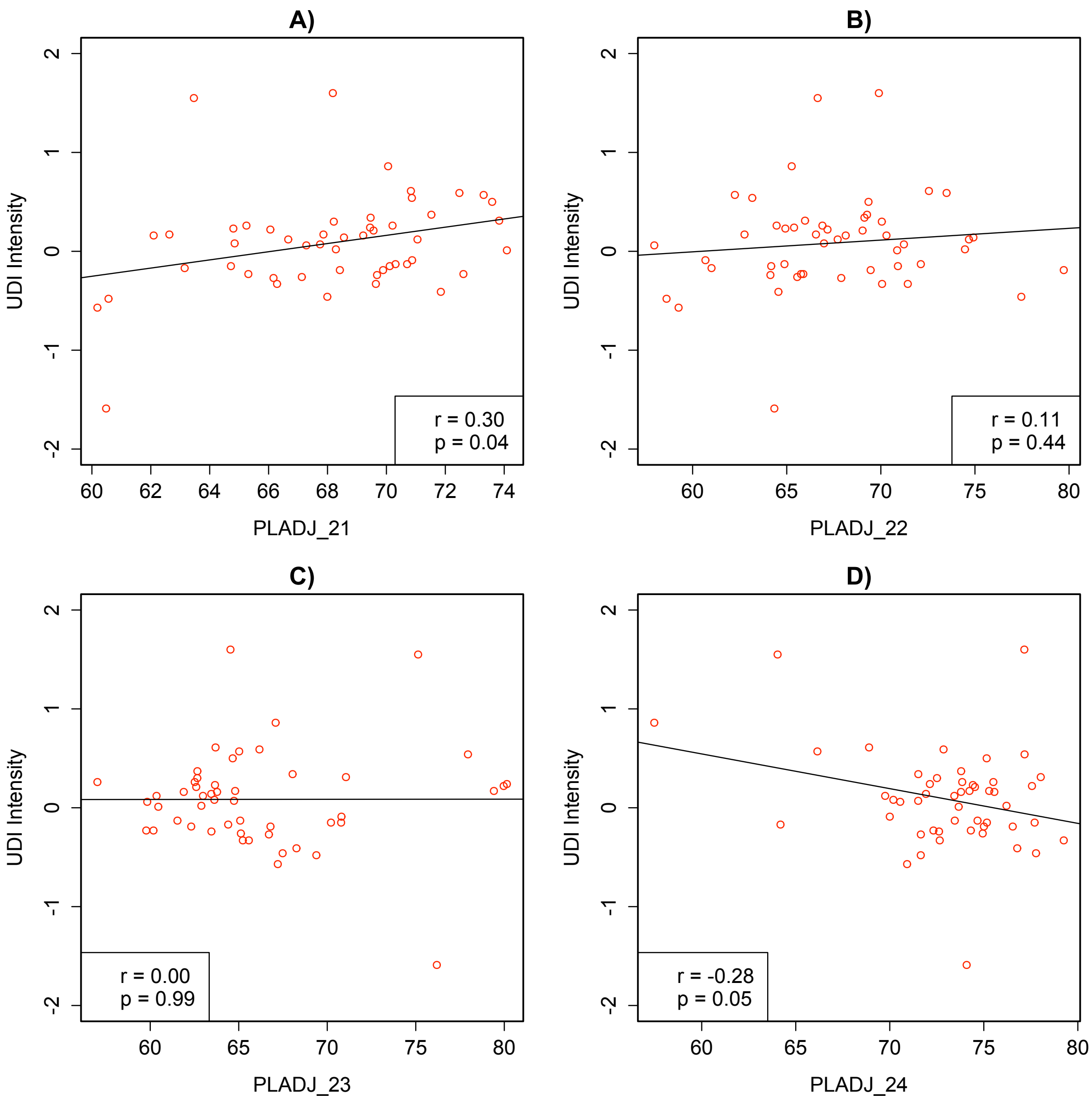

Figure 4.26. Relationships Between Annual Average UDI Intensity in 2010 and Urban Spatial Metrics

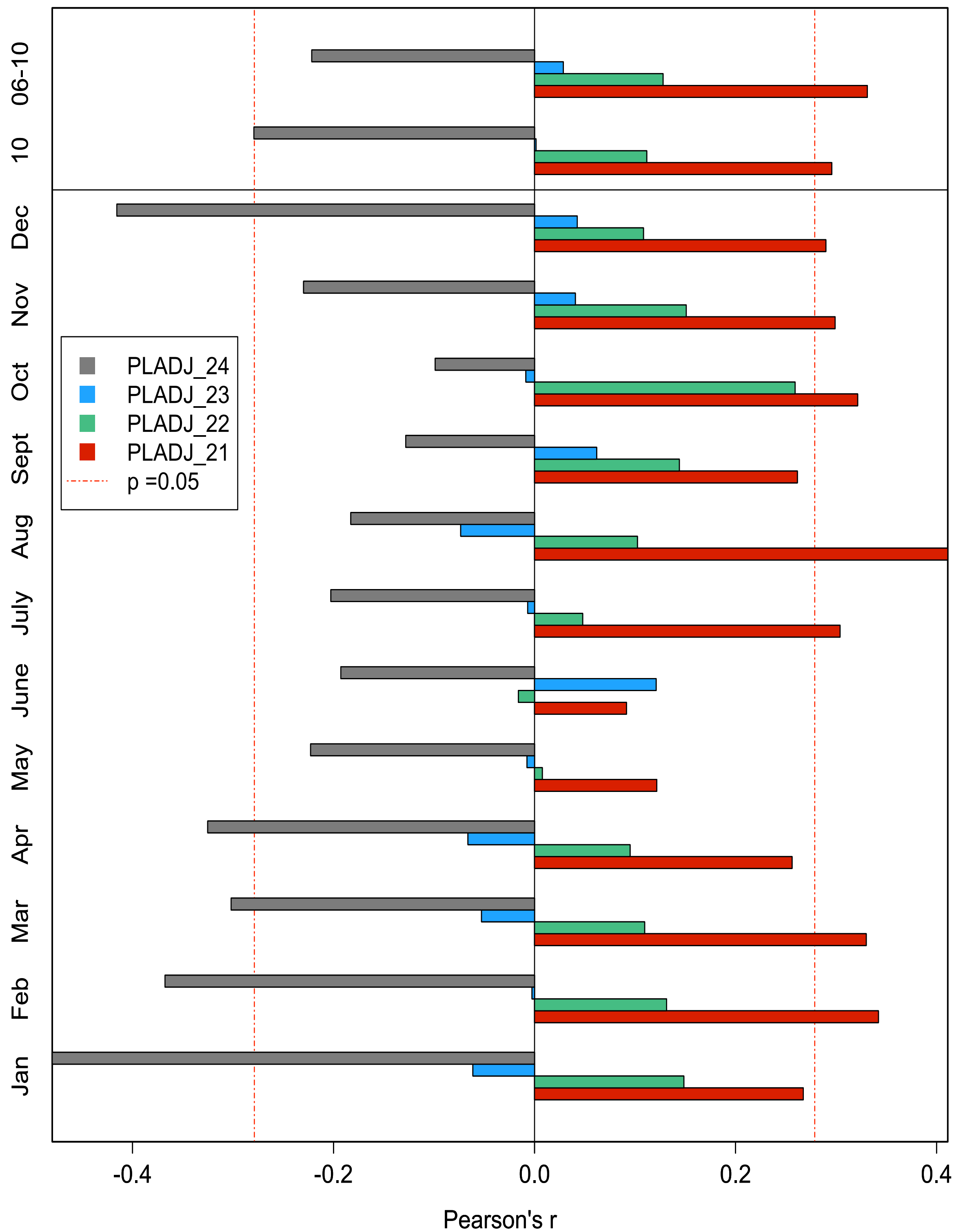

Figure 4.27. Variability in the Relationships Between UDI Intensity and Urban Spatial Metrics by Month in 2010

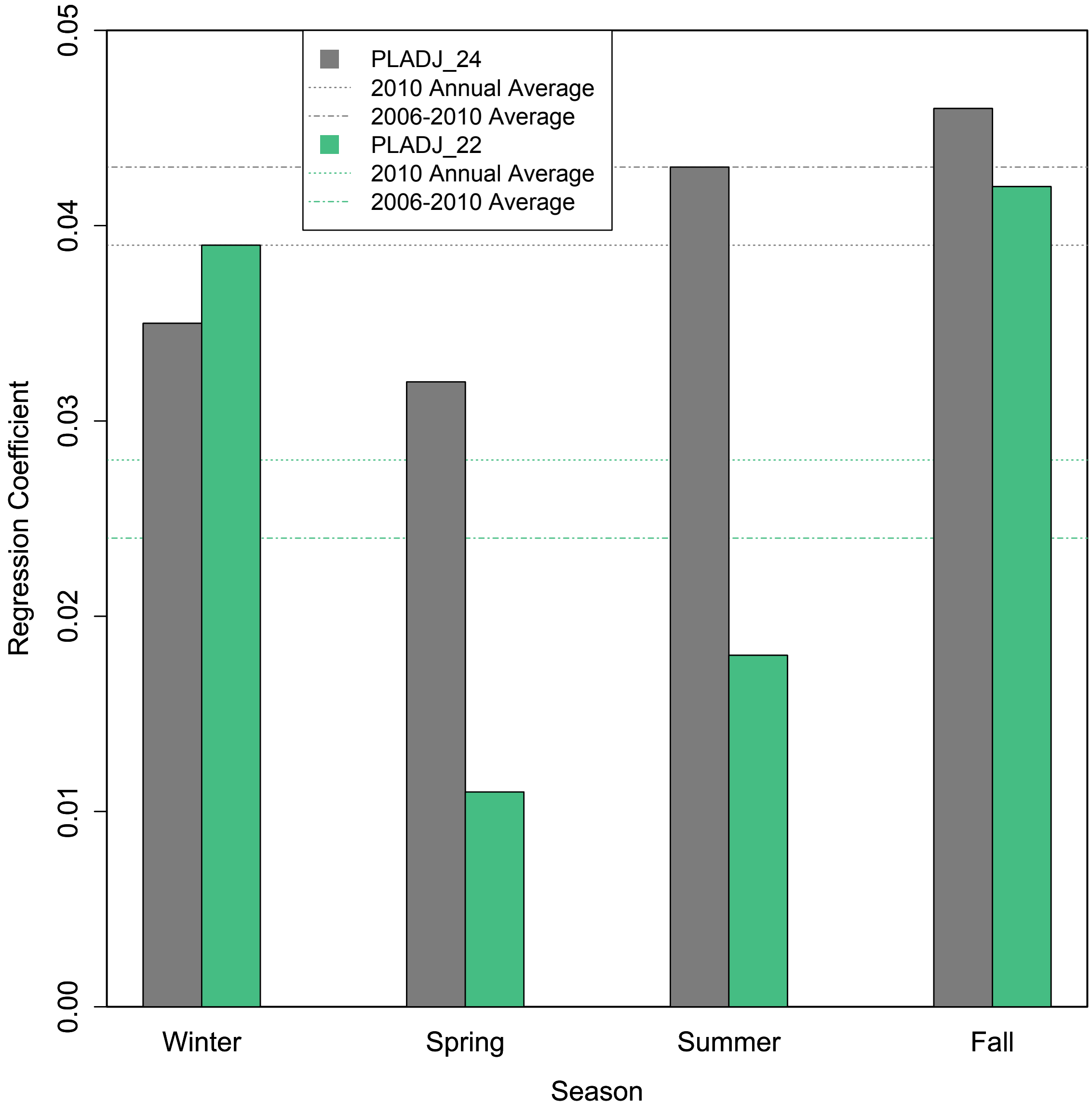

Figure 4.28. Regression Coefficients for PLADJ_24 and PLADJ_22 in the UHI Intensity Models

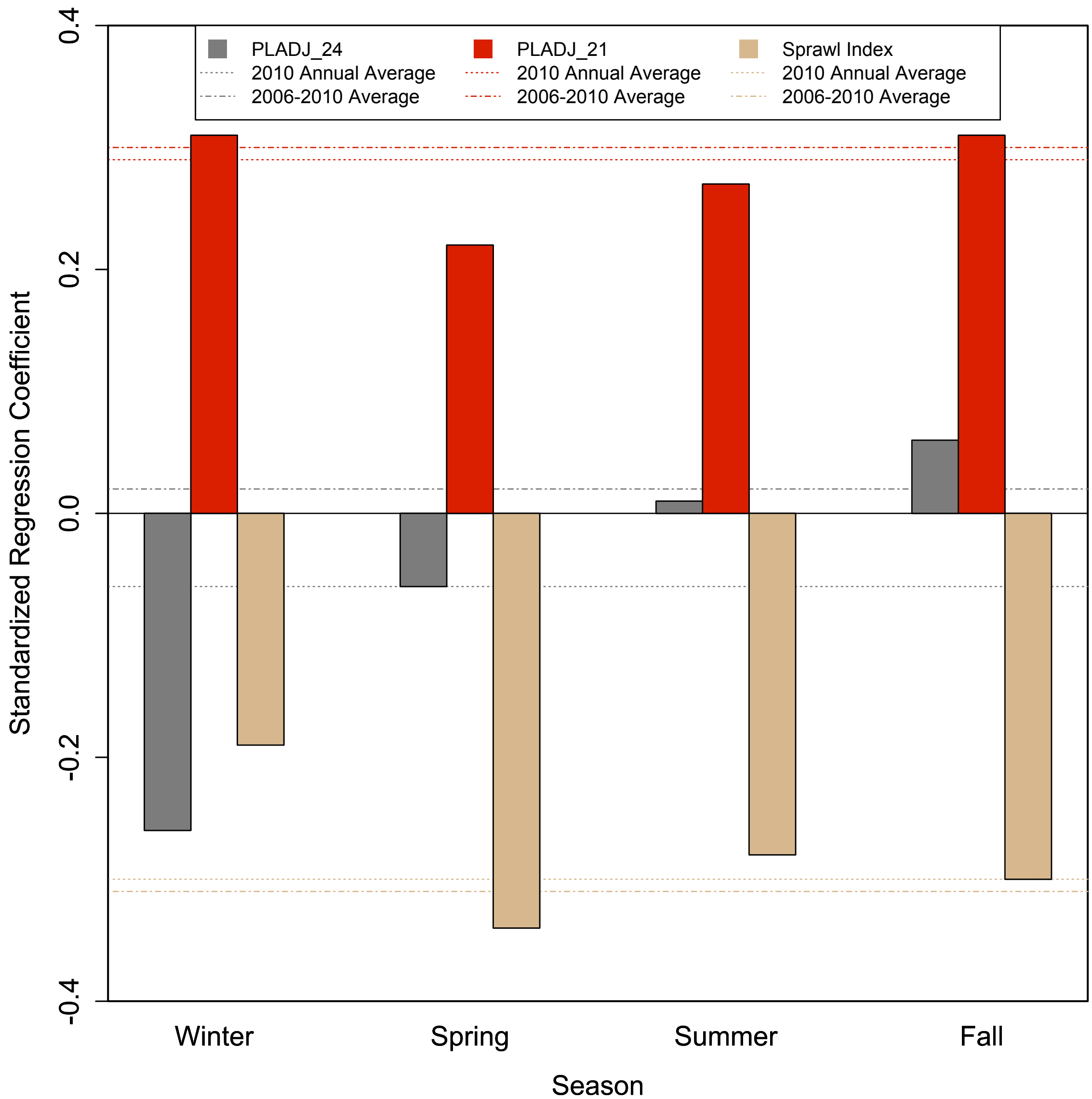

Figure 4.29. Standardized Regression Coefficients for PLADJ_24, PLADJ_21 and Sprawl Index in the UDI Intensity Models

Table 4.1. Ten Most Intense UHIs by Each Rural Definition

MSA	50 km Buffer	MSA	Elevation Control	MSA	Elevation and Urban Control
Salt Lake City	2.65	Miami	1.35	Salt Lake City	1.49
Sacramento	2.46	Salt Lake City	1.26	Miami	1.34
Phoenix	2.32	Louisville	1.12	Louisville	1.12
Los Angeles	2.32	Cleveland	1.06	Cleveland	1.04
Denver	2.01	Jacksonville	0.91	Jacksonville	0.92
San Diego	1.96	Los Angeles	0.90	Baltimore	0.89
Seattle	1.83	Minneapolis	0.82	Los Angeles	0.85
Portland	1.73	Tampa	0.81	San Francisco	0.85
Miami	1.35	Dallas	0.74	Tampa	0.84
New York	1.32	San Francisco	0.74	Minneapolis	0.82

Table 4.2. Standard Deviations of the Three UHI Intensities Calculated by Each Rural Definition

MSA	UHI Std. Dev.	MSA	UHI Std. Dev.
Sacramento	1.14	Chicago	0.09
San Diego	1.13	Detroit	0.07
Denver	1.11	Columbus	0.07
Las Vegas	1.06	Memphis	0.07
Phoenix	0.95	Minneapolis	0.06
Los Angeles	0.83	Washington	0.06
Portland	0.81	Raleigh	0.05
Buffalo	0.80	St. Louis	0.05
Seattle	0.75	Richmond	0.05
Salt Lake City	0.75	Atlanta	0.04
Boston	0.68	Cleveland	0.04
Providence	0.48	Charlotte	0.03
New York	0.43	Birmingham	0.03
Riverside	0.37	Milwaukee	0.03
Pittsburgh	0.35	Indianapolis	0.02
San Francisco	0.28	Austin	0.02
San Antonio	0.24	Nashville	0.02
Hartford	0.23	Tampa	0.02
Philadelphia	0.18	Orlando	0.02
Houston	0.18	Louisville	0.01
Dallas	0.14	Kansas City	0.01
Baltimore	0.14	Miami	0.01
Cincinnati	0.12	Jacksonville	0.00
New Orleans	0.10	Oklahoma City	0.00
San Jose	0.09	Virginia Beach	0.00

Table 4.3. Ten Most Intense UDIs by Each Rural Definition

MSA	50 km Buffer	MSA	Elevation Control	MSA	Elevation and Urban Control
Las Vegas	-0.41	Las Vegas	-1.59	Las Vegas	-1.59
Atlanta	-0.36	Boston	-0.61	Boston	-0.57
Milwaukee	-0.35	Chicago	-0.42	Providence	-0.48
Charlotte	-0.27	New York	-0.39	Chicago	-0.46
Chicago	-0.24	Milwaukee	-0.37	New York	-0.41
Richmond	-0.18	Seattle	-0.35	Milwaukee	-0.33
Oklahoma City	-0.15	Richmond	-0.25	Seattle	-0.33
New Orleans	-0.09	Hartford	-0.23	Washington	-0.27
Kansas City	-0.05	Atlanta	-0.22	Philadelphia	-0.26
Austin	-0.03	Washington	-0.21	Richmond	-0.24

Table 4.4. Standard Deviations of the Three UDI Intensities Calculated by Each Rural Definition

MSA	UDI Std. Dev.	MSA	UDI Std. Dev.
Los Angeles	2.51	Birmingham	0.09
San Diego	2.29	Atlanta	0.08
Sacramento	1.75	Cincinnati	0.07
Denver	0.99	Nashville	0.07
Seattle	0.97	Columbus	0.06
Salt Lake City	0.94	Raleigh	0.06
Portland	0.80	New Orleans	0.06
Las Vegas	0.68	Austin	0.05
Boston	0.55	Louisville	0.05
Buffalo	0.54	Memphis	0.05
San Jose	0.52	St. Louis	0.04
Riverside	0.41	Charlotte	0.04
Providence	0.39	Kansas City	0.04
Phoenix	0.32	Baltimore	0.04
Hartford	0.31	Cleveland	0.04
New York	0.29	Richmond	0.03
Washington	0.22	Milwaukee	0.02
San Antonio	0.22	Minneapolis	0.02
Houston	0.20	Tampa	0.01
Pittsburgh	0.18	Oklahoma City	0.01
Dallas	0.14	Jacksonville	0.01
Philadelphia	0.13	Orlando	0.00
San Francisco	0.12	Miami	0.00
Chicago	0.11	Indianapolis	0.00
Detroit	0.09	Virginia Beach	0.00

Table 4.5. UHI Rankings in 2010 Based on Annual Average Minimum Temperature

MSA	UHI	MSA	UHI
Salt Lake City	1.49	Charlotte	0.31
Miami	1.34	New Orleans	0.29
Louisville	1.12	Milwaukee	0.29
Cleveland	1.04	Houston	0.28
Jacksonville	0.92	Hartford	0.26
Baltimore	0.89	Atlanta	0.25
Los Angeles	0.85	Kansas City	0.25
San Francisco	0.85	San Jose	0.25
Tampa	0.84	Oklahoma City	0.23
Minneapolis	0.82	Indianapolis	0.17
Dallas	0.74	Orlando	0.17
Birmingham	0.71	Memphis	0.17
St. Louis	0.71	Raleigh	0.13
Detroit	0.68	Austin	0.11
Phoenix	0.67	Denver	0.09
Virginia Beach	0.67	Nashville	0.08
Washington	0.63	Cincinnati	0.07
New York	0.57	Philadelphia	0.02
Seattle	0.53	San Diego	0.01
Chicago	0.52	Buffalo	-0.14
Sacramento	0.47	Richmond	-0.19
San Antonio	0.47	Boston	-0.43
Columbus	0.44	Providence	-0.61
Pittsburgh	0.34	Las Vegas	-0.76
Portland	0.32	Riverside	-1.37

Table 4.6. UDI Rankings in 2010 Based on Annual Average Dew Point Temperature

MSA	UDI	MSA	UDI
Las Vegas	-1.59	Orlando	0.12
Boston	-0.57	St. Louis	0.12
Providence	-0.48	Denver	0.14
Chicago	-0.46	Minneapolis	0.16
New York	-0.41	Birmingham	0.16
Milwaukee	-0.33	Baltimore	0.17
Seattle	-0.33	San Diego	0.17
Washington	-0.27	Nashville	0.21
Philadelphia	-0.26	Los Angeles	0.22
Richmond	-0.24	Pittsburgh	0.23
Atlanta	-0.23	San Jose	0.24
Charlotte	-0.23	San Antonio	0.26
Dallas	-0.19	Louisville	0.26
New Orleans	-0.19	Jacksonville	0.30
Hartford	-0.17	Detroit	0.31
Houston	-0.15	Tampa	0.34
Portland	-0.15	Columbus	0.37
Oklahoma City	-0.13	Memphis	0.50
Buffalo	-0.13	San Francisco	0.54
Sacramento	-0.09	Raleigh	0.57
Indianapolis	0.01	Miami	0.59
Kansas City	0.02	Cleveland	0.61
Austin	0.06	Phoenix	0.86
Virginia Beach	0.07	Riverside	1.55
Cincinnati	0.08	Salt Lake City	1.60

Table 4.7. UHI Intensity Decadal Rate of Change from 1950 – 2012

MSA	Decadal Change	MSA	Decadal Change
Las Vegas	0.35	New Orleans	0.01
Salt Lake City	0.18	Orlando	0.01
Phoenix	0.11	Dallas	0.00
Sacramento	0.08	Atlanta	0.00
Miami	0.07	Portland	0.00
Kansas City	0.05	Washington	0.00
Columbus	0.05	Nashville	-0.01
Riverside	0.05	San Francisco	-0.01
Tampa	0.04	Philadelphia	-0.01
Louisville	0.04	Raleigh	-0.01
Oklahoma City	0.04	Detroit	-0.01
Minneapolis	0.04	San Jose	-0.02
Cleveland	0.04	Hartford	-0.02
Jacksonville	0.03	Indianapolis	-0.02
Richmond	0.03	St. Louis	-0.02
Austin	0.03	Boston	-0.03
Birmingham	0.03	Providence	-0.03
Seattle	0.03	Memphis	-0.03
Charlotte	0.02	Los Angeles	-0.04
Chicago	0.02	Buffalo	-0.04
Baltimore	0.02	Pittsburgh	-0.07
Milwaukee	0.02	Virginia Beach	-0.08
New York	0.02	San Diego	-0.09
San Antonio	0.02	Cincinnati	-0.09
Houston	0.01	Denver	-0.10

Table 4.8. UDI Intensity Decadal Rate of Change from 1950 – 2012

MSA	Decadal Change	MSA	Decadal Change
San Jose	-0.11	Indianapolis	-0.02
Jacksonville	-0.10	Columbus	-0.02
Salt Lake City	-0.08	Hartford	-0.01
Washington	-0.08	Philadelphia	-0.01
Sacramento	-0.08	Providence	-0.01
Nashville	-0.07	Atlanta	-0.01
Richmond	-0.06	Pittsburgh	-0.01
Dallas	-0.06	Phoenix	-0.01
San Francisco	-0.05	Cincinnati	-0.01
Raleigh	-0.05	Milwaukee	-0.01
Birmingham	-0.05	Charlotte	0.00
Virginia Beach	-0.04	Boston	0.00
Oklahoma City	-0.04	New York	0.00
Denver	-0.04	Los Angeles	0.00
Louisville	-0.04	San Diego	0.01
Orlando	-0.03	St. Louis	0.01
Cleveland	-0.03	San Antonio	0.01
Minneapolis	-0.03	Buffalo	0.01
Portland	-0.03	Tampa	0.02
Detroit	-0.03	Memphis	0.02
New Orleans	-0.03	Austin	0.02
Kansas City	-0.03	Baltimore	0.02
Houston	-0.03	Seattle	0.12
Chicago	-0.03	Riverside	0.14
Miami	-0.02	Las Vegas	0.31

Table 4.9. Regression Model 1: Annual Average UHI Intensity in 2010 is the Dependent Variable (No Cities were Omitted)

Independent Variable	Coefficient	Std. Coefficient	P-Value	Sig. Level
Constant	-1.929		0.18	
PLADJ_22	0.011	0.10	0.43	
PLADJ_24	0.043	0.33	0.02	*
PLAND_31	-0.142	-0.30	0.04	*
AWMPFD_41	-0.720	-0.40	0.00	**
PLAND_52	-0.047	-0.39	0.04	*
Aridity	-0.017	-0.37	0.02	*
R-Squared	0.44			
Adjusted R-Squared	0.37			
F-Statistic	5.71		0.00	***

Sig Levels: - = p<0.10; * = p<0.05; ** = p< 0.01; *** = p ~ 0.000

Table 4.10. Regression Model 2: Annual Average UHI intensity in 2010 is the Dependent Variable (Miami, Tampa, Phoenix, Las Vegas and Riverside were Omitted)

Independent Variable	Coefficient	Std. Coefficient	P-Value	Sig. Level
Constant	-9.857		0.00	***
PLADJ_22	0.028	0.33	0.02	*
PLADJ_24	0.039	0.30	0.03	*
PLAND_31	0.380	0.28	0.03	*
AWMPFD_41	5.161	0.42	0.00	**
PLAND_52	-0.028	-0.16	0.28	
Aridity	-0.020	-0.49	0.00	**
R-Squared	0.46			
Adjusted R-Squared	0.38			
F-Statistic	5.46		0.00	***

Sig Levels: - = p<0.10; * = p<0.05; ** = p< 0.01; *** = p ~ 0.000

Table 4.11. Regression Model 3: Annual Average UHI Intensity from 2006 to 2010 is the Dependent Variable (Miami, Tampa, Phoenix, Las Vegas and Riverside were Omitted)

Independent Variable	Coefficient	Std. Coefficient	P-Value	Sig. Level
Constant	-8.463		0.00	***
PLADJ_22	0.024	0.28	0.05	-
PLADJ_24	0.043	0.32	0.02	*
PLAND_31	0.390	0.28	0.03	*
AWMPFD_41	4.046	0.32	0.02	*
PLAND_52	-0.039	-0.23	0.14	
Aridity	-0.023	-0.55	0.00	***
R-Squared	0.46			
Adjusted R-Squared	0.38			
F-Statistic	5.47		0.00	***

Sig Levels: - = p<0.10; * = p<0.05; ** = p< 0.01; *** = p ~ 0.000

Table 4.12. Regression Model 4: Average Winter UHI Intensity in 2010 is the Dependent Variable (Miami, Tampa, Phoenix, Las Vegas and Riverside were Omitted)

Independent Variable	Coefficient	Std. Coefficient	P-Value	Sig. Level
Constant	-9.921		0.00	***
PLADJ_22	0.039	0.42	0.00	**
PLADJ_24	0.035	0.24	0.07	-
PLAND_31	0.432	0.29	0.03	*
AWMPFD_41	4.776	0.35	0.01	*
PLAND_52	-0.054	-0.29	0.06	-
Aridity	-0.021	-0.44	0.00	**
R-Squared	0.47			
Adjusted R-Squared	0.38			
F-Statistic	5.55		0.00	***

Sig Levels: - = p<0.10; * = p<0.05; ** = p< 0.01; *** = p ~ 0.000

Table 4.13. Regression Model 5: Average Spring UHI Intensity in 2010 is the Dependent Variable (Miami, Tampa, Phoenix, Las Vegas and Riverside were Omitted)

Independent Variable	Coefficient	Std. Coefficient	P-Value	Sig. Level
Constant	-7.194		0.01	**
PLADJ_22	0.011	0.14	0.39	
PLADJ_24	0.032	0.26	0.09	-
PLAND_31	0.341	0.27	0.07	-
AWMPFD_41	4.291	0.37	0.02	*
PLAND_52	-0.028	-0.18	0.31	
Aridity	-0.019	-0.47	0.01	**
R-Squared	0.32			
Adjusted R-Squared	0.21			
F-Statistic	3.00		0.02	*

Sig Levels: - = p<0.10; * = p<0.05; ** = p< 0.01; *** = p ~ 0.000

Table 4.14. Regression Model 6: Average Summer UHI Intensity in 2010 is the Dependent Variable (Miami, Tampa, Phoenix, Las Vegas and Riverside were Omitted)

Independent Variable	Coefficient	Std. Coefficient	P-Value	Sig. Level
Constant	-10.598		0.00	***
PLADJ_22	0.018	0.23	0.10	-
PLADJ_24	0.043	0.35	0.01	*
PLAND_31	0.247	0.20	0.12	
AWMPFD_41	5.950	0.53	0.00	***
PLAND_52	0.007	0.05	0.76	
Aridity	-0.015	-0.40	0.01	**
R-Squared	0.46			
Adjusted R-Squared	0.38			
F-Statistic	5.42		0.00	***

Sig Levels: - = p<0.10; * = p<0.05; ** = p< 0.01; *** = p ~ 0.000

Table 4.15. Regression Model 7: Average Fall UHI Intensity in 2010 is the Dependent Variable (Miami, Tampa, Phoenix, Las Vegas and Riverside were Omitted)

Independent Variable	Coefficient	Std. Coefficient	P-Value	Sig. Level
Constant	-11.728		0.00	***
PLADJ_22	0.042	0.39	0.01	**
PLADJ_24	0.046	0.27	0.04	*
PLAND_31	0.503	0.29	0.03	*
AWMPFD_41	5.631	0.35	0.01	*
PLAND_52	-0.035	-0.16	0.29	
Aridity	-0.027	-0.50	0.00	**
R-Squared	0.48			
Adjusted R-Squared	0.39			
F-Statistic	5.78		0.00	***

Sig Levels: - = p<0.10; * = p<0.05; ** = p< 0.01; *** = p ~ 0.000

Table 4.16. Regression Model 8: Average Annual UDI/UME Intensity in 2010 is the Dependent Variable

Independent Variable	Coefficient	Std. Coefficient	P-Value	Sig. Level
Constant	-7.148		0.04	*
PLADJ_21	0.041	0.29	0.03	*
PLADJ_24	-0.007	-0.06	0.70	
Sprawl Index	-0.006	-0.30	0.03	*
AWMPFD_71	4.569	0.24	0.08	-
AWMSI_82	0.156	0.19	0.18	
Land Area	-3.67E-11	-0.14	0.29	
R-Squared	0.40			
Adjusted R-Squared	0.31			
F-Statistic	4.35		0.00	**

Sig Levels: - = p<0.10; * = p<0.05; ** = p< 0.01; *** = p ~ 0.000

Table 4.17. Regression Model 9: Annual Average UDI/UME Intensity from 2006 to 2010 is the Dependent Variable

Independent Variable	Coefficient	Std. Coefficient	P-Value	Sig. Level
Constant	-8.983		0.01	*
PLADJ_21	0.044	0.30	0.02	*
PLADJ_24	0.003	0.02	0.87	
Sprawl Index	-0.006	-0.31	0.02	*
AWMPFD_71	5.416	0.28	0.04	*
AWMSI_82	0.147	0.18	0.22	
Land Area	-4.60E-11	-0.17	0.19	
R-Squared	0.41			
Adjusted R-Squared	0.32			
F-Statistic	4.57		0.00	**

Sig Levels: - = p<0.10; * = p<0.05; ** = p< 0.01; *** = p ~ 0.000

Table 4.18. Regression Model 10: Average Winter UDI/UME Intensity in 2010 is the Dependent Variable

Independent Variable	Coefficient	Std. Coefficient	P-Value	Sig. Level
Constant	-3.214		0.26	
PLADJ_21	0.039	0.31	0.01	*
PLADJ_24	-0.029	-0.26	0.07	-
Sprawl Index	-0.003	-0.19	0.13	
AWMPFD_71	2.141	0.13	0.32	
AWMSI_82	0.231	0.32	0.02	*
Land Area	-1.11E-11	-0.05	0.70	
R-Squared	0.48			
Adjusted R-Squared	0.40			
F-Statistic	5.98		0.00	***

Sig Levels: - = p<0.10; * = p<0.05; ** = p< 0.01; *** = p ~ 0.000

Table 4.19. Regression Model 11: Average Spring UDI/UME Intensity in 2010 is the Dependent Variable

Independent Variable	Coefficient	Std. Coefficient	P-Value	Sig. Level
Constant	-5.922		0.14	
PLADJ_21	0.035	0.22	0.10	-
PLADJ_24	-0.008	-0.06	0.69	
Sprawl Index	-0.008	-0.34	0.02	*
AWMPFD_71	4.060	0.19	0.18	
AWMSI_82	0.155	0.17	0.25	
Land Area	-4.28E-11	-0.14	0.28	
R-Squared	0.35			
Adjusted R-Squared	0.25			
F-Statistic	3.52		0.01	**

Sig Levels: - = p<0.10; * = p<0.05; ** = p< 0.01; *** = p ~ 0.000

Table 4.20. Regression Model 12: Average Summer UDI/UME Intensity in 2010 is the Dependent Variable

Independent Variable	Coefficient	Std. Coefficient	P-Value	Sig. Level
Constant	-10.27		0.02	*
PLADJ_21	0.045	0.27	0.05	*
PLADJ_24	0.002	0.01	0.93	
Sprawl Index	-0.007	-0.28	0.05	-
AWMPFD_71	6.735	0.30	0.04	*
AWMSI_82	0.101	0.10	0.48	
Land Area	-5.79E-11	-0.18	0.17	
R-Squared	0.36			
Adjusted R-Squared	0.26			
F-Statistic	3.61		0.01	**

Sig Levels: - = p<0.10; * = p<0.05; ** = p< 0.01; *** = p ~ 0.000

Table 4.21. Regression Model 13: Average Fall UDI/UME Intensity in 2010 is the Dependent Variable

Independent Variable	Coefficient	Std. Coefficient	P-Value	Sig. Level
Constant	-9.163		0.02	*
PLADJ_21	0.045	0.31	0.02	*
PLADJ_24	0.007	0.06	0.72	
Sprawl Index	-0.006	-0.30	0.04	*
AWMPFD_71	5.274	0.27	0.06	-
AWMSI_82	0.143	0.17	0.26	
Land Area	-3.43E-11	-0.12	0.35	
R-Squared	0.36			
Adjusted R-Squared	0.26			
F-Statistic	3.68		0.01	**

Sig Levels: - = p<0.10; * = p<0.05; ** = p< 0.01; *** = p ~ 0.000

CHAPTER 5

CONCLUSIONS

5.1 Summary of Major Findings

Although it has been well documented that urban land surfaces alter regional moisture and energy balances, the precise nature of how the spatial configuration of cities influences these effects is still not fully understood. The extant literature has suggested that both sprawling (Stone and Rodgers 2001) and high-density (Coutts et al. 2007) urban development can amplify the UHI effect and these potential linkages have been under researched with regard to UDI/UME intensities. The overarching goal of this thesis was to elucidate how urban morphology, or the spatial configuration of cities, impacts the UHI and UDI/UME effects. The research was broken down into three primary objectives: 1) develop a systematic grid-based methodology to estimate the canopy level UHI/UDI intensities, 2) quantify urban form at the MSA scale using spatial metrics and 3) evaluate the degree of association between the spatial arrangement of cities and their subsequent UHI/UDI intensities.

A systematic technique that utilized PRISM climate data was developed to estimate the UHI and UDI/UME intensities of the 50 largest MSAs in the United States. In 2010, the average annual UHI intensity of all fifty cities was 0.37 degrees Celsius. Although the magnitude of the annual average UHI effect was much less than the documented maximum UHI intensity, it was expected since the annual average incorporated both those nights that were ideally and very poorly suited for UHI formation. The most intense UHIs were observed in Salt Lake City, Miami and Louisville while the strongest UCIs occurred in Riverside and Las Vegas. The hotspot analysis revealed that the clusters of UCIs in the Southwest and Northeast portions of the country were significant. The ANOVA largely corroborated these findings, as cities located in the Northeastern Census Region had significantly less intense UHI effects. With regard to the seasonality of the UHI effect in 2010, there was no clear overarching trend. Instead, it appeared that the seasonality was dependent upon the highly localized characteristics of each city. Historically from 1950 to 2012, the average UHI intensity has increased by 0.013 degrees Celsius per decade. This is of comparable magnitude to the UHI growth observed by Hansen et al. (2001) but noticeably smaller than the estimates of Stone (2007). Since rural temperature trends are affected by any warming attributable to greenhouse gas emissions, finding that most cities are characterized by increasing UHI intensities suggests that urban areas are warming at a faster rate than the planet as a whole. The combined effect of increasing UHI intensities and broader scale climate change is likely to produce exceedingly warm urban environments in the future.

In terms of the UDI/UME effect, dew point temperatures were on average 0.08 degrees Celsius higher within cities relative to their surrounding natural environments in 2010. Intense UMEs occurred in Phoenix, Riverside and Salt Lake City while the strongest UDI effect was observed in Las Vegas. A hotspot analysis was conducted to analyze the geography of the UDI/UME effect, which indicated that the cluster of UDIs in the Northeast was statistically significant. The ANOVA supported these findings since it revealed that the UDI effect was significantly more intense for cities in the Northeastern Census Region. Similar to the intra-annual variability of the UHI effect, no overarching seasonal pattern in UDI/UME intensities was identified. Instead, the seasonality seemed to be governed by conditions very specific to each city. Historically, there was also no clear trend in UDI/UME intensities partially because the recent portion of the record was fairly volatile and suspected to be potentially influenced by station inhomogeneities.

A positive relationship between UHI intensity and UME intensity was observed. This suggests that more intense UHIs allow evapotranspiration to continue longer within cities relative to the surrounding natural environment after sunset, which would increase the moisture content of the urban atmosphere. This positive correlation held true when analyzing the annual average effects as well as the individual seasonal effects. Overall, since urban environments have a propensity to be warmer, a feedback is established that can make them relatively moister as well. This poses serious health ramifications since urban dwellers are not only exposed to more heat but also higher levels of atmospheric moisture, which undoubtedly increases heat stress.

To fulfill objective two, the urban morphologies of each city were quantified using a suite of spatial metrics. The most substantial differences in urban morphology existed between the cities located in the Western and Southern Census Regions. On average, the proportion of high-intensity urban development in Western cities was 8%, which was twice as much as a typical Southern city. The dominance of the largest high-intensity urban patch was also significantly different, as it occupied over 1% of the urban landscape in Western cities but only approximately 0.5% in Southern cities. The spatial contiguity of high-intensity urban development did not vary by Census Region but the contiguity of developed open space was substantially greater in Southern cities. Collectively, the lack of high-intensity urban development (as indicated by PLAND_24), the poorly defined urban cores (as indicated by LPI_24) and the highly contiguous developed open space (as indicated by PLADJ_21) characteristic of Southern cities are indicative of the general sprawling urban morphologies located in that portion of the United States. Contrastingly, the urban cores of Western cities were better defined and more dominant. To test how the spatial metrics related to existing measures of urban form, correlations between the metrics and the Ewing et al. (2003) Sprawl Index were calculated. Overall, the majority of metrics displayed significant relationships with the Sprawl Index. A noticeable exception was the spatial contiguity of developed open space (PLADJ_21), which seemed to evaluate a unique aspect of urban form.

Both bivariate and multivariate statistical techniques were used to address the third objective, which was to analyze how the spatial configuration of cities influenced the UHI/UDI intensities. First, bivariate correlations were calculated between the 2010 annual average UHI intensities and a series of hypothesized control variables. Surprisingly, no significant relationships were observed between UHI intensity and city area, water area, population, population density, aridity or wind speed. Of the spatial metrics calculated for each urban LULC category, spatial contiguity (PLADJ) had the strongest correlations with UHI intensity. It is worth noting that the amount of urban land cover was not as strongly correlated with the UHI effect, which suggest that the spatial configuration of urban development, not merely its quantity, is of importance. More contiguous developed open space, low-intensity urban development and high-intensity urban development were all associated with an amplification of the UHI effect. This suggests that sprawling and high-density urban development patterns both have the propensity to enhance UHI intensities if they are highly contiguous, which partially reconciles the contrasting findings of Stone (2012) and Coutts et al. (2007). Of course, these relationships varied seasonally with the contiguity of high-intensity urban development being most strongly correlated with the UHI effect in the summer. Contrastingly, the contiguity of low-intensity urban development and developed open space were more strongly related to the UHI effect in the winter.

The multivariate regression models estimated for the UHI effect generally corroborated the findings from the bivariate analysis. Overall, the models performed fairly well as they explained between roughly 30% and half of the variability in UHI intensities. The estimated partial slope coefficients suggested that increasing the contiguity of urban development across a spectrum of intensity levels would enhance the UHI effect, even when accounting for potential confounding factors and the influence of non-urban LULCs. Specifically, a ten percentage point increase in the spatial contiguity of low or high-intensity urban development was predicted to enhance the UHI effect by a tenth to almost half a degree Celsius.

A similar bivariate and multivariate approach was used to investigate the relationships between urban morphology and UDI/UME intensities. In terms of the potential control variables, no strong correlations were observed between UDI/UME intensity and city area, water area, population, population density or wind speed. The relationship between the UDI/UME effect and aridity was marginally significant, with more arid conditions generally associated with more intense UMEs. For the urban development LULC categories, spatial contiguity (PLADJ) was the most strongly correlated metric with UDI/UME intensities. More contiguous developed open space was associated with an enhancement of the UME effect while more contiguous high-intensity development was generally indicative of a stronger UDI effect. The relationship between UDI intensity and the contiguity of high-intensity urban development displayed a notable seasonal trend, as they were most strongly correlated during the winter. Contrastingly, the correlations between UME intensity and the spatial contiguity of developed open space were fairly stable throughout the year with the exceptions of May and June.

The multivariate regression models estimated for the UDI/UME effect reaffirmed the findings from the bivariate analysis. Overall, the models had respectable predictive power as they explained between 35% and almost half of the variability in UDI/UME intensities. The individual partial slope coefficients suggested that increasing the spatial contiguity of developed open space would enhance the UME effect while increasing the spatial contiguity of high-intensity development would magnify the UDI intensity. Specifically, a ten percentage point increase in the spatial contiguity of developed open space was predicted to amplify the UME effect by 0.35 to 0.45 degrees Celsius. Contrastingly, a ten percentage point increase in the spatial contiguity of high-intensity urban development was predicted to increase the winter UDI effect by roughly 0.3 degrees Celsius. It should be noted, however, that this winter relationship was only marginally significant and not observed in any other season or with respect to the annual averages. In addition to the urban spatial metrics, the Ewing et al. (2002) Sprawl Index also had a significant partial effect, which indicated that more sprawling morphologies generally amplified UME intensities. It appears that highly contiguous developed open space and sprawling urban morphologies achieve a delicate balance between the heat contributed by urban land surfaces to power evapotranspiration and maintaining enough vegetation and water vapor sources to create strong UMEs.

5.2 Policy Implications

One underlying motive of this research was to clarify if increasing urban densities is a viable UHI mitigation strategy. Stone (2012) has strongly advocated for urban densification as a measure to mitigate the UHI effect while Coutts et al. (2007) posited that increasing densities would be counteractive since it actually enhances UHI intensities. Based on the correlations and multiple regression models, it was concluded that increasingly contiguous urban development across a range of intensity levels would magnify the UHI effect. Therefore, simply increasing urban densities, which would presumably also increase the contiguity of high-intensity urban development (PLADJ_24), is not likely a viable UHI mitigation strategy. Advocating for increased densities is a particularly troubling mitigation plan given the seasonality exhibited by the correlations. The contiguity of high-intensity urban development was most strongly related with UHI intensities during the summer months, which is precisely when cities are most vulnerable to heat waves. At the opposite end of the urban intensity spectrum, contiguous low-intensity urban development and developed open space also appeared to enhance the UHI effect. However, these relationships were strongest during the winter months. Since this amplification occurred during the colder portion of the year, contiguous low-intensity urban development and developed open space could potentially be beneficial, as it would reduce the amount of energy used to heat buildings.

Interpreting the statistical models very literally, it appears that any morphology that reduces the contiguity of urban development would help mitigate the UHI effect. Obviously, in reality there are certain LULC types that would more successfully accomplish this goal. The inclusion of urban green spaces and parks would decrease the contiguity of urban development while simultaneously providing a cooling influence. Therefore, while increasing densities alone would be injudicious, if the increased densities were accompanied by relevant mitigation strategies that reduced the contiguity of high-intensity urban development, UHI intensities could be successfully reduced. Additionally, mitigation strategies, such as white roofs and green roofs, become more economically feasible at higher density levels (Stone 2012).

One concern for greening urban cores is the interesting result that contiguous developed open space simultaneously enhanced the UHI and UME effects. This would create a dangerous combination from a health perspective since the urban environment would be both hotter and moister. It appears that highly contiguous developed open space achieved a delicate balance between the amount of heat contributed by urban land surfaces to power evapotranspiration and maintaining an adequate quantity of vegetation and water vapor sources to create an UME. It is difficult to determine from this analysis if such an effect needs to be considered when developing urban greening mitigation strategies. However, a more conservative approach would be to focus on albedo altering measures since they provide cooling by directly altering the thermal properties of urban surfaces and therefore do not establish a feedback that could contribute more water vapor to the urban atmosphere.

Overall, planning to reduce UHI intensities is very complex and the policies will likely need to be tailored to individual cities. This is particularly true given that the seasonality of the UHI effect, an important component when evaluating the benefits of a warmer winter versus the detriments of a warmer summer, was very localized to each city. Additionally, policies have to comprehensively address the entire urban system and not simply focus on the UHI and UDI/UME effects in isolation. For example, increased densities can improve air quality, increase the feasibility of public transit, decrease energy consumption and promote more active lifestyles. Therefore, any UHI mitigation strategy must take into account the entire urban metabolism and its complex array of feedbacks, such as the work of Martilli (2014). When the entire urban system is considered qualitatively within the context of this work, it appears that discontiguous high-intensity urban development may be an ideal city configuration.

5.3 Future Research

Throughout the course of this thesis multiple avenues for future research were identified. Firstly, the sample size could be expanded to include more cities. Incorporating additional cities, specifically urban environments in arid climatological settings, could potentially reduce the severity of the influential observations that in some cases made the multivariate regression analysis challenging. Additionally, considering a wider range of city sizes would help more directly test if the often-hypothesized relationship between UHI intensity and population size deteriorated in this particular case because only fifty very large cities were evaluated. Although the methodologies and data sources used herein were tailored to analyze cities in the United States, it would be worthwhile to analyze how the relationships between urban morphology and UHI/UDI intensities for American cities compare to urban environments in other portions of the world.

In addition to increasing the geographical scope of the analysis, additional datasets could be used to characterize both the urban climatological phenomena and the urban morphologies. At the time of writing, PRISM was transitioning to an updated and expanded version of their datasets, which incorporated observations from new station networks. Although a brief portion of the sensitivity analysis used the updated PRISM data, a more detailed and extensive evaluation of the new datasets would enable a useful comparison. Additionally, other gridded climate datasets, such as the product created by the Northeast Regional Climate Center (Beier et al. 2012), could be used to assess the accuracy of the UHI and UDI/UME intensity estimates derived from PRISM. With regard to urban morphology, other LULC data could be used to calculate the spatial metrics. Although NLCD 2011 has yet to be released (it was scheduled to be released in December 2013), using the newer LULC data when it becomes available would more accurately characterize the urban morphologies of the cities included in the study. Another potential alternative would be to explore more detailed LULC datasets that are obtained from sensors with higher resolutions than Landsat.

Due to the plethora of spatial metrics that can be calculated using FRAGSTATS, only those metrics relevant to urban environments, as indicated by previous literature (e.g. Herold et al. 2005; Bereitschaft, and Debbage 2013a), were explored in this investigation. Of course, it would be beneficial to test if any additional spatial metrics are potentially related to urban climatological phenomena. One avenue for future improvement is the more accurate characterization of building heights and the subsequent urban canyons within a given city. This thesis only explicitly analyzed the spatial configuration of cities in a two-dimensional sense, although information regarding the third dimension can be implicitly obtained from the urban intensity levels. Nevertheless, more directly addressing the nature of the urban canyon via the inclusion of additional metrics that consider the height dimension, such as the frontal area index (e.g. Wong et al. 2010), could improve the analysis.

Although steps were taken to control for many possible confounding factors during the multiple regression modeling, the inclusion of all potentially relevant variables is often challenging. The wind speed variable included in the analysis was obtained from fairly coarse resolution re-analysis data and could be improved by using a different re-analysis product (i.e. NARR instead of NCEP/NCAR) or data from meteorological stations. Other meteorological variables that influence UHI and UDI/UME intensities, such as atmospheric pressure and cloud coverage, could also be included in the regression analysis. Additionally, factors that govern the UHI and UDI/UME effects but are not directly related to meteorology, such as energy consumption, the thermal properties of urban materials and pollution, could be incorporated into future models.

Even when considering only the datasets currently included in this investigation, further analysis could be conducted. For example, the UHI and UDI/UME records for the individual cities warrant more attention. A small portion of analysis in this vein was presented when the monthly UHI and UDI/UME intensities for Riverside, Boston and Providence were correlated with meteorological conditions. However, this level of more detailed examination could be expanded to include other cities. In particular, Salt Lake City is of interest since it was hypothesized that the temperature inversions characteristic of the wintertime high-pressure systems were at least partially responsible for its intense UHI effect.

REFERENCES

Ackerman, B. 1987. Climatology of Chicago Area Urban-Rural Differences in Humidity. *Journal of Climate and Applied Meteorology*, 26: 427 – 430.

Arnold, C. & Gibbons, J. 1996. Impervious Surface Coverage: The Emergence of a Key Environmental Indicator. *Journal of the American Planning Association*, 62(2): 243 – 258.

Atkinson, B. 2003. Numerical Modeling of Urban Heat-Island Intensity. *Boundary-Layer Meteorology*, 109(3) 285 – 310.

Beier, C., Signell, S., Luttman, A. & DeGaetano, A. 2012. High-Resolution Climate Change Mapping with Gridded Historical Climate Products. *Landscape Ecology*, 27: 327 – 342.

Bereitschaft, B. & Debbage, K. 2013a. Urban Form, Air Pollution, and CO_2 Emissions in Large U.S. Metropolitan Areas. *The Professional Geographer*, 65(4): 612 – 635.

Bereitschaft, B. & Debbage, K. 2013b. Regional Variations in Urban Fragmentation Among U.S. Metropolitan and Megapolitan Areas. *Applied Spatial Analysis and Policy*, doi: 10.1007/s12061-013-9092-9.

Bhatta, B. 2010. *Analysis of Urban Growth and Sprawl from Remote Sensing Data*. Springer, New York, NY.

Bornstein, R. & Lin, Q. 2000. Urban Heat Islands and Summertime Convective Thunderstorms in Atlanta: Three Case Studies. *Atmospheric Environment*, 34(3): 507 – 516.

Chandler, T. J. 1964. City Growth and Urban Climates, *Weather*, 19: 170 – 171.

Charciarek, T. 2003. Daily Course of Vapor Pressure and Relative Humidity Differences Between Urban and Rural Site in Lodz. *5th International Conference on Urban Climate*, 51 – 54. Available Online: http://nargeo.geo.uni.lodz.pl/~icuc5/text/P_4_14.pdf.

Connors, J., Galletti, C. & Chow, W. 2013. Landscape Configuration and Urban Heat Island Effects: Assessing the Relationship Between Landscape Characteristics and Land Surface Temperature in Phoenix, Arizona. *Landscape Ecology*, 28: 271 – 283.

Coutts, A., Beringer, J. & Tapper, N. 2007. Impact of Increasing Urban Density on Local Climate: Spatial and Temporal Variations in the Surface Energy Balance in Melbourne, Australia. *Journal of Applied Meteorology and Climatology*, 46: 477 – 493.

Daly, C., Halbleib, M., Smith, J., Gibson, W., Doggett, M., Taylor, G., Curtis, J. & Pasteris, P. 2008. Physiographically Sensitive Mapping of Climatological Temperature and Precipitation across the Conterminous United States. *International Journal of Climatology*, 28(15): 2031 – 2064.

De Martonne, E. 1926. Une Nouvelle Fonction Climatologique: L'indice D'Aridite. *La Meteorologie*, 2: 449 – 458.

Emmanuel, R. & Fernando, H. 2007. Urban Heat Islands in Humid and Arid Climates: Role of Urban Form and Thermal Properties in Colombo, Sri Lanka and Phoenix, USA. *Climate Research*, 34: 241 – 251.

Environmental Protection Agency. 2008. Reducing Urban Heat Islands: Compendium of Strategies. Available Online: http://www.epa.gov/hiri/resources/pdf/Basics Compendium.pdf.

Ewing, R., Pendall, R. & Chen, D. 2002. Measuring Sprawl and Its Impact. Available Online: http://www.smartgrowthamerica.org/documents/MeasuringSprawl.PDF.

Ewing, R. & Rong, F. 2008. The Impact of Urban Form on U.S. Residential Energy Use. *Housing Policy Debate*, 19(1): 1 – 30.

Filoso, S., Martinellis, L., Howarth, R., Boyer, E. & Dentener, F. 2006. Human Activities Changing the Nitrogen Cycle in Brazil. *Biogeochemistry*, 79: 61 – 89.

Forman, R. & Godron, M. 1986. *Landscape Ecology*. New York: John Wiley & Sons.

Gaffin, S., Rosenzweig, C., Khanbilvardi, R., Parshall,L., Mahani, S., Glickman, H., Goldberg, R., Blake, R., Slosberg, R. & Hillel, D. 2008. Variations in New York City's Urban Heat Island Strength Over Time and Space. *Theoretical and Applied Climatology*, 94: 1 – 11.

Gallo, K., McNab, A., Karl, T., Brown, J., Hood, J. & Tarpley, J. 1993. The Use of NOAA AVHRR Data for Assessment of the Urban Heat Island Effect. *Journal of Applied Meteorology*, 32: 899 – 908.

Gottmann, J. 1961. *Megalopolis: The Urbanized Northeastern Seaboard of the United States*. New York: Twentieth-Century Fund.

Gustafson, E. 1998. Quantifying Landscape Spatial Pattern: What Is the State of the Art? *Ecosystems*, 1(2): 143 – 156.

Hafner, J. & Kidder, S. 1999. Urban Heat Island Modeling in Conjunction with Satellite-Derived Surface/Soil Parameters. *Journal of Applied Meteorology*, 38: 448 – 465.

Hage, K. D. 1975. Urban-Rural Humidity Differences. *Journal of Applied Meteorology*, 14: 1277 – 1283.

Hamilton, L. 1992. *Regression with Graphics: A Second Course in Applied Statistics*. Pacific Grove, CA: Brooks/Cole Publishing Company.

Herold, M., Couclelis, H. & Clarke, K. 2005. The Role of Spatial Metrics in the Analysis and Modeling of Urban Land Use Change. *Computers, Environment and Urban Systems*, 29: 369 – 399.

Herold, M., Scepan, J. & Clarke, K. 2002. The Use of Remote Sensing and Landscape Metrics to Describe Structures and Changes in Urban Land Uses. *Environment and Planning A*, 34: 1443 – 1458.

Holmer, B. & Eliasson, I. 1999. Urban-Rural Vapor Pressure Differences and Their Role in the Development of Urban Heat Islands. *International Journal of Climatology*, 19: 989 – 1009.

Howard, L. 1833. *The Climate of London*. Available Online: http://urban-climate.com/wp3/resources/classic-texts/luke-howard-the-climate-of-london.

Hu, X., Klein, P., Xue, M., Lundquist, J., Zhang, F. & Qi, Y. 2013. Impact of Low-Level Jets on the Nocturnal Urban Heat Island Intensity in Oklahoma City. *Journal of Applied Meteorology and Climatology*, 52: 1779 – 1802.

Huang, J., Lu, X. & Sellers, J. 2007. A Global Comparative Analysis of Urban From: Applying Spatial Metrics and Remote Sensing. *Landscape and Urban Planning*, 82: 184 – 197.

Imhoff, M., Bounoua, L., DeFries, R., Lawrence, W., Stutzer, D., Tucker, C. & Ricketts, T. 2004. The Consequences of Urban Land Transformation on Net Primary Productivity in the United States. *Remote Sensing of Environment*. 89: 434 – 443.

Imhoff, M., Zhang, P., Wolfe, R. & Bounoua, L. 2010. Remote Sensing of the Urban Heat Island Effect Across Biomes in the Continental USA. *Remote Sensing of Environment*, 114: 504 – 513.

Jacobson, M. 2010. Enhancement of Local Air Pollution by Urban CO_2 Domes. *Environmental Science and Technology*, 44: 2497 – 2502.

Jat, M., Garg, P. K. & Khare, D. 2008. Monitoring and Modeling of Urban Sprawl Using Remote Sensing and GIS Techniques. *International Journal of Applied Earth Observation and Geoinformation*, 10: 26 – 43.

Ji, W., Ma, J., Twibell, R. & Underhill, K. 2006. Characterizing Urban Sprawl Using Multi-Stage Remote Sensing Images and Landscape Metrics. *Computers, Environment and Urban Systems*, 30: 861 – 879.

Jin, M. 2012. Developing an Index to Measure Urban Heat Island Effect Using Satellite Land Skin Temperature and Land Cover Observations. *Journal of Climate*, 25: 6193 – 6201.

Kaufmann, R., Seto, K., Schneider, A., Liu, Z., Zhou, L. & Wang, W. 2007. Climate Response to Rapid Urban Growth. Evidence of a Human-Induced Precipitation Deficit. *Journal of Climate*, 20(10): 2299 – 2306.

Kennedy, C., Cuddihy, J. & Engel-Yan, J. 2007. The Changing Metabolism of Cities. *Journal of Industrial Ecology*, 11(2): 43 – 59.

Kuttler, W., Weber, S., Schonnefeld, J. & Hesselschwerdt, A. 2007. Urban/Rural Atmospheric Water Vapor Pressure Differences and Urban Moisture Excess in Krefeld, Germany. *International Journal of Climatology*, 27: 2005 – 2015.

Lang, R. & Knox, P. 2009. The New Metropolis: Rethinking Megalopolis. *Regional Studies,* 43(6): 789 – 802.

Lewis, P. 1983. The Galactic Metropolis, in Pratt, R. and Macinko, G. (Eds) *Beyond the Urban Fringe*, 60 – 91. Minneapolis: University of Minnesota Press.

Li, D. & Bou-Zeid, E. 2013. Synergistic Interactions between Urban Heat Islands and Heat Waves: The Impact in Cities Is Larger than the Sum of Its Parts. *Journal of Applied Meteorology and Climatology*, 52: 2051 – 2064.

Li, X., He, H., Bu, R., Wen, Q., Chang, Y., Hu, Y. & Li, Y. 2005. The Adequacy of Different Landscape Metrics for Various Landscape Patterns. *Pattern Recognition*, 38: 2626 – 2638.

Liu, H. & Weng Q. 2008. Seasonal Variations in the Relationship Between Landscape Pattern and Land Surface Temperature in Indianapolis, USA. *Environmental Monitoring and Assessment*, 144: 199 – 219.

Makido, Y., Dhakal, S. & Yamagata, Y. 2012. Relationship Between Urban Form and CO_2 Emissions: Evidence From Fifty Japanese Cities. *Urban Climate*, 2: 55 – 67.

Martilli, A. 2014. An Idealized Study of City Structure, Urban Climate, Energy Consumption, and Air Quality. *Urban Climate*, doi: http://dx.doi.org/10.1016/j.uclim.2014.03.003

Matzarakis, A., De Rocco, M., & Najjar, G. 2009. Thermal Bioclimate in Strasbourg – The 2003 Heat Wave. *Theoretical and Applied Climatology*, 98(3 – 4): 209 – 220.

McGarigal, K., Cushman, S. & Ene, E. 2012. FRAGSTATS v4: Spatial Pattern Analysis Program for Categorical and Continuous Maps. Computer software program produced by the authors at the University of Massachusetts, Amherst. Available Online: http://www.umass.edu/landeco/research/fragstats/fragstats.html.

Mills, G. 2008. Luke Howard and the Climate of London. *Weather*, 63(6): 153 – 157.

Mladenoff, D. & DeZonia, B. 1997. APACK 2.0 User's Guide. Department of Forest Ecology and Management, University of Wisconsin-Madison.

Mote, T., Lacke, M. & Shepherd, J. M. 2007. Radar Signatures of the Urban Effect on Precipitation Distribution: A Case Study for Atlanta, Georgia. *Geophysical Research Letters*, 34: DOI 10.1029/2007GL031903.

Myrup, L. 1969. A Numerical Model of the Urban Heat Island. *Journal of Applied Meteorology*, 8: 908 – 918.

Naveh, Z. & Lieberman, A. 1984. *Landscape Ecology: Theory and Application*. New York: Springer-Verlag.

Oke, T. R. 1973. City Size and the Urban Heat Island. *Atmospheric Environment*, 7: 769 – 779.

Oke, T. R. 1976. The Distinction Between Canopy and Boundary-Layer Urban Heat Islands. *Atmosphere*, 14(4): 268 – 277.

Oke, T. R. 1982. The Energetic Basis of the Urban Heat Island. *Quarterly Journal of the Royal Meteorological Society*, 108: 1 – 24.

Oke, T. R. 1987. *Boundary Layer Climates*. New York: Methuen.

Oke, T. R. 1997. Urban Climates and Global Environmental Change, in Thompson, R. and Perry, A. (Eds) *Applied Climatology: Principles & Practices*, 273 – 287. New York: Routledge.

Oke, T. R., Johnson, C., Steyn, D. & Watson, I. 1991. Simulation of Surface Urban Heat Islands Under "Ideal" Conditions at Night. Part 2: Diagnosis of Causation. *Boundary-Layer Meteorology*, 56: 339 – 358.

Oke, T. R. & Maxwell, G. B. 1975. Urban Heat Island Dynamics in Montreal and Vancouver. *Atmospheric Environment*, 9: 191 – 200.

Peng, S., Piao, S., Ciais, P., Friedlingstein, P., Ottle, C., Breon, F., Nan, H., Zhou, L. & Myneni, R. 2011. Surface Urban Heat Island Across 419 Global Cities. *Environmental Science and Technology*, 46: 696 – 703.

Pope, C. A., Muhlestein, J., May, H., Renlund, D., Anderson, J. & Horne, B. 2006. Ischemic Heart Disease Events Triggered by Short-Term Exposure to Fine Particulate Air Pollution. *Circulation*, 114: 2443 – 2448.

Population Reference Bureau. 2012. World Population Datasheet. Available Online: http://www.prb.org/pdf12/2012-population-data-sheet_eng.pdf

PRISM Climate Group. Oregon State University. http://prism.oregonstate.edu.

Robine, J., Cheung, S., Le Roy, S., Van Oyen, H., Griffiths, C., Michel, J., & Herrmann, F. 2008. Death Toll Exceeded 70,000 in Europe During the Summer of 2003. *Comptes Rendus Biologies*, 331(2): 171 – 178.

Rosenfeld, A., Akbari, H., Romm, J., & Pomerantz, M. 1998. Cool Communities: Strategies for Heat Island Mitigation and Smog Reduction. *Energy and Buildings*, 28: 51 – 62.

Roth, M., Oke, T. R. & Emery, W. J. 1989. Satellite-Derived Urban Heat Islands from Three Costal Cities and the Utilization of Such Data in Urban Climatology. *International Journal of Remote Sensing*, 10(11): 1699 – 1720.

Semádeni-Davies, A. & Bengtsson, L. 1998. Snowmelt Sensitivity to Radiation in the Urban Environment. *Hydrological Sciences Journal,* 43(1): 67 – 89.

Shepherd, J. M. In Press. Impacts of Urbanization on Precipitation and Storms: Physical Insights and Vulnerabilities. *Climate Vulnerability*. Ed. Roger Pielke.

Sisterson, D. & Dirks, R. 1977. The Urban Moisture Climate. *Proceedings of the Conference on Metropolitan Physical Environment*, 26 – 35. Available Online: http://www.nrs.fs.fed.us/pubs/gtr/gtr_ne25/gtr_ne25_026.pdf

Stewart, I. 2011. A Systematic Review and Scientific Critique of Methodology in Modern Urban Heat Island Literature. *International Journal of Climatology*, 31(2): 200 – 217.

Stone, B. 2007. Urban and Rural Temperature Trends in Proximity to Large US Cities: 1951 – 2000. *International Journal of Climatology*, 27: 1801 – 1807.

Stone, B. 2012. *The City and the Coming Climate: Climate Change in the Places We Live.* New York: Cambridge University Press.

Stone, B., Hess, J. & Frumkin, H. 2010. Urban Form and Extreme Heat Events: Are Sprawling Cities More Vulnerable to Climate Change Than Compact Cities? *Environmental Health Perspectives*, 118(10): 1425 – 1428.

Stone, B. & Rodgers, M. 2001. Urban Form and Thermal Efficiency: How the Design of Cities Influences the Urban Heat island Effect. *Journal of the American Planning Association*, 67(2): 186 – 198.

Streutker, D. 2003. Satellite-Measured Growth of The Urban Heat Island of Houston. *Remote Sensing of Environment*, 85: 282 – 289.

Souch, C. & Grimmond, S. 2006. Applied Climatology: Urban Climate. *Progress in Physical Geography*, 30(2): 270 – 279.

Sutton, P., Goetz, A., Fildes, S., Forster, C. & Ghosh, T. 2010. Darkness on the Edge of Town: Mapping Urban and Peri-Urban Australia Using Nighttime Satellite Imagery. *The Professional Geographer*, 62(1): 119 – 133.

Todhunter, P., Xu, F. & Buttle, J. 1992. A Model of Net Radiation Over Suburban Snowpacks. *Atmospheric Environment,* 26B: 17 – 27.

United Nations. 2012. World Urbanization Prospects The 2011 Revision Highlights. Available Online: http://esa.un.org/unup/pdf/WUP2011_Highlights.pdf

Voogt, J. A. & Oke, T. R. 1997. Complete Urban Surface Temperatures. *Journal of Applied Meteorology*, 36: 1117 – 1132.

Wickham, J., Stehman, S., Gass, L., Dewitz, J., Fry, J. & Wade, T. 2013. Accuracy Assessment of NLCD 2006 Land Cover and Impervious Surface. *Remote Sensing of Environment*, 130: 294 – 304.

Wei, J., Ma, J., Twibell, R. & Underhill, K. 2006. Characterizing Urban Sprawl Using Multi-Stage Remote Sensing Images and Landscape Metrics. *Computers, Environment and Urban Systems*, 30: 861 – 879.

Wolters, D. & Brandsma, T. 2012. Estimating the Urban Heat Island in Residential Areas in the Netherlands Using Observations by Weather Amateurs. *Journal of Applied Meteorology and Climatology*, 51: 711 – 721.

Wong, M. S., Nichol, J., To, P. H. & Wang, J. 2010. A Simple method for Designation of Urban Ventilation Corridors and its Application to Urban Heat Island Analysis. *Building and Environment*, 45: 1880 – 1889.

Xi, W. & Yan, G. 2010. The Impact of an Urban Dry Island on the Summer Heat Wave and Sultry Weather in Beijing City. *Chinese Science Bulletin*, 55(16): 1657 – 1661.

Yuan, F. & Bauer, M. 2006. Comparison of Impervious Surface Area and Normalized Difference Vegetation Index as Indicators of Surface Urban Heat Island Effects in Landsat Imagery. *Remote Sensing of Environment*, 106(3): 375 – 386.

Zhang, D., Shou, Y. & Dickerson, R. 2009. Upstream Urbanization Exacerbates Urban Heat Island Effects. *Geophysical Research Letters*, 36 L24491, doi:10.1029/2009GL041082.

Zhou, B., Rybski, D. & Kropp, J. 2013. On the Statistics of Urban Heat Island Intensity. *Geophysical Research Letters*, 40: 1 – 6. doi: 10.1002/2013GL057320.

Zhou, Y. & Shepherd, J. M. 2010. Atlanta's Urban Heat Island Under Extreme Heat Conditions and Potential Mitigation Strategies. *Natural Hazards*, 52: 639 – 668.